The Impact of Climate Change on Groundwater Resources: The Climate Sensitivity of Groundwater Recharge in Australia

Article · January 2010

CITATIONS
23

READS
477

9 authors, including:

Olga Barron
The Commonwealth Scientific and Industrial Research Organisation
56 PUBLICATIONS **1,421** CITATIONS
SEE PROFILE

Russell S. Crosbie
The Commonwealth Scientific and Industrial Research Organisation
114 PUBLICATIONS **3,521** CITATIONS
SEE PROFILE

Warrick R. Dawes
The Commonwealth Scientific and Industrial Research Organisation
107 PUBLICATIONS **6,187** CITATIONS
SEE PROFILE

Freddie Simon Mpelasoka
The Commonwealth Scientific and Industrial Research Organisation
29 PUBLICATIONS **1,670** CITATIONS
SEE PROFILE

National Research FLAGSHIPS
Water for a Healthy Country

CSIRO

The impact of climate change on groundwater resources: The climate sensitivity of groundwater recharge in Australia

Olga Barron, Russell Crosbie, Warrick Dawes, Daniel Pollock, Steve Charles, Freddie Mpelasoka, Santosh Aryal, Michael Donn and Ben Wurcker

October 2010

Water for a Healthy Country Flagship Report series ISSN: 1835-095X

Australia is founding its future on science and innovation. Its national science agency, CSIRO, is a powerhouse of ideas, technologies and skills.

CSIRO initiated the National Research Flagships to address Australia's major research challenges and opportunities. They apply large scale, long term, multidisciplinary science and aim for widespread adoption of solutions. The Flagship Collaboration Fund supports the best and brightest researchers to address these complex challenges through partnerships between CSIRO, universities, research agencies and industry.

The Water for a Healthy Country Flagship aims to provide Australia with solutions for water resource management, creating economic gains of $3 billion per annum by 2030, while protecting or restoring our major water ecosystems. The work contained in this report is collaboration between the National Water Commission, CSIRO and SKM.

For more information about Water for a Healthy Country Flagship or the National Research Flagship Initiative visit www.csiro.au/org/HealthyCountry.html

Citation: Barron O., Pollock D., Crosbie R., Dawes W., Charles S., Mpelasoka F., Aryal S., Donn M. and Wurcker B. 2010. The impact of climate change on groundwater resources: The climate sensitivity of groundwater recharge in Australia. CSIRO: Water for a Healthy Country Report to National Water Commission.

Cover Photograph:

Aerial view of a groundwater spring at Lake Eyre, South Australia, by Dr Paul Shand, CSIRO Land and Water © 2010 CSIRO

TABLE OF CONTENTS

Acknowledgements ix

Executive Summary x

Introduction 1

1. Climate change and groundwater: Literature Review 3

    1.1. General approach for projecting the impact of climate change on groundwater resources 3

    1.2. Effect of climate on groundwater recharge: process understanding 7

    1.3. Knowledge gaps 8

2. Methods 10

    2.1. Estimation of climate type transitions 10

    2.2. Climate parameters and diffuse groundwater recharge 13

    2.3. Effect of climate data downscaling on diffuse groundwater recharge 16

3. Historical and projected climate types in Australia 25

    3.1. Current baseline climate type 25

    3.2. Historical change in the extent of climate types 27

    3.3. Projected changes for 2030 29

    3.4. Projected changes for 2050 32

    3.5. Potential risk to changes in land cover 34

    3.6. Conclusions 36

4. Effect of individual climate characteristics and their combination on diffuse groundwater recharge 37

    4.1. Selected climate type characterisation 38

    4.2. Recharge frequency 40

    4.3. Relative importance of climate characteristics in recharge estimation 41

    4.4. Effect of rainfall characteristics on estimated recharge 44

    4.5. Recharge sensitivity to rainfall and its intensity 48

4.6. Conclusions 55

5. Effect of GCMs, downscaling methods and selection of hydrological models on recharge projection under future climate 58

5.1. Climate data 58

5.2. Calibration of hydrological models 66

5.3. Recharge under a future climate 68

5.4. Conclusions 77

Appendix A 79

References 91

LIST OF FIGURES

Figure 2-1. Relationship between modelled recharge and soil hydraulic conductivity (as geometric mean between hydraulic conductivity of topsoil and subsoil): see Table 2-2 for climate types acronyms . 15

Figure 2-2. Conceptual diagram of the WAVES model. 20

Figure 2-3. Conceptual model of HELP. 21

Figure 2-4. Conceptual model of SIMHYD 22

Figure 2-5. Location of three sites chosen for calibration of the recharge models 23

Figure 3-1. Current Australian baseline Köppen-Geiger climate type map (1970–2009) 26

Figure 3-2. Land cover map for Australia (BRS, 2008) 26

Figure 3-3. Historical series of Australian Köppen-Geiger climate type maps: 1939–1969, 1949–1979, 1959–1989, 1969–1999 and 1979–2009. 28

Figure 3-4. Percentage of Australia territory under different climate types 29

Figure 3-5. Percentage of Australia territory under different climate types, per degree of global warming (low, medium, and high projections for 2030 and 2050) 30

Figure 3-6. 2030 medium global warming projections: (a) mode climate type; (b) frequency of the mode climate type; (c) mode climate type compared to baseline climate type, 0 – no difference, 1 – different; (d) number of different projected climate types 31

Figure 3-7. 2050 medium global warming projections: (a) mode climate type; (b) frequency of the mode climate type; (c) mode climate type compared to baseline climate type, 0 – no difference, 1 – different; (d) number of different projected climate types 33

Figure 3-8. Mode projected climate type change (medium projection for 2030) and current land cover (BRS, 2008) 35

Figure 3-9. Mode projected climate type change (medium projection for 2050) and current land cover (BRS, 2008) 35

Figure 4-1. Probability of exceedance of annual rainfall for selected climate types 39

Figure 4-2. Locations where climate data was extracted for recharge modelling shown in relation to (a) climate type, (b) mean annual temperature (MAT, ºC), derived from daily maximum and minimum temperature, (c) mean annual precipitation (MAP, mm), and (d) fraction of mean annual precipitation during summer period (F_{smap}) 39

Figure 4-3. Probability of exceedance of annual recharge for various vegetation, climate types and soil types 40

Figure 4-4. Relative importance of all considered climate characteristics 42

Figure 4-5. Relative importance of the considered climate characteristics other than annual rainfall 43

Figure 4-6. Relative importance of climate characteristics (all but rainfall) in recharge estimation for three vegetation types and soil K > 1 m/d 44

Figure 4-7. Average increase in relative importance when selected climate characteristics are considered in addition to annual rainfall 44

Figure 4-8. Comparison of the correlation coefficients (R^2) for the recharge and rainfall relationship: (X-axis) with total annual rainfall and (Y-axis) derived annual rainfall characteristics which reflect intra-annual rainfall patterns (as a best fit for considered range) 45

Figure 4-9. Comparison of the correlation coefficients (R^2) for the recharge and rainfall relationship: (X-axis) with total annual rainfall and (Y-axis) derived annual rainfall characteristics: (a) sum of the daily rainfall above the identified thresholds; (b) sum of the daily rainfall within the identified bands; (c) sum of the daily rainfall as moving average with identified intervals and daily thresholds; and (d) sum of 95th and 99th percentile daily rainfall 46

Figure 4-10. Slope of the R and RF relation at individual sites and the mean annual rainfall at the same site for all locations (a) and for annual vegetation only (b); square symbols are used for annuals, circles for perennials and triangular symbols for trees 48

Figure 4-11. Annual rainfall and recharge relationship (a) contribution of high intensity daily rainfall to total annual average rainfall, (b) the annual average recharge, and (c) at three selected locations under soil with K > 1m/d 49

Figure 4-12. Annual rainfall and recharge relationship at two selected locations 50

Figure 4-13. Relationship between annual rainfall (ARF) and percent of rainfall greater than 20 mm (ARF_{20}/ARF): example is given for site 'L' 50

Figure 4-14. Annual average recharge and a (slope) of the relationship between recharge and annual average rainfall for annual, perennial vegetation and trees under soil with high hydraulic conductivity, plotted over annual average rainfall 51

Figure 4-15. Annual average recharge and a (slope) of the relationship between recharge and annual average rainfall for annual, perennial vegetation and trees under soil with high hydraulic conductivity, plotted over annual average rainfall, plotted over the map of summer rainfall as proportion of total annual rainfall 52

Figure 4-16. Slopes of the recharge and rainfall relationship, when the total annual (left column) and only rainfall of high intensity (right column) were considered for combination of soils and vegetations under BSh3, BSk, BWh and Cfa climate types 53

Figure 4-17. Slopes of the recharge and rainfall relationship, when the total annual (left column) and only rainfall of high intensity (right column) was considered for combination of soils and vegetations under Aw, BSh4 and Dfc climate types 54

Figure 5-1. Observed annual series of rainfall at each site for the historical period (red line shows the average). 59

Figure 5-2. Average annual rainfall from the GCMs without downscaling for each of the three sites showing the current climate period (black), future climate period (grey) and the observed annual average for comparison (red line) 59

Figure 5-3. Comparison of change in rainfall for the downscaling methods for each GCM and site 60

Figure 5-4. Boxplots of the change in rainfall at the three sites comparing the differences in GCMs and downscaling methods. The red line in the box represents the mean. 61

Figure 5-5. Probability of exceedances of daily rainfall for the current and future climates for Gnangara. 'Stochastic 10', 'Stochastic 50', and 'Stochastic 90' refer to the 10th, 50th and 90th percentile replicates (in terms of mean annual rainfall change) extracted from 100 stochastic replicates. P_H refers to the historical rainfall and P_F refers to the future rainfall 63

Figure 5-6. Probability of exceedances of daily rainfall for the current and future climates for Moorook. 'Stochastic 10', 'Stochastic 50', and 'Stochastic 90' refer to the 10th, 50th and 90th percentile replicates (in terms of mean annual rainfall change) extracted from 100 stochastic replicates. P_H refers to the historical rainfall and P_F refers to the future rainfall. 64

Figure 5-7. Probability of exceedances of daily rainfall for the current and future climates for Livingston Creek. 'Stochastic 10', 'Stochastic 50', and 'Stochastic 90' refer to the 10th, 50th and 90th percentile replicates (in terms of mean annual rainfall change) extracted from 100 stochastic replicates. P_H refers to the historical rainfall and P_F refers to the future rainfall. 65

Figure 5-8. Scatter plot of monthly modelled and simulated runoff for the Livingstone Creek catchment..67

Figure 5-9. The change in recharge estimated from each hydrological model for every combination of future climate projected by the GCMs and downscaling methods 69

Figure 5-10. Comparison of the change in recharge at each site aggregated by GCM. The red line in the box represents the mean....70

Figure 5-11. Comparison between the change in recharge for the different GCMs at the different sites. The colour filled symbols indicate that the recharge from the two GCMs are different according to a paired t-test....71

Figure 5-12. The relationship between the change in rainfall and the change in recharge for the different GCMs at the different sites....72

Figure 5-13. Comparison of the change in recharge at each site aggregated by downscaling method. The red line in the box represents the mean....72

Figure 5-14. Comparison between the change in rainfall and the change in recharge for the different downscaling methods at the different sites. The colour filled symbols indicate that the rainfall or recharge from the two downscaling methods are different according to a paired t-test. 73

Figure 5-15. The relationship between the change in rainfall and the change in recharge for the different downscaling methods at the different sites 74

Figure 5-16. Comparison of the change in recharge at each site as aggregated by hydrological model. The red line in the box represents the mean....74

Figure 5-17. Comparison between the change in recharge for the different hydrological models at the different sites. The colour filled symbols indicate that the recharge from the two hydrological models are different according to a paired t-test. 75

Figure 5-18. The relationship between the change in rainfall and the change in recharge for the different hydrological models at the different sites 76

Figure 5-19. Comparison between the change in recharge and change in runoff at Livingston Creek where runoff is the sum of overland flow (OF) and lateral flow (LF) 77

In Appendix A

Figure A-1. Relationship between annual rainfalls, temperature solar radiation and vapour pressure deficit for Aw climate type....80

Figure A-2. Relationship between annual rainfalls, temperature solar radiation and vapour pressure deficit for BSh4 climate type....81

Figure A-3. Relationship between annual rainfalls, temperature solar radiation and vapour pressure deficit for BSh3 climate type....82

Figure A-4. Relationship between annual rainfalls, temperature solar radiation and vapour pressure deficit for BSk climate type 83

Figure A-5. Relationship between annual rainfalls, temperature solar radiation and vapour pressure deficit for BWh climate type 84

Figure A-6. Relationship between annual rainfalls, temperature solar radiation and vapour pressure deficit for Cfa climate type 85

Figure A-7. Relationship between annual rainfalls, temperature solar radiation and vapour pressure deficit for Dfc climate type 86

Figure A-8. Probability of exceedance of annual recharge for various vegetation, climate types and clay soil (K=0.01m/d) 87

Figure A-9. Probability of exceedance of annual recharge for various vegetation, climate types and light soil (K=0.1m/d) 88

Figure A-10. Probability of exceedance of annual recharge for various vegetation, climate types and highly permeable soils (K=1m/d) 89

Figure A-11. Annual average recharge (a, c and e) and a (slope) of the relationship between recharge and annual average rainfall (b, d and f) for annual vegetation (a and b), perennial vegetation (c and d), trees (e and f) under soil with high hydraulic conductivity, plotted over the climate types 90

LIST OF TABLES

Table 2-1. Criteria for determining the precipitation threshold (P_{thres}) from mean annual temperature (MAT), conditional on the fraction of mean annual precipitation that falls in summer (F_{smap}) 11

Table 2-2. Köppen-Geiger climate type descriptions and classification criteria 11

Table 2-3. The minimum daily rainfall event fully accounted in moving-average analysis over the set of considered periods and daily thresholds 15

Table 3-1. Change in percentage occurrence from baseline to 2030 (low, medium and high projections) 32

Table 3-2. Change in percentage occurrence from baseline to 2050 (low, medium and high projections) 34

Table 4-1. Characterisation of the selected climate types 38

Table 4-2. Annual rainfall characteristics with highest R^2 for recharge estimation 47

Table 4-3. Summary for perennial vegetation and K ≥ 1.0 m/d 56

Table 5-1. Summary of the annual averages of the water balance terms from the calibrated hydrological models at Gnangara 66

Table 5-2. Summary of the annual averages of the water balance terms from the calibrated hydrological models at Moorook 66

Table 5-3. Summary of the annual averages of the water balance terms from the calibrated hydrological models at Livingston Creek 67

ACKNOWLEDGEMENTS

The project team would like to acknowledge the National Water Commission for providing funding to support current studies under the National Groundwater Action Plan. We would like to thank Riasat Ali, Richard and Geoff Hodgson for their contribution to the report, as well as Ian Jolly and Marie Ekstrom, who reviewed the report and provided us with the most useful comments.

EXECUTIVE SUMMARY

Australia has experienced increasing pressures on groundwater resources due to a drier climate and an increased scarcity of surface water resources. In 2004 the Council of Australian Governments agreed to the National Water Initiative (NWI) which aimed to ensure the implementation of a transparent planning framework that would avoid over-allocation of water resources, including groundwater. Changes in entitlements can occur, but under the NWI it is necessary to assign the risk associated with changes in entitlements due to climate change and variability. This risk assignment will require a good understanding of the processes impacting on water resources from climate change.

In response to these issues the National Water Commission has commissioned a project 'Investigating the impact of climate change on groundwater resources' within the National Groundwater Action Plan (NGAP). The primary objective of the project is to determine how the temporal variability in rainfall and temperature due to climate change will impact on groundwater recharge and groundwater resources across different aquifer types in different climatic types across Australia.

The project is built upon the work carried out by CSIRO in the Murray-Darling Basin Sustainable Yields (MDBSY), Northern Australia Sustainable Yields (NASY), South-West Western Australia Sustainable Yields (SWSY) and Tasmania Sustainable Yields (TasSY) Projects, but also will provide additional information on the impact of changes in groundwater systems that affect groundwater-dependent ecosystems, agricultural production, and stock and domestic water supply in those regions not covered by the CSIRO sustainable yields projects.

This report presents the results of a number of project activities, identified within the third milestone of the project plan, with objectives to:

- review scientific publication and summarise the current knowledge of the effect of climate change on groundwater recharge and resources
- analyse climate types and climate type transitions across Australia for the historical period beginning in 1930 and under projected future climates for 2030 and 2050
- investigate the specifics of diffuse recharge within different climate types
- assess the differences in global climate models (GCMs), downscaling methods and hydrological models for projecting future recharge under the A2 scenario for 2050 using three contrasting field sites as examples.

Literature review

The literature review highlighted the paucity of studies worldwide investigating the impact of climate change on groundwater resources. A common approach to the investigation of climate change effect on groundwater was apparent: climate projections derived from climate models were applied as an input in hydrological models, which in turn were used to define the changes in water fluxes. However, the results of published analyses did not adequately account for uncertainties inherent in using only a single GCM, downscaling method and hydrological model to make projections of groundwater resources under a future climate. The literature review identified the following knowledge gaps:

- Previous comparisons of different hydrological models have focused on their ability to simulate observed conditions. However, model structure has never been evaluated as a determinant in the projections of recharge under a future climate.

- Only two published studies were identified that reported a comparison of the impact on recharge of different downscaling techniques; however, the methods used in these studies are not commonly used in Australia.
- There has not been a study of the influence of climate types upon recharge anywhere in world.

The analyses undertaken within this project are expected to advance our knowledge in some of these areas.

Historical and future projection of changes in climate types in Australia

Analysis of historical (from the 1930s to the present) climate types suggests a transition from desert to steppe conditions in central and northern Australia that may be attributed to an observed increase in mean annual precipitation. Over the same time, there was a shift to drier summers in parts of south-western Victoria, and in south-west Western Australia there was a transition from temperate (with hot dry summers) to steppe conditions.

Projected climates are characterised by a decrease in precipitation in central Australia, as well as an overall increase in temperature. As a result, an increase in the occurrence of arid conditions (both desert and steppe) is projected as well as a general reduction in the occurrence of temperate conditions.

In addition to projected changes from the GCMs for rainfall and temperature across the country, the climate type analysis led to the identification of areas where a combined variation in rainfall and temperature led to a change of climate type. Such circumstances may cause changes in vegetation cover, which in turn may have an additional impact on water resources, which will be considered in a later stage of the project.

Climate types and their effect on diffuse recharge

The analysis was undertaken for the NASY and MBDSY regions where recharge estimation was available to the project. It identified that:

- Annual rainfall is a major factor influencing recharge. However, for the majority of the considered climate types the total annual rainfall had a weaker correlation with recharge than the rainfall parameters reflecting rainfall intensity.
- Annual recharge is more sensitive to daily rainfall intensity in regions with winter-dominated rainfall, where it is also less sensitive to absolute changes in annual rainfall.
- In regions with winter-dominated rainfall, annual recharge under the same annual rainfall, soils and vegetation conditions is less than in regions with summer-dominated rainfall. This was attributed to the differences in rainfall patterns associated with monsoons/cyclones with predominately heavy rains in the north, and frontal weather systems with prolonged periods of light daily rainfall in the south.
- The relative importance of climate parameters other than rainfall is higher for recharge under annual vegetation, but overall is highest in the tropical climate type. Solar radiation and vapour pressure deficit (VPD) show greater relative importance than average annual daily mean temperature. Climate parameters have lowest relative importance in the arid climate type (with cold winters) and the temperate climate type.
- Episodic recharge is more likely associated with the desert climate type; the probability of episodic recharge reduces in the climate type sequence: arid>temperate>cold. However, episodic recharge may also occur in areas with high

annual rainfall but less permeable soils (such as vertosols) and with trees as a land cover.

The results highlight the importance of the rainfall intensity projection under future climate scenarios, particularly in the southern region of the country

Effect of climate data downscaling and selection of recharge models on the projection of recharge changes under future climate

As the analysis did not aim to define the best GCM, downscaling method or hydrological model for projection of recharge changes under the future climate, the results are reported in terms of differences between them. The five GCMs chosen (CSIRO Mk3.5, GFDL 2.0, GFDL 2.1, MIROC 3.2 midres, and MPI-ECHAM5) are amongst the better-performing GCMs available in terms of reproducing El Niño Southern Oscillation and Indian Ocean Dipole signals, both of which are important for predicting climate patterns across Australia. However, there is considerable variability in their projections of rainfall under the A2 scenario for 2050. The GCMs' projections at all three sites were not consistent, showing both increase and decrease in future rainfall.

The results of the three downscaling methods (daily scaling (daily), stochastic downscaling model (ST), and daily scaling using dynamical downscaling model Cubic Conformal Atmospheric Model (CCAM) results (CCAM-scaled)) showed a trend in rainfall projection where CCAM-scaled would project the highest rainfall, followed by the daily scaling method with the stochastic downscaling projecting the least rainfall. Daily scaling resulted in the greatest range of projected changes in rainfall.

The four hydrological models (WAVES with and without plant growth, HELP, and SIMHYD) were all successfully calibrated using the recharge estimated from field measurements. Each model differs considerably in its conceptualisation and therefore its ability to simulate physical processes. Though sensitivity of the modelling to changes in those processes will be undertaken in a later stage, an observation from the modelling is that at two out of three sites HELP projected significantly lower recharge than both of the WAVES models.

There were considerable differences in the change in recharge projected by the different combinations of GCM, downscaling method and hydrological model at each site.

- At Gnangara, where historical recharge was the highest of all three sites (~360 mm), the range of recharge projections was the most consistent and ranged from +17% to –55% with a median of –31% from –18% projected change in rainfall. Only one combination of GCM/downscaling (CSIRO/daily) resulted in an increase in recharge at this site. All other combinations projected a reduction in future recharge except for CSIRO/ST with the SIMHYD and WAVES-C (constant annual pattern of leaf area index) hydrological models.
- At Moorook, where the recharge and rainfall was particularly low, the range of recharge projections was from +553% to –80% with a median of –37% from –18% projected change in rainfall. The largest change in recharge projections was from the HELP model.
- At Livingston Creek, with predominately clay-rich soils, the range of recharge projections was from +101% to –68% with a median of –7% from –2% projected change in rainfall. At this site increases in recharge were consistently projected when recharge modelling was based on CCAM-scaled downscaling for the majority of GCMs.

The range of projections across the sites highlights the uncertainty in making projections of recharge under a future climate, and indicates that the application of a single GCM,

downscaling method and hydrological model could be inadequate for future groundwater resources projection.

INTRODUCTION

The effect of climate change on water resources, and consequently on water availability, is one of the most challenging aspects of long-term sustainable water management. National and international studies most often focus on climate change impacts to surface water resources; climate change effects on groundwater resources have not been systematically addressed. This is despite the fact that many regions are greatly dependant on groundwater resources for irrigation, industrial use including mining, and urban supply.

Australia has experienced increasing pressures on groundwater resources. In 2004 the Coalition of Australian Governments agreed to the National Water Initiative (NWI) which aimed to bring over-allocated groundwater systems back to sustainable levels, and to ensure the implementation of a transparent planning framework that would avoid future over-allocation. Changes in entitlements can occur for a number of reasons, but under the NWI it is necessary to assign the risk associated with changes to entitlement due to climate change and variability. This risk assignment will require a good understanding of the processes impacting on water resources from climate change.

The rainfall decline in many Australian regions over recent years has seen both reductions in recharge and increases in groundwater use, as surface water resources become increasingly scarce. The 2007 Biennial Assessment of Progress against the NWI led to the identification of several concerns with respect to groundwater. This subsequently led to the National Groundwater Action Plan (NGAP) of which the main component, the National Groundwater Assessment Initiative, aimed to improve the understanding of groundwater resources and support NWI implementation.

In response to these issues, the National Water Commission has commissioned a project 'Investigating the impact of climate change on groundwater resources' within the NGAP to investigate the impact of climate change on groundwater resources. The aim of this project is to quantify the impacts of spatial and temporal change in climate on groundwater resources in representative aquifer systems across Australia as a national snapshot.

The project builds upon the work carried out by CSIRO in the Murray-Darling Basin Sustainable Yields (MDBSY), Northern Australia Sustainable Yields (NASY), South-West Western Australia Sustainable Yields (SWSY) and Tasmania Sustainable Yields (TasSY) Projects. The project will provide additional information on the impact of changes in groundwater systems that affect groundwater-dependent ecosystems, agricultural production, and stock and domestic water supply in those regions not covered by the CSIRO sustainable yield projects.

The primary objective of the project is to determine how the temporal variability in rainfall and temperature due to climate change will impact on groundwater recharge and groundwater resources across different aquifer types in different climatic zones across Australia. In order to achieve this objective the project will focus on the following activities:

- quantifying the influence of climate characteristics on groundwater recharge, including total rainfall, rainfall intensity and sequencing, seasonal distribution, temperature, solar radiation, humidity, and the consequences of variation in land use
- characterising groundwater systems, including hydrogeological characterisation, aquifer types, groundwater recharge and discharge zones, depth to groundwater and contribution to baseflow
- assessing future interaction between climate change and groundwater resources, taking into account changes in both magnitude and sequencing in climate characteristics and the impact of these on groundwater recharge and baseflow.

This report presents the results of the first phase of the project activities in defining sensitivity of groundwater resources to climate variability and projected changes in future climate. It includes the following:

- literature review – summarising the current knowledge on climate change effects on groundwater recharge and resources; presented in Chapter 1
- detailed methodology – set out in Chapter 2
- analysis of climate types and climate type transitions, using Köppen-Geiger climate classification – includes characterisation of historical trends, for the period beginning in 1930, and assessing the impact of projected climates under a number of global warming scenarios for 2030 and 2050; discussed in Chapter 3
- discussion on the specifics of diffuse recharge within the different climate types – presented in Chapter 4
- assessment of the differences in GCMs, downscaling methods and hydrological models for projecting future recharge at three locations – results are summarised in Chapter 5.

The outcomes of the undertaken analyses are given as conclusions in the end of each individual chapter, and are also summarised in the Executive Summary of the report.

1. CLIMATE CHANGE AND GROUNDWATER: LITERATURE REVIEW

The assessment reports of the Intergovernmental Panel on Climate Change (IPCC) are considered to be the authoritative reviews of climate change research globally across all disciplines. The second assessment report had this to say about groundwater research (Watson et al., 1996):

> *Despite the critical importance of groundwater resources in many parts of the world, there have been very few direct studies of the effect(s) of global warming on groundwater recharge.*

Little had changed by the time the third assessment report was released five years later (McCarthy et al., 2001):

> *Groundwater is the major source of water across much of the world, particularly in rural areas in arid and semiarid regions, but there has been very little research on the potential effects of climate change.*

The fourth assessment came to a very similar conclusion (Parry et al., 2007):

> *Despite its significance, groundwater has received little attention from climate change impact assessments, compared to surface water resources.*

The literature review presented here aims to summarise current knowledge of climate change effects on groundwater. It is subdivided into three sections:

- a review of approaches used to estimate the impact of climate change on groundwater resources
- a review of what has been learned from studies of the impact of climate change on groundwater
- an assessment of the knowledge gaps that still exist in our understanding of how climate change will impact on groundwater.

1.1. General approach for projecting the impact of climate change on groundwater resources

There is a general approach to estimating the impact of climate change on groundwater that most studies have followed. It includes:

- obtaining projections of the future climate change based on the output of one or more global climate model (GCM)
- downscaling projections from the coarse-grid scale of a GCM to a finer scale as required by hydrological models
- undertaking groundwater recharge modelling for the newly created time series of future climate to create a time series of recharge
- applying the projected future recharge time series as an input to a groundwater model.

1.1.1. Choice of GCM

GCMs are unanimous in their projections of globally increasing temperature (albeit with a large range, depending on the emissions scenario and the model used) with an increase in CO_2 concentration. There is much less consensus on the impact of increasing CO_2 concentration on rainfall. Different GCMs can project increases as well as decreases in rainfall that also differ in the magnitude of change for the same region using the same emissions scenario. For this reason it is generally recommended that impact studies use the output of multiple GCMs to investigate this source of uncertainty.

This is rarely undertaken in groundwater investigations, as commonly only one GCM is used (Austin et al., 2010; Bouraoui et al., 1999; Candela et al., 2009; Green et al., 2007; Herrera-Pantoja and Hiscock, 2008; Holman et al., 2009; Mileham et al., 2009; Scibek and Allen, 2006a; Scibek and Allen, 2006b; Scibek et al., 2007; Toews and Allen, 2009; van Roosmalen et al., 2009). When one GCM is chosen for investigation, this is generally the GCM produced in the country of the study. For instance, in Australia the CSIRO GCM has been used (Austin et al., 2010; Green et al., 2007), studies in Canada have favoured the CGCM1 model (Scibek and Allen, 2006a; Scibek and Allen, 2006b; Scibek et al., 2007; Toews and Allen, 2009) and UK-based researchers have used the HadCM3 model (Herrera-Pantoja and Hiscock, 2008; Holman et al., 2009; Mileham et al., 2009). Using two (Croley and Luukkonen, 2003; Doll, 2009; Goderniaux et al., 2009) or three (Brouyère et al., 2004; Hanson and Dettinger, 2005; Rosenberg et al., 1999) GCMs provides little improvement in understanding compared to using just one GCM. This is often because the differences between GCMs contribute the largest source of uncertainty in the projected hydrological response.

A step up in complexity of the future climate analysis is to use ensemble climate projections; this involves using the average of several GCMs as the input to hydrological models. Vaccaro (1992) used the average of three GCMs and the extreme case, and Serrat-Capdevila et al. (2007) used the average of 17 GCMs and four extreme cases. Using ensemble projections would appear to be a useful method of reducing the computation burden of investigating many GCMs but this may limit the assessment of the full uncertainty range of future projections. This is illustrated by the following example.

Through the Sustainable Yields Projects, it was found that the change in rainfall was not necessarily the best indicator of the change in recharge, and the rank of the GCMs for change in rainfall was never the same as the rank of the GCMs for the change in recharge (Crosbie et al., 2008; Crosbie et al., 2009). This illustrates that choosing the extreme GCMs for rainfall does not necessarily produce the extremes of recharge.

To better assess the range of possible future changes in climate, it appears that inclusion of a larger GCM model suite is beneficial. Several studies have used as many GCMs as they could get access to, Eckhardt and Ulbrich (2003) used five GCMs available under the ACACIA project, Loáiciga et al. (2000) used six GCMs available under the VEMAP project, and Crosbie et al. (2010b) used 15 GCMs available under the CMIP3 project.

1.1.2. Choice of downscaling method

Whilst GCMs are the preeminent tool for quantifying climate change representing atmospheric, oceanic, land surface and sea-ice processes and their feedbacks, their relatively coarse spatial resolution (several hundred km grid lengths) precludes their direct use in regional and local-scale impact assessment of the hydrological impacts of climate change scenarios (Fowler et al., 2007). GCM precipitation characteristics are often that of constant ‘drizzle’ as they cannot resolve circulation patterns that produce extreme hydrological events [Maraun, 2010 #160]. Thus ‘downscaling’ techniques are needed to

bridge the gap between the resolution of GCMs and the meteorological inputs required by hydrological models.

Techniques to transfer GCM-scale information to the scale required for impacts modelling can be broadly classified into two categories: statistical downscaling and dynamical downscaling. This project compares two statistical downscaling techniques (using methods based on scaling and stochastic downscaling) and one dynamical downscaling technique.

Statistical downscaling is a commonly used technique for which comprehensive guidelines and reviews are provided in Wilby et al. (2004), Fowler et al. (2007) and Maraun et al. (2010). The simplest methods use 'change factors', modifying observed climate series by factors calculated from the relative changes between current and future GCM simulations for the variables and seasons of interest. One of the limitations of the change factors approach is that it uses 'constant' scaling factors for all precipitation amounts whereas model evidence suggests the upper tail of the precipitation distribution may experience greater relative change, i.e. extreme daily rainfalls may increase proportionally more than moderate and low intensity daily rainfalls. Thus, 'daily scaling' has been developed to account for different relative changes for different percentiles of the daily precipitation probability density distribution (Mpelasoka and Chiew, 2009).

More advanced statistical downscaling techniques predominantly involve regression, weather typing, or weather generator approaches. These are also discussed in detail in the review articles cited above. Major issues for successful statistical downscaling application include predictor selection and careful assessment of performance for current and future climate (e.g. Charles et al., 2007; 1999; 2004).

Of those studies that have used statistical downscaling for climate change recharge or groundwater level modelling, the majority have used either scaling (constant scaling or pattern scaling) (Allen et al., 2004; Brouyère et al., 2004; Croley and Luukkonen, 2003; Eckhardt and Ulbrich, 2003; Jyrkama and Sykes, 2007; Kingston and Taylor, 2010; Loaiciga et al., 2000; Rosenberg et al., 1999; Serrat-Capdevila et al., 2007) or weather generators with parameters modified according to projected GCM changes (Bouraoui et al., 1999; Candela et al., 2009; Green et al., 2007; Herrera-Pantoja and Hiscock, 2008; Ng et al., 2010; Scibek and Allen, 2006a; Scibek and Allen, 2006b; Toews and Allen, 2009; Vaccaro, 1992; Vivoni et al., 2009).

Dynamical downscaling relies on regional climate models (RCMs) which account for the same physical atmospheric processes as GCMs but at a higher spatial resolution (less than 100 km) over a region. Although RCMs are much better at representing the spatial and temporal characteristics of precipitation compared to GCMs, most tend to have biases of too many simulated wet days concurrent with an underestimation of high intensity daily rainfalls ('drizzle effect'). Therefore there will always be discrepancies between RCM precipitation, which represents an areal average, and station data used in impacts modelling (Maraun et al., 2010). Such biases are evident in investigations that have used RCM outputs for recharge or groundwater modelling, as there has been a need to re-scale or bias correct the dynamically downscaled data to make it suitable as model input. For example, van Roosmalen et al. (2009) applied monthly change factors, derived from RCM 1961–1990 versus 2071–2100 changes, to observed daily precipitation, temperature and (calculated) Penman-Montieth evapotranspiration (ET) because RCM biases precluded the direct use of the RCM output in their groundwater modelling. Goderniaux et al. (2009) bias corrected daily precipitation and temperature simulations from six RCMs using quantile mapping (Wood et al., 2004) so that the RCM distributions for their current climate simulations matched those of the observed data, and then applied the same corrections to the future climate projections. Herrera-Pantoja and Hiscock (2008) and Holman et al. (2009) modified weather generator parameters according to an RCM's projected changes.

Only a few studies have evaluated the effect of different downscaling techniques on recharge projections. Mileham et al. (2009) used simple scaling and RCM transformation techniques in Uganda to demonstrate that the delta factor technique did not capture the increases in rainfall intensity simulated by the RCM and therefore grossly underestimated future recharge relative to the transformed climate time series. Holman et al. (2009) compared recharge estimates obtained from using a change factor scaling approach (for precipitation and potential evapotranspiration (PET) on a monthly basis) and a stochastic weather generator (also modified by change factors), and concluded that the deterministic change factors approach underestimates the uncertainty in recharge projections that are due to variability in runs of wet and dry years as simulated by the stochastic weather generator approach.

1.1.2. Choice of recharge model

There are many models used to estimate recharge and they differ greatly in their complexity. They range from simple empirical relationships to physically based numerical models.

Simple regression equations have been used to estimate recharge where annual recharge is assumed to vary linearly with annual rainfall after some rainfall threshold has been reached (Hanson and Dettinger, 2005; Serrat-Capdevila et al., 2007). This method assumes that an empirical relationship developed under historical climate conditions will hold under a future climate; this has been shown not to be true in the Murray-Darling Basin (Crosbie et al., 2010a).

'Bucket' models are commonly used to estimate recharge. These models have a series of cascading storages used to simulate the water stored in different soil layers. Some of the more common bucket models used for estimating recharge under climate change scenarios are HELP (Allen et al., 2004; Jyrkama and Sykes, 2007; Scibek and Allen, 2006a; Scibek and Allen, 2006b; Toews and Allen, 2009), SWAT (Eckhardt and Ulbrich, 2003; Kingston and Taylor, 2010; Rosenberg et al., 1999) and EPIC (Brouyère et al., 2004).

Models that rely on solving Richard's equation have the strongest conceptual basis from a theoretical point of view, but suffer from comparatively long computation times and many parameters that need to be estimated. Examples of these models that have been used in climate change studies include SWAP (Ng et al., 2010) and WAVES (Crosbie et al., 2010b; Green et al., 2007; McCallum et al., 2010).

Integrated models are the most complex hydrological models; these models solve the water balance in the unsaturated zone, saturated zone and river channel within the one model. Examples of these models that have been used for studies of climate change impact on groundwater include MIKE-SHE (van Roosmalen et al., 2009) and HydroGeoSphere (Goderniaux et al., 2009).

1.1.3. Groundwater modelling

The groundwater modelling component of an impact of climate change study is a simple scenario analysis commonly applied in groundwater modelling. If the groundwater model is not coupled with the unsaturated flow modules (as those mentioned in the previous section), each climate scenario has its own recharge time series that provides the input to the groundwater modelling. MODFLOW is by far the most commonly used groundwater model (Allen et al., 2004; Candela et al., 2009; Croley and Luukkonen, 2003; Hanson and Dettinger, 2005; Scibek and Allen, 2006a; Scibek and Allen, 2006b; Scibek et al., 2007; Serrat-Capdevila et al., 2007; Toews and Allen, 2009; Woldeamlak et al., 2007).

1.2. Effect of climate on groundwater recharge: process understanding

1.2.1. Sensitivity to climate parameters

McCallum et al. (2010) designed a numerical experiment to determine the sensitivity of recharge to climate parameters in three locations across Australia characterised by different climate types. They found that rainfall was the most important climate parameter influencing recharge and that rainfall intensity and temperature also caused significant changes in recharge. Furthermore, the change in recharge induced by changes in CO_2 concentration, solar radiation and vapour pressure deficit were relatively minor.

The direction of the change in recharge is generally the same as the change in rainfall (Allen et al., 2004; Serrat-Capdevila et al., 2007), but there are too many exceptions (Crosbie et al., 2010b; Doll, 2009; Rosenberg et al., 1999) to say that a change in rainfall is an adequate predictor of change in recharge.

The change in the frequency and seasonality of rainfall may also influence changes in recharge. Vivoni et al. (2009) demonstrated for a catchment in New Mexico that either an increase in the intensity of summer rainfall or an increase in the frequency of winter rainfall can lead to an increase in recharge. In semi-arid areas, higher intensity rainfall could lead to higher episodic recharge even under projections of decreased total rainfall (Crosbie et al., 2010a; Ng et al., 2010).

After rainfall, recharge is most sensitive to the climate parameter of temperature. In most studies this dependence of recharge on temperature was studied for cold climates which is associated with variation in snowfall, snowmelt and frozen ground under different temperature conditions (Eckhardt and Ulbrich, 2003; Jyrkama and Sykes, 2007; Okkonen et al., 2010; Vivoni et al., 2009). In addition, Rosenberg et al. (1999) found that recharge could even decrease with an increase in rainfall due to higher temperatures in the Ogallala Aquifer. In the Upper Nile Basin it was found that recharge increased as rainfall increased up to a 3°C temperature increase but for larger temperature increases evapotranspiration increases lead to reductions in recharge (Kingston and Taylor, 2010). Increased recharge was simulated in the Murray-Darling Basin despite a decrease in rainfall, which was attributed to a reduction in transpiration, i.e. the transpiration reduced due to the effect of temperature on vegetation when the optimum temperature for vegetation growth was exceeded (Crosbie et al., 2010b).

1.2.2. Sensitivity to vegetation

An increase in CO_2 affects plant growth and subsequently may affect groundwater recharge. Elevated CO_2 allows plants to increase their water-use efficiency, thereby assimilating more carbon per unit of water transpired. This can lead to an increase in leaf area, a reduction in transpiration or both. There are few models used to estimate recharge that can incorporate these effects. Eckhardt and Ulbrich (2003) used a modified version of SWAT that forced an increase in maximum leaf area and a reduction in maximum stomatal conductance to account for the physiological effects of elevated CO_2. The WAVES model has a carbon balance within the model and so is better equipped to simulate the effect of elevated CO_2. McCallum et al. (2010) used a slightly modified version of WAVES so that the elevated CO_2 is simulated in the same manner as Hatton et al. (1992), this allows the vegetation to grow within the model as a response to environmental conditions.

A very different approach to the investigation of vegetation effects on recharge was used by Ng et al. (2010). They used a probabilistic approach and selected the vegetation parameters,

such as leaf area index (LAI) and rooting depth amongst others, from a probability distribution conditioned on historical climate modelling and field observations. The Monte Carlo analysis assumed that soils, vegetation and climate are independent of each other, in this way the future vegetation has the same distribution as the historical vegetation and cannot respond to changes in climate.

1.2.3. Sensitivity to land use change

As the effect of vegetation on groundwater recharge is significant, it is likely that if land use were to change significantly because of climate change, the indirect effect of climate change on recharge may be greater than changes in rainfall or temperature themselves. Crosbie et al. (2010b) highlighted that the difference in recharge between annuals, perennials and trees is greater than the projected changes in recharge due to climate change in the Murray-Darling Basin. Austin et al. (2010) had a land use change scenario where the entire Murray-Darling Basin was reafforested, not surprisingly this unrealistic scenario produced much greater reductions in water yield than climate change alone. van Roosmalen et al. (2009) used a more plausible land use change scenario where areas of grassland were converted to forest, this had a very minor impact on recharge in an environment where rainfall is much greater than potential evapotranspiration.

1.3. Knowledge gaps

Recharge and runoff

During the Northern Australia Sustainable Yields Project (CSIRO, 2009), it was noticed that in the same region using the same input data the runoff modelling could predict an decrease in runoff while the recharge modelling could predict an increase in recharge. It has not been resolved as to whether this is a fundamental difference between recharge and runoff or whether the different models used for runoff and recharge estimation respond differently to changes in climate. In this case the scale of the modelling was the same between the recharge and runoff.

Model choice

Previous comparisons of different models have focused on their ability to simulate observed conditions (Scanlon et al., 2002). However, model structure has never been evaluated as a determinant in the projections of recharge under a future climate.

Downscaling

There have only been two studies that have compared the impact on recharge of different downscaling techniques (Holman et al., 2009; Mileham et al., 2009); however, the methods used in these studies are not commonly used in Australia.

All the recharge/groundwater studies that have used statistical downscaling techniques have used precipitation from GCMs or RCMs, either to modify observed time series (change factors, constant scaling or pattern scaling), or to modify the parameters of a weather generator, or used bias corrected RCM rainfall. Thus they rely on the relative changes in regional rainfall simulated by climate models, despite the acknowledged poor performance of climate models in reproducing observed rainfall characteristics. Only a few recharge/ groundwater studies have applied statistical downscaling techniques using atmospheric predictors (Fowler et al., 2007; Maraun et al., 2010). Thus there has not been any comparison of recharge/groundwater response to projections obtained from change factor,

statistical downscaling using atmospheric predictors, and dynamical downscaling approaches.

Additionally, there has not been a study of the influence of climate type on recharge anywhere in world.

2. METHODS

This chapter outlines the detailed methodology used for climate type mapping under historical and projected climates, the investigation of specifics of diffuse groundwater recharge within selected climate types, and the investigation of the effect of GCM downscaling methods and selection of groundwater models on modelled groundwater recharge.

2.1. Estimation of climate type transitions

The climate classification method used in this project was the Köppen-Geiger method as described in Peel et al. (2007), which is largely based on monthly summaries of precipitation and temperature. This information was available from the Australian Bureau of Meteorology (BOM), which produces Australia-wide historical and current monthly climate grids for rainfall, minimum temperature and maximum temperature (Jones et al., 2009). Convenient access to these climate grids made it possible to generate Australia-wide Köppen-Geiger climate type maps for any period between 1900 and 2009.

2.1.1. Generating Australia-wide Köppen-Geiger climate type maps

The time series of national-scale climate grids maintained by BOM were used to produce monthly climate summaries of precipitation and temperature for selected periods, resulting in national summary grids of precipitation and temperature for each calendar month and pertaining to the selected period. For example, if the selected period was 1970 to 2009, all relevant national-scale climate grids within that period would be used to calculate a national-scale climate grid for, say total January precipitation, and so on. These climate summary grids were then used to produce:

- mean annual precipitation (MAP)
- mean annual temperature (MAT)
- temperature of the hottest month (T_{hot})
- temperature of the coldest month (T_{cold})
- number of months with a temperature greater than 10 (T_{mon10})
- precipitation of the driest month (P_{dry})
- precipitation of the wettest month in summer (P_{swet})
- precipitation of the driest month in summer (P_{sdry})
- precipitation of the wettest month in winter (P_{wwet})
- precipitation of the driest month in winter (P_{wdry})
- fraction of mean annual precipitation that falls in summer[1] (F_{smap})
- precipitation threshold (P_{thres}).

Table 2-1 illustrates how precipitation threshold was defined. Köppen-Geiger climate type maps were subsequently produced using the approach illustrated in

[1] Summer is defined as the hotter period out of October to March and April to September.

Table 2-2. The Köppen-Geiger climate types were mapped for a series of historical periods and projected climate scenarios for 2030 and 2050.

Table 2-1. Criteria for determining the precipitation threshold (P_{thres}) from mean annual temperature (MAT), conditional on the fraction of mean annual precipitation that falls in summer (F_{smap})

Criteria	**P_{thres}**
F_{smap} < 0.3	2 × MAT
F_{smap} >= 0.7	(2 × MAT) + 28
Other	(2 × MAT) + 14

Table 2-2. Köppen-Geiger climate type descriptions and classification criteria

1st Type	**2nd Type**	**3rd Type**	**Description**	**Criteria**
A			Tropical	not B and T_{cold} >= 18
	Af		Rainforest	P_{dry} >= 60
	Am		Monsoon	P_{dry} >= (100 - (MAP / 25))
	Aw		Savannah	P_{dry} < (100 - (MAP / 25))
B			Arid	MAP < (10 × P_{thres})
	BW		Desert	MAP < (5 × P_{thres})
	BS		Steppe	MAP >= (5 × P_{thres})
		B-h	*Hot*	*MAT >= 18*
		B-k	*Cold*	*MAT < 18*
C			Temperate	T_{hot} > 10 and T_{cold} > 0 and T_{cold} < 18
	Cs		Dry Summer	P_{sdry} < 40 and P_{sdry} < (P_{wwet} / 3)
	Cw		Dry Winter	P_{wdry} < (P_{swet} / 10)
	Cf		Without dry season	not Cs or Cw
		C-a	*Hot summer*	T_{hot} >= *22*
		C-b	*Warm summer*	T_{mon10} >= *4*
		C-c	*Cold summer*	T_{mon10} >= *1 and* T_{mon10} < *4*
D			Cold	T_{hot} > 10 and T_{cold} <= 0
	Ds		Dry Summer	P_{sdry} < 40 and P_{sdry} < (P_{wwet} / 3)
	Dw		Dry Winter	P_{wdry} < (P_{swet} / 10)
	Df		Without dry season	not Ds or Dw
		D-a	*Hot summer*	T_{hot} >= *22*
		D-b	*Warm summer*	T_{mon10} >= *4*
		D-c	*Cold summer*	*not a, b, or d*
		D-d	*Very cold winter*	T_{cold} < *-38*
E			Polar	T_{hot} < 10
	ET		Tundra	T_{hot} > 0
	EF		Frost	T_{hot} <= 0

Note: The criteria were generally assessed in the order presented in the table, with the following exceptions – where there is a 'not' condition (e.g. A and D-c) and for C and D, F_{smap} was used to discriminate in cases that fit the criteria of both Dry Summer and Dry Winter

2.1.2. Historical Köppen-Geiger climate type maps

Historical Australian Köppen-Geiger climate type maps were produced for the periods 1930–2009 and 1970–2009. The 1930–2009 period provided a longer-term view on climate types within Australia, while the 1970–2009 period is considered to be the baseline for current climate. In addition, a historical change series of climate type maps were produced for the periods: 1939–1969, 1949–1979, 1959–1989, 1969–1999, and 1979–2009. This 30-year moving average series was used to assess historical transitions in climate type.

2.1.3. Projected Köppen-Geiger climate type maps

Projected Australian Köppen-Geiger climate type maps were generated to represent plausible low, medium and high global warming scenarios for 2030 and 2050. Based on the range of IPCC Fourth Assessment Review (AR4) projections (IPCC, 2007), low, medium and high global warming scenarios for 2030 were 0.7, 1.0 and 1.3 ºC and for 2050 were 1.0, 1.7 and 2.4 ºC, respectively.

The changes in rainfall and temperature per degree of global warming were calculated on a monthly basis for 17 available GCMs relative to the GCM's 1975–2005 baseline climate. A detailed description of this pattern scaling methodology can be found in Chiew et al. (2008). These GCM grid-scale changes were applied to the BOM national grid current baseline (1970–2009) rainfall and temperature climate summaries. This scaled data was then used to produce projected Köppen-Geiger climate type maps. For each projection (2030 or 2050) and global warming scenario (low, medium or high) 17 projected Köppen-Geiger climate type maps (one per GCM) were compared for consistency in climate type projection, and whether the projection represented a change from baseline climate type.

Two sources of uncertainty are accounted for using this methodology. Firstly, global warming uncertainty associated with greenhouse gas emission projections and global climate sensitivity is accounted for by the use of three levels of global warming. Secondly, the uncertainty in GCM projections of rainfall and temperature changes over Australia is accounted for by using 17 GCMs.

2.1.4. Summarising the projected climate type maps

A single climate projection, characterised by a global warming scenario (low, medium, or high), and a year (2030 or 2050), realised 17 climate types maps (one per GCM). The following approach was used to summarise the 17 realisations into a single climate type map for the scenario, while maintaining some information about the level of agreement between the 17 results. The 17 projected climate type maps were treated with equal weight, and were summarised to a single climate type map by identifying (logically, for each grid cell) the:

- most common (mode) projected climate type
- frequency of the mode projected climate type
- commonality of the current baseline climate type with the mode projected climate type
- climate type variety, as a measure of consistency (essentially this is the number of different climate types projected by the 17 CGMs for a single global warming scenario).

This summary indicates where, for a given scenario, the projected Köppen-Geiger climate type maps were consistent, the most common climate type, and where the most common climate type was different from the baseline climate type.

2.1.5. Assessing climate type transition

At this stage of analysis there were three series of climate type maps:

- historical climate types, based on 30-year moving averages of historical climate data
- 2030 projected climate types, including baseline climate type and mode projected climate type for global warming scenarios: low, medium and high warming of 0.7, 1.0, 1.3 ºC, respectively
- 2050 projected climate types, including baseline climate type and mode projected climate type for global warming scenarios: low, medium and high warming of 1.3, 1.7, and 2.4 ºC, respectively.

Climate type transitions were assessed for each of these series. The frequency of each climate type was determined for each map in a series, and these frequencies were converted to a percentage. A linear regression model was then used to quantify trends in climate type frequencies for the series. In addition, a transition matrix was constructed from the climate type maps in the series, to identify the dominant transitions between climate types.

2.2. Climate parameters and diffuse groundwater recharge

The methodology of the investigation on the effect of climate characteristics and their combination within individual climate types on diffuse recharge was based on statistical analysis of the climate data and corresponding modelled recharge data for the selected climate types.

2.2.1. Groundwater recharge data

The diffuse groundwater recharge was previously estimated during the course of the Northern Australia Sustainable Yields Project (NASY) and recharge assessment for the Murray-Darling Basin Authority reported earlier within the scope of this project. The recharge estimation methodology and modelling results for each region are given in Crosbie et al. (2009) and Crosbie et al. (2010b), respectively. The WAVES model (Dawes et al., 2004; Zhang et al., 1996) was used in both cases to simulate deep drainage, below 4 m of the soil profile, which hereafter is referred as recharge.

In the NASY and Murray-Darling Basin (MDB) work, the recharge modelling was undertaken for a number of soil types in the regions and three vegetation types, but under various growth conditions. For northern Australia, summer-growing vegetation was assumed, while in the MDB winter-growing vegetation was modelled. These were chosen as the most likely grazing cover as the main growing period for grasses will be in the wetter season. However, due to differences in soil types, rainfall frequency and intensity, and physiological activity this does not mean that the same annual recharge will be modelled for the same annual rainfall in both areas.

The soil profile was modelled as a two-layer system, with 0.5 m topsoil and 3.5 m subsoil. Hydraulic characteristics of soils were derived from Johnston et al. (2003) with topsoil typically being more permeable than subsoil. Between the two regions, soils of a similar type were more permeable in northern Australia. As a result the direct comparison between recharge under similar soil types for two regions was undertaken with caution. It was observed that the modelled recharge in both regions showed a similar trend in relationship between soil permeability and recharge. As illustrated in Figure 2-1, the range of the

estimated recharge is the greatest for soils with hydraulic conductivity less than 1 m/day, expressed as a geometric mean of the topsoil and subsoil hydraulic conductivity values. For all considered scenarios of soil and vegetation, the estimated recharge was not significantly different for soil with K > 1.5 m/day. For this reason some reported results were presented only for three soil types with low, medium and high hydraulic conductivity, approximately defined as 0.01, 0.1 and 1.0 m/day, respectively.

It is important to note that the modelled recharge was not validated with field data. Therefore the modelled deep drainage estimates are only considered as an approximation of the recharge; comparisons between climate types are also only reported in relative terms.

The available data falls into five climate types and only those types were considered in the analysis (see Figure 4-2 in Chapter 4).

The analyses included:

- frequency of exceedance of the annual recharge in various climate types
- relative importance of rainfall, temperature, solar radiation and vapour pressure deficit for various climate types
- correlation between recharge and rainfall parameters other than total annual rainfall
- sensitivity of recharge to rainfall.

2.2.2. Time-series data preparation

The daily time series was limited to the time period 1930 to 2006 to ensure that all of the available series were complete. The daily series were aggregated to an annual frequency, with the start date being dependent on summer rainfall. In areas that experienced summer-dominated rainfall, the aggregation period began in September; otherwise the aggregation period began in March. Rainfall and recharge (deep drainage) were aggregated by summation, while other climate variables were averaged (using the mean values). Additional methods for aggregating rainfall were also used, and these involved summation of rainfall events that were:

- above a threshold value (5 mm, 10 mm, 20 mm, 40 mm, 60 mm)
- within a range (0–20 mm, 20–40 mm, 40–60 mm)
- larger than the 95th or 99th percentile rainfall event.

A moving-average approach was also applied to account for the effect of a prolonged rainfall period on recharge. This involved calculating the moving average of the daily rainfall series applying a 7, 14, and 21 day window, and then aggregating the averaged rainfall values that were above a threshold of 2.5 mm/day or 5 mm/day (Table 2-3).

The Koppen-Geiger climate type was calculated for each series, using the daily rainfall and mean daily temperature (mean of the T_{min} and T_{max} series), aggregated to a monthly sum. That is, a mean monthly value for the whole period, not for each year.

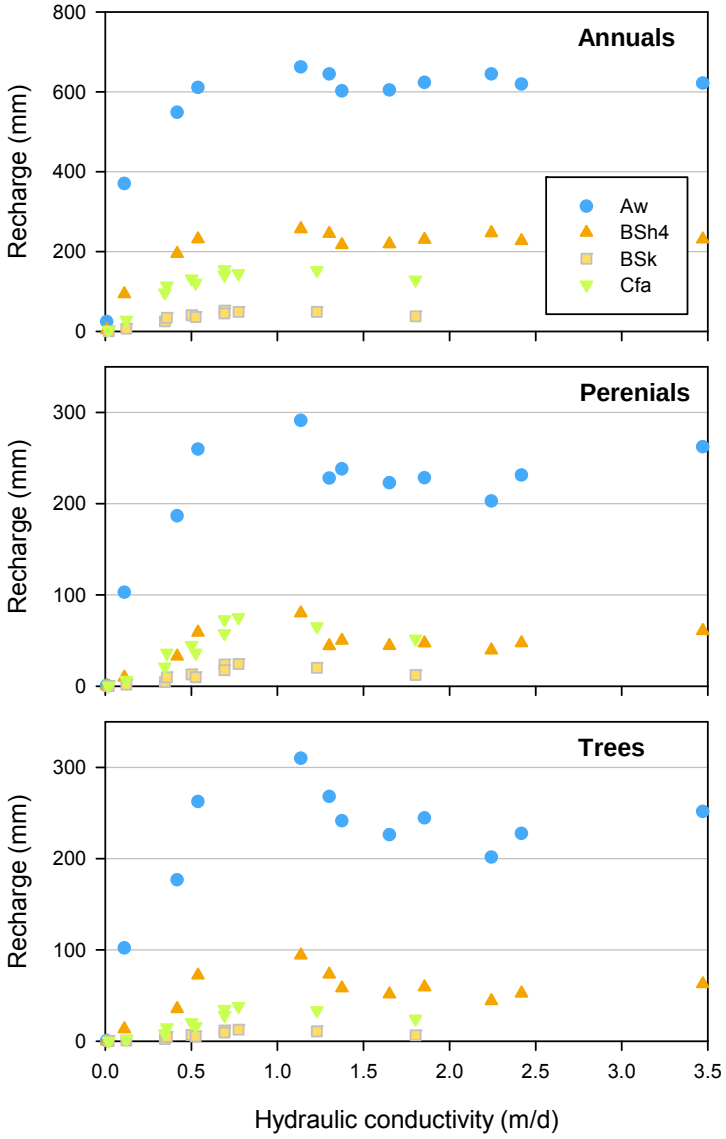

Figure 2-1. Relationship between modelled recharge and soil hydraulic conductivity (as geometric mean between hydraulic conductivity of topsoil and subsoil): see Table 2-2 for climate types acronyms

Table 2-3. The minimum daily rainfall event fully accounted in moving-average analysis over the set of considered periods and daily thresholds

Moving average period and threshold (mm/day)		**Daily rain as a single event over the defined period (mm)**
7 days	2.5	17.5
	5.0	35
14 days	2.5	35
	5.0	70
21 days	2.5	52.5
	5.0	105

2.2.3. Time-series data analysis

A variety of approaches were utilised to assess the sensitivity of recharge to variability in climate. The data were subset in several ways by:

- maintaining individual model runs, or
- grouping model runs with the same soil and vegetation type, or
- grouping model runs with the same climate, soil and vegetation type.

In all cases the annual aggregates of the variables were used. Two measures were used to quantify the independent effect of climate variables on recharge; these were Pearson's Product Moment Correlation Coefficient, and the slope of the linear regression between the climate variable and recharge. Relative importance measures (Groemping, 2006) were then used to assess the contribution of climate variables to explain variance in recharge (within the context of a multiple regression model). The relative importance measure used in this case was the approach proposed by Lindeman et al. (1980), as recommended by Gromping (2006).

Frequency of exceedance of annual recharge was calculated for combinations of soil, vegetation, and climate type, using an empirical cumulative distribution function (ecdf), and plotting recharge (y-axis) against 1-ecdf (recharge) (x-axis).

2.3. Effect of climate data downscaling on diffuse groundwater recharge

Three (MDBSY, NASY and SWSY) of the four sustainable yields projects completed so far have used daily scaling to downscale the future climate projections from various GCMs. This method was chosen for pragmatic reasons as stochastic downscaling is currently not possible on a continental scale and the tight time frames of the projects prevented the use of dynamical downscaling. It has not yet been tested whether the choice of downscaling method affected the recharge modelling results in these projects.

All four sustainable yields projects used the WAVES model (Zhang and Dawes, 1998) for estimating recharge under the future climate projections. Three (MDBSY, NASY and TasSY) of the four used WAVES in its dynamic vegetation growth mode and the other (SWSY) used WAVES with a fixed LAI throughout the year. These models have not been compared to investigate if they differ under future climate conditions; they have also not been compared to other conceptually simpler models.

This part of the project compared the recharge estimated under projections of a future climate from five GCMs using three different downscaling methods, four different hydrological models and at three contrasting field sites.

2.3.1. Description of GCM downscaling methods and climate change projections

Three techniques (a scaling approach, a stochastic downscaling model, and a dynamical downscaling model) were compared that transfer information from the coarse spatial resolution of GCMs, typically 200 to 300 km grid lengths, to specific locations required for recharge modelling. The aim was to compare the technique that only modifies magnitudes (the scaling approach) with more sophisticated approaches that also account for changes in

frequencies and sequencing of wet days, and to determine and explain their impact on recharge.

GCM projections

For consistency the three downscaling techniques were applied using the same baseline period (observed data) of 1981–2000 and a projection period of 2046–2065. This was pre-determined by the availability of daily data from the IPCC AR4 [IPCC, 2007 #18] GCMs, which only archive daily projections for 2046–2065 and 2081–2100. For AR4 runs for the historical period, they archive daily data for 1961–2000, and so to use the same period length as the future projection the last 20 years (1981–2000) were selected. The future projection emissions scenario used was the A2 scenario, which projects the greatest temperature increase of those for which daily data is archived. An emissions scenario is a plausible representation of the future development of emissions of substances that are potentially radiatively active (e.g. greenhouse gases, aerosols), based on a coherent and internally consistent set of assumptions about driving forces (such as demographic and socioeconomic development, technological change) and their key relationships.

Daily data is required by both the daily scaling and stochastic downscaling techniques. We used the available data from five of the AR4 GCMs: the CSIRO Mk3.5, GFDL 2.0, GFDL 2.1, MIROC 3.2 midres, and MPI-ECHAM5. These five GCMs were selected on the basis that they are used with the CSIRO dynamical downscaling model (see below).

It is important to emphasis the crucial differences between 'projections', as used in this project, and 'predictions' as used, for example, in weather forecasting. Climate projections are defined by the IPCC:

> *A projection of the response of the climate system to emission or concentration scenarios of greenhouse gases and aerosols, or radiative forcing scenarios, is often based on simulations by climate models. Climate projections are distinguished from climate predictions in order to emphasise that climate projections depend upon the emission/concentration/radiative forcing scenario used, which are based on assumptions concerning, for example, future socioeconomic and technological developments that may or may not be realised and are therefore subject to substantial uncertainty.* [IPCC, 2007 #18]

Thus climate projections are not simulations that attempt to estimate the actual evolution of the climate in the future in terms of seasonal, interannual or interdecadal time scales. Therefore the downscaled scenarios presented here represent possible future climates, conditional on the assumptions inherent in the emissions scenario and climate models used, in order to assess possible potential impacts of climate change on recharge.

Daily scaling

The scaling approach used is termed 'daily scaling'. Typical scaling approaches calculate seasonal or monthly 'change factors' based on differences between current and future climate GCM simulations and then scale/adjust the daily observed records. This produces a projected daily series of the same length and sequencing as the observed, but with the magnitudes of the climate variables changed. Such seasonal scaling is applied to temperature, relative humidity and solar radiation variables used to calculate potential evapotranspiration. For rainfall an extension of this methodology, 'daily scaling', is used that in addition to the seasonal-scale changes also accounts for varying changes for different rainfall amounts. The GCM-projected changes for higher percentile, i.e. more extreme, daily rainfalls often increase more than lower percentile daily rainfall amounts, and this approach accounts for these changes (Chiew et al., 2008; Mpelasoka and Chiew, 2009).

The seasonal (non-precipitation variables) and daily (precipitation) scaling is applied on a seasonal basis (summer – Dec/Jan/Feb; autumn – Mar/Apr/May; winter – Jun/Jul/Aug; and spring – Sep/Oct/Nov). The scaling factors were calculated using the 1981–2000 and 2046–2065 precipitation (daily) and temperature, solar radiation and relative humidity (monthly) variables from the five GCMs.

Stochastic downscaling

The Nonhomogeneous Hidden Markov Model (NHMM) is a stochastic (i.e. able to generate multiple realisations Monte Carlo style) downscaling model, that relates synoptic-scale, atmospheric circulation variables ('predictors') to multisite daily precipitation via a finite number of unobserved ('hidden') weather states. A given day's precipitation is conditioned on the weather state for that day and the daily weather state sequence is a first-order Markov process. The process is nonhomogeneous as the weather state transition probabilities depend on the atmospheric predictors and hence vary from day to day (Charles et al., 1999; Hughes et al., 1999). The latest NHMM version was used here (Kirshner, 2005). The NHMM has been used extensively for hydrological investigations into climate change impacts on surface water across several regions of Australia including Western Australia (Berti et al., 2004; Charles et al., 2007; Kitsios et al., 2006), South Australia (Charles et al., 2008) and the MDB (Chiew et al., 2010). In all these cases out-of-sample validation of NHMMs, calibrated to station networks that included the three stations used in this project, successfully reproduced validation period daily to interdecadal station precipitation variability, notably often including periods with rainfall characteristics outside the range of the calibration data, e.g. wetter or drier periods than seen in calibration. In this study, 100 stochastic daily rainfall sequences were generated for each input atmospheric predictor series. The algorithms used by the NHMM to stochastically generate daily precipitation series are described in Appendix 2 of [Hughes, 1994 #199].

NHMM model selection involved an iterative calibration and testing process to determine the optimum number of weather states and sets of atmospheric predictors. The aim was to select a parsimonious model that describes the calibration data, with out-of-sample validation used to confirm adequate reproduction of the full range of rainfall variability observed in the available historical record. Models were calibrated separately for winter and summer half-years, to account for different rainfall generation processes and hence atmospheric predictors. For calibration, we used daily atmospheric predictors extracted from the NCEP/NCAR Reanalysis available on a 2.5º by 2.5º grid (Kalnay et al., 1996).

Dynamical downscaling

Dynamical downscaling has been undertaken across Australia at a 60 km grid resolution using CSIRO's Cubic Conformal Atmospheric Model (CCAM) (McGregor, 2005). Monthly data from the five IPCC AR4 GCMs mentioned above for SRES A2 was used to force CCAM, producing 6-hourly output for 1961 to 2100. The required climate variables were extracted over the three locations of interest for the two twenty-year periods.

Given biases in CCAM precipitation, when compared to observed station rainfall of the three stations, it was decided that direct use of CCAM climate variables in recharge modelling would not be consistent with the other downscaling approaches. In order to produce a set of consistent input series the CCAM variables were used to determine seasonal scaling factors and daily scaling factors as described using GCM data above. This is a simple approach to bias correcting dynamical downscaling output (van Roosmalen et al., 2009) but unfortunately reduces the information utilised from the CCAM runs as only magnitudes are changed in the observed record and not frequencies or sequencing of events. More sophisticated quantile matching approaches have been used in the literature (Goderniaux et al., 2009), but were

not possible to implement given the limited resources and tight delivery time frames of this project.

2.3.2. Description of models adopted for groundwater recharge estimation

A number of groundwater recharge models were compared to investigate differences in recharge estimation under a future climate, which was projected using a number of GCM models and three downscaling techniques described in the previous section. The following section gives a brief outline and key reference for each of the models used in the evaluation phase.

WAVES model

The WAVES model was developed by CSIRO Land and Water as a stand-alone vertical model that could be integrated into other larger projects. The following description is taken from the WAVES 3.5 User Manual (Dawes et al., 1998).

"WAVES is designed to simulate energy, water, carbon, and solute balances of a one-dimensional soil-canopy-atmosphere system (Dawes and Short, 1993; Zhang et al., 1996) on a daily time step. It is a process-based model and it integrates soil, canopy and atmosphere with a consistent level of process detail. WAVES predicts the dynamic interactions and feedbacks between the processes. Thus, the model is well suited to investigations of hydrological and ecological responses to changes in land management and climatic variation.

The model is based on five balances (Figure 2-2):

1. Energy Balance: partitions available energy into canopy and soil for plant growth and evapotranspiration (Beer's law);
2. Water Balance: handles infiltration, runoff, evapotranspiration (Penman-Monteith equation), soil moisture redistribution (Richards equation), lateral flow, drainage, and watertable interactions;
3. Carbon Balance: calculates carbon assimilation using integrated rate method and dynamically allocates carbon to leaves, stems, and roots, and to estimate canopy resistance for plant transpiration;
4. Solute Balance: estimates conservative solute transport within the soil column and the impact of salinity on plants (osmotic effect only);
5. Balance of complexity, usefulness, and accuracy.

WAVES emphasises the physical aspects of soil water fluxes and the physiological control of water loss through transpiration. It can be used to simulate the hydrological and ecological effects of scenario vegetation management options (e.g. for recharge control), or the water balance implications of changed climatic conditions. The model strikes a good balance between generality, realism and accuracy, and provides a powerful tool for water balance studies.

Soil moisture in WAVES is handled with the non-linear Richards Equation, which assumes a continuity of soil moisture potential through the profile, and controls the vertical and horizontal movement of water. Both the flux of water and content of water through the entire soil profile are solved simultaneously, using relationships between unsaturated soil water potential, moisture content and hydraulic conductivity."

Two versions of WAVES were compared in this project: a dynamic vegetation growth mode (WAVES-G) and a constant annual pattern of LAI (WAVES-C).

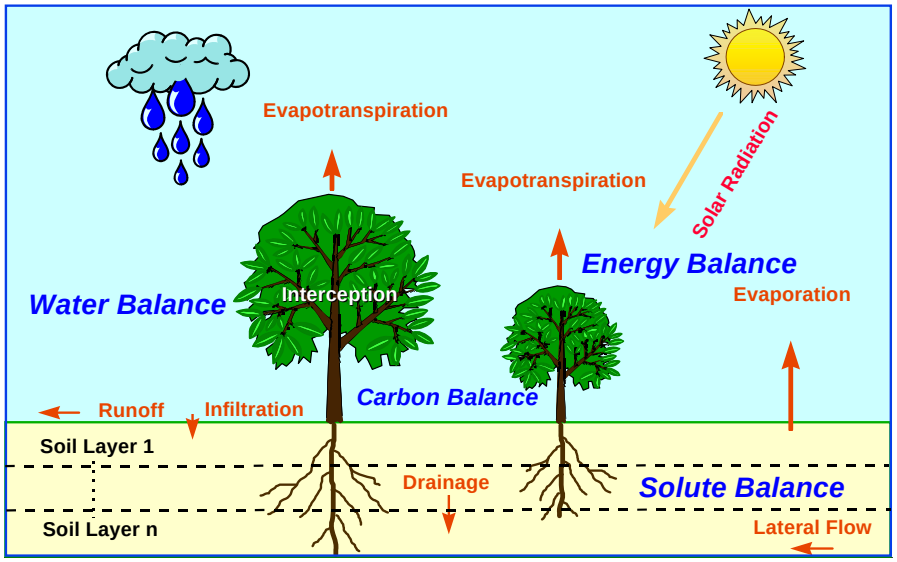

Figure 2-2. Conceptual diagram of the WAVES model.

HELP Model

The computer program HELP was developed by the US Environmental Protection Agency (Schroeder et al., 1994) and the acronym for 'hydrologic evaluation of landfill performance' is illustrative of the focus and intent of the product. The following is taken from the abstract of the user manual, and describes the model in general:

"The Hydrologic Evaluation of Landfill Performance (HELP) computer program is a quasi-two-dimensional hydrologic model of water movement across, into, through and out of landfills. The model accepts weather, soil and design data and uses solution techniques that account for surface storage, snowmelt, runoff, infiltration, vegetative growth, evapotranspiration, soil moisture storage, lateral subsurface drainage, leachate recirculation, unsaturated vertical drainage, and leakage through soil, geomembrane or composite liners. Landfill systems including combinations of vegetation, cover soils, waste cells, lateral drain layers, barrier soils, and synthetic geomembrane liners may be modelled. The program was developed to conduct water balance analyses of landfills, cover systems, and solid waste disposal facilities. As such, the model facilitates rapid estimation of the amounts of runoff, evapotranspiration, drainage, leachate collection, and liner leakage that may be expected to result from the operation of a wide variety of landfill designs. The primary purpose of the model is to assist in the comparison of design alternatives as judged by their water balances."

HELP is a tipping bucket model, that is moisture accumulates in a conceptual layer until the field capacity of the soil is exceeded then an amount of water dependent on conductivity is allowed to leak vertically downward to the next lowest layer (Figure 2-3). This process occurs with the addition of rainfall at the surface in a cascading manner downward through the soil profile.

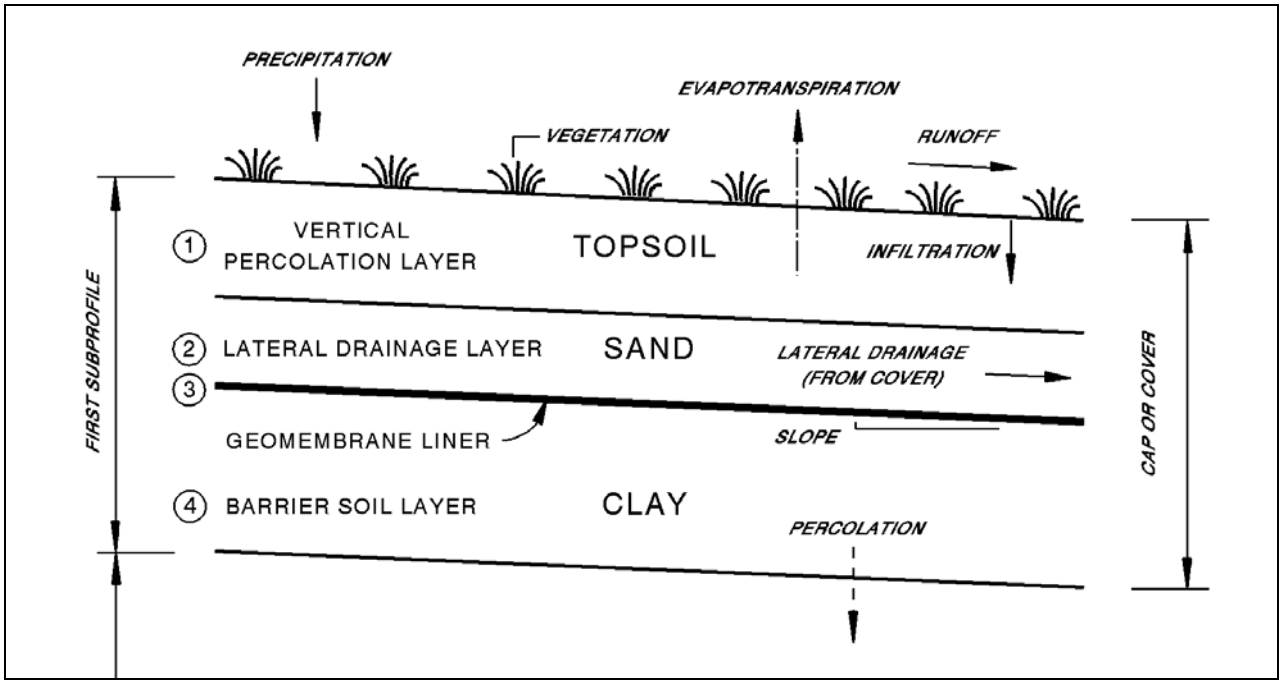

Figure 2-3. Conceptual model of HELP.

SIMHYD Model

SIMHYD is a lumped rainfall-runoff model with seven parameters (Chiew et al., 2002). It simulates runoff using input rainfall and areal potential evapotranspiration on a daily time step. Streamflow generated with this model has three flow components: surface runoff, interflow and baseflow. The SIMHYD structure and its algorithms describing flux movement into and out of the storages are shown inFigure 2-4. There are seven parameters in SIMHYD which can be optimised in calibration using shuffle complex evolution algorithms. Of the three research sites, only the Livingston Creek at Wagga Wagga has streamflow records. Although the record shows available flow data from 2002 to 2007, it is fragmented with missing periods of data throughout. A detailed check of the consistency of the rainfall and streamflow data showed that, for the most part, rainfall and flow data do not match each other except during the earlier record period. Accordingly, six months of flow data available for 2003 was used to calibrate the SIMHYD model.

The shuffle complex evolution optimisation technique (Duan, 1994) was used to optimise the model parameter using daily data. The objective function given by Nash-Sutcliffe efficiency (NSE) (Nash and Sutcliffe, 1970) of daily runoff was used. NSE is a common measure in water resource modelling and is calculated as:

$$NSE = 1 - \frac{\Sigma(Q_O - Q_A)^2}{\Sigma(Q_O - \bar{Q}_O)^2}$$

where Q_O is the observed flow, $\bar{Q}_O$ is the mean of the observed flow and Q_A is the flow simulated by the model. The NSE is an estimate of the variance in model error between simulated and observed data. Values can vary from $-\infty$ to 1, with 1 indicating a perfect fit and a value of zero indicating that the model is no better than assuming an average flow over the period. A negative NSE value implies a bad prediction which is hard to interpret, and is worse

than simply assuming a fixed average flow. An undue influence of high flows can be an issue with this indicator; however, the NSE is a reliable statistic for assessing the goodness of fit of hydrological models and is recommended for a variety of model types.

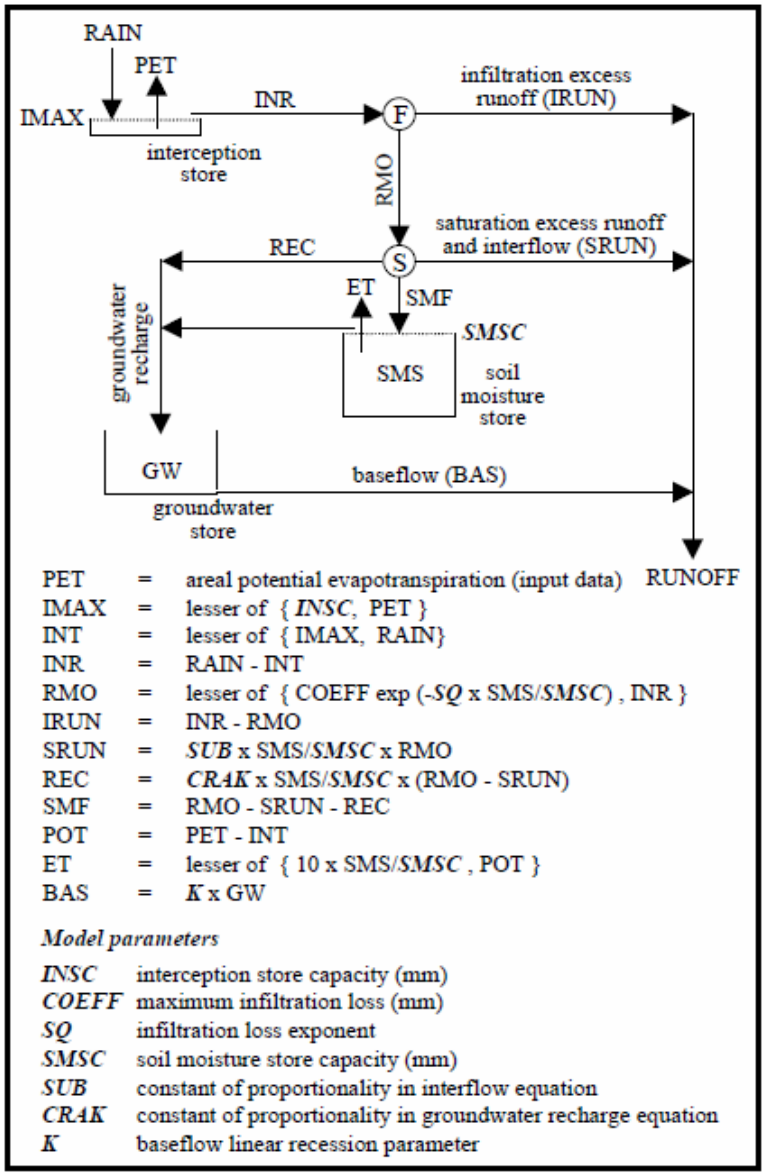

Figure 2-4. Conceptual model of SIMHYD

2.3.3. Selection and description of the sites used for calibration of the selected recharge models

Three sites were chosen for their contrasting hydrological regimes (Figure 2-5). The Wanneroo site is on the Swan coastal plain in Western Australia and has high rainfall and high recharge (Sharma et al., 1991). The Moorook site is in the Riverland in South Australia and has low rainfall and low recharge (Cook et al., 2004). The Livingston Creek site is in the Murrumbidgee catchment in New South Wales and has medium rainfall and low recharge; it is the only one of the three sites to have any runoff (Summerell, 2004).

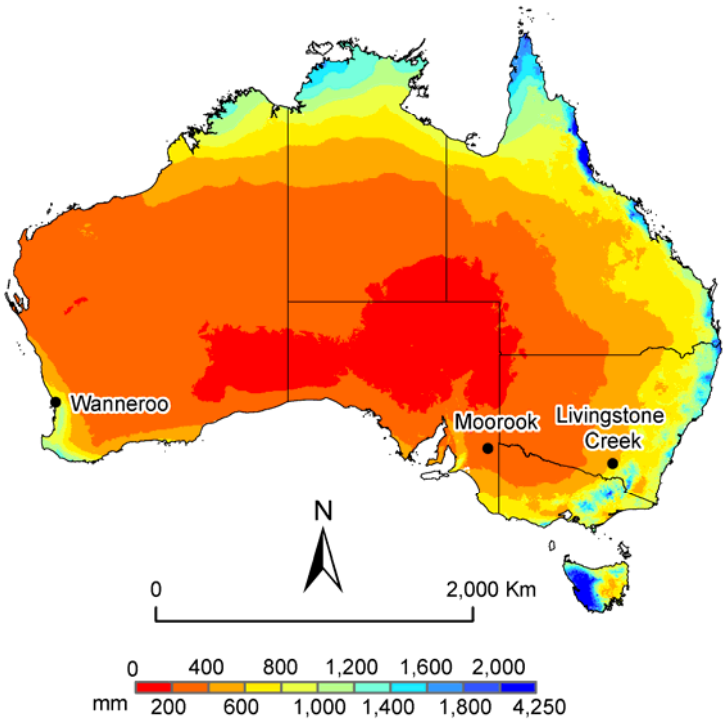

Figure 2-5. Location of three sites chosen for calibration of the recharge models

Wanneroo, Western Australia

The site description is summarised from Raper and Sharma (1989) and Sharma et al. (1991). The soil is described as a uniform coarse deep sand, locally known as Bassendean Sand. It consists of 85–95% coarse sand, 5–10% fine sand, and very small fractions of silt and clay. The bulk density is approximately 1.7 g/cm^3, with a saturated water content of 32%, residual water content of 2%, and field-measured hydraulic conductivity of 30 m/day. For modelling purposes the deep watertable site was used, with a watertable between 5 and 7 m, thus free drainage at 4 m was assumed.

The area has a Mediterranean climate with a dry, hot summer and mild, wet winter. Average annual rainfall is 750 mm and Class-A pan evaporation is approximately 1800 mm. Climate data was taken from the Wanneroo station #9105, using the SILO PPD data record.

Sharma et al. (1991) reported on a site with perennial tuft veldt grass of average quality, which was occasionally grazed, and had little other management. LAI pattern over the year was not reported, but maximum rooting depth was set to 1.5 m as determined from moisture content profiles.

Moorook, South Australia

The data for this site is extracted from a report by Cook et al. (2004). The soil profile is often described simply by fractions of sand and clay in the top 2 m, and annual recharge relationships derived from contents from 1 to 30%, while watertables are of variable depth ranging from 10 to 68 m. The site with highest estimated drainage rate was 6HC with only 4% clay in the top 2 m of soil, and the soil is described as sandy loam. From this general soil texture some indicative soil hydraulic parameters were derived. A deep uniform profile to 15 m was used with free gravity drainage at the base; the watertable at 6HC was 34 m.

Mallee vegetation is usually found in arid areas with mean annual rainfall ranging from 250 to 500 mm. Climate data was the Moorook station #24010 taken from SILO PPD, which has a very long rainfall record, back to the 1920s. The mean annual rainfall over the study period is 267 mm and Class-A pan evaporation is 1840 mm.

The vegetation is annual grasses and sparse native mallee scrub. For the annual grasses a winter-growing season was used with a peak LAI between 1 and 2, and a maximum rooting depth of 1 m. With tree cover the LAI was much lower, averaging around 0.25, and the maximum rooting depth was set to 10 m as determined from soil water potential measurements.

Livingstone Creek, New South Wales

The Livingston Creek site is described by Summerell (2004). The data for soil description is taken from Zhang et al. (1999) for a 161 ha cropping catchment named ‘Mona Vale’, near Wagga Wagga. The gentle side slope soil is described as a red podzolic, with a weakly developed A2 horizon over a red clay B horizon. Parameters for the various layers are taken from Zhang et al. (1999), and for modelling purposes the same lower boundary at 2 m was used.

Climate data was taken from the Wagga Wagga AMO station #72150, using the SILO PPD data record. The average annual rainfall is 570 mm, while Class-A pan evaporation is 1800 mm.

The vegetation was modelled only as perennial grass (some generic mixed pasture). Maximum rooting depth was 1 m, and peak LAI was between 1 and 2 but non zero at all times.

3. HISTORICAL AND PROJECTED CLIMATE TYPES IN AUSTRALIA

Climate is variable across Australia, as illustrated by climate parameters with wide ranges, including:

- annual rainfall, ranging from less than 200 mm to more than 4000 mm;
- seasonality of rainfall, with summer rainfall composing from less than 15% to more than 96% of annual rainfall;
- temperature, with mean annual temperatures ranging from less than 5 ºC to over 29 ºC.

Combinations of these factors define climate type, and the occurrence of climate type may vary depending on the climatic variability. Climate type variability has resulted in significant differences in native vegetation across the country and influenced the type of agricultural activities which have been adopted in different regions.

In this chapter the results of climate type mapping, based on the Köppen-Geiger approach, are discussed in terms of the climate type transitions over the period from 1930 to 2009 and potential changes to their frequency/occurrence under projected climates for 2030 and 2050. This analysis will facilitate the investigation of the effect of climate change on land use, and the assessment of climate type transitions for projected climate scenarios.

It is important to note that quantification of climate type transitions were based on the frequency/occurrence of climate types, i.e. the number of grid cells with a particular climate type within a climate type map, and not actual area. This distinction is important because the spatial data used in this analysis was in a geographic coordinate system (0.05 degree cell size), and each grid cell does not represent the same area.

3.1. Current baseline climate type

The climate classification scheme divides the climate into five main groups and several types and subtypes (see Table 2-2 in Chapter 2). The current Australian baseline Köppen-Geiger climate type map was estimated for the period 1979–2009 (Figure 3-1), and shows that 40.3% of the continent is characterised by an arid climate type with hot desert conditions (BWh). The next most frequent climate type is arid, steppe and hot (BSh) which occurs in 28.4% of the country. In total, the arid climate type accounts for 76.9% of Australia, while the temperate climate type constitutes 14.4% and the tropical climate type makes up 8.7%.

Under current climatic conditions, the main production of annual crop is associated with a few climate types (Figure 3-2):

- in the south-west: arid, steppe and hot and cold (BSh and BSk), temperate dry summer hot and warm (Csa and Csb), and temperate without dry season warm (Cfb)
- in the south-east: arid, steppe and cold (BSk), temperate dry summer hot and warm (Csa and Csb) and temperate without dry season hot and warm (Cfa and Cfb).

The majority of the country is covered by perennial vegetation. Native trees and bushland largely occur in more temperate climate types as well as in tropical climate types.

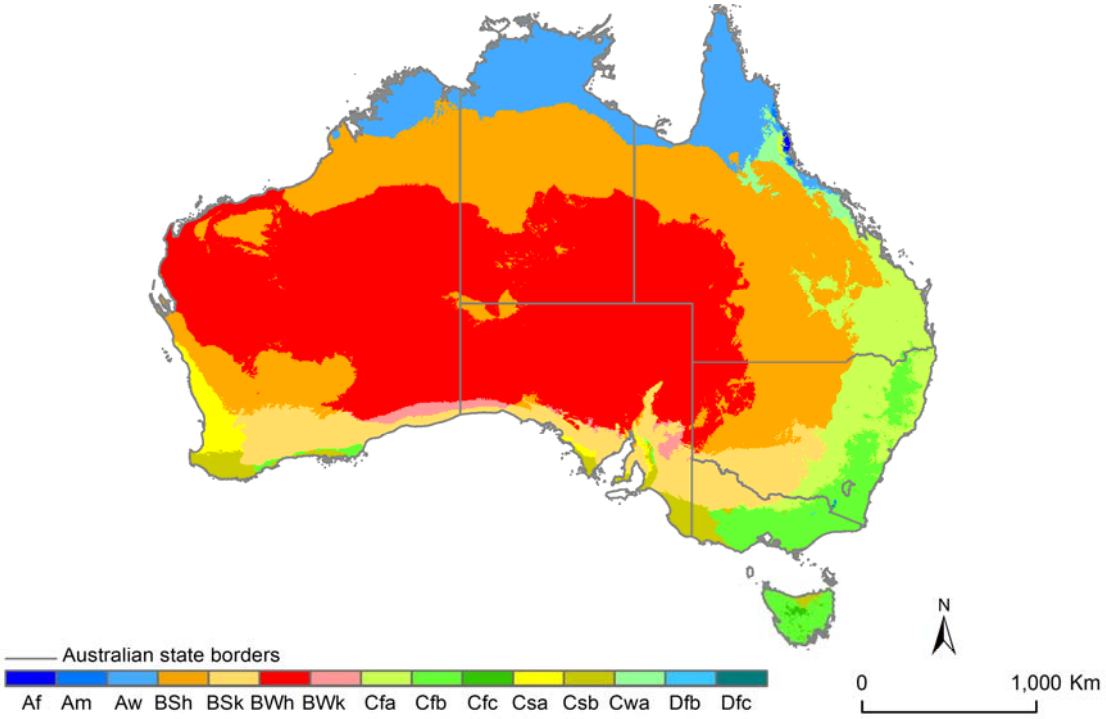

Figure 3-1. Current Australian baseline Köppen-Geiger climate type map (1970–2009)

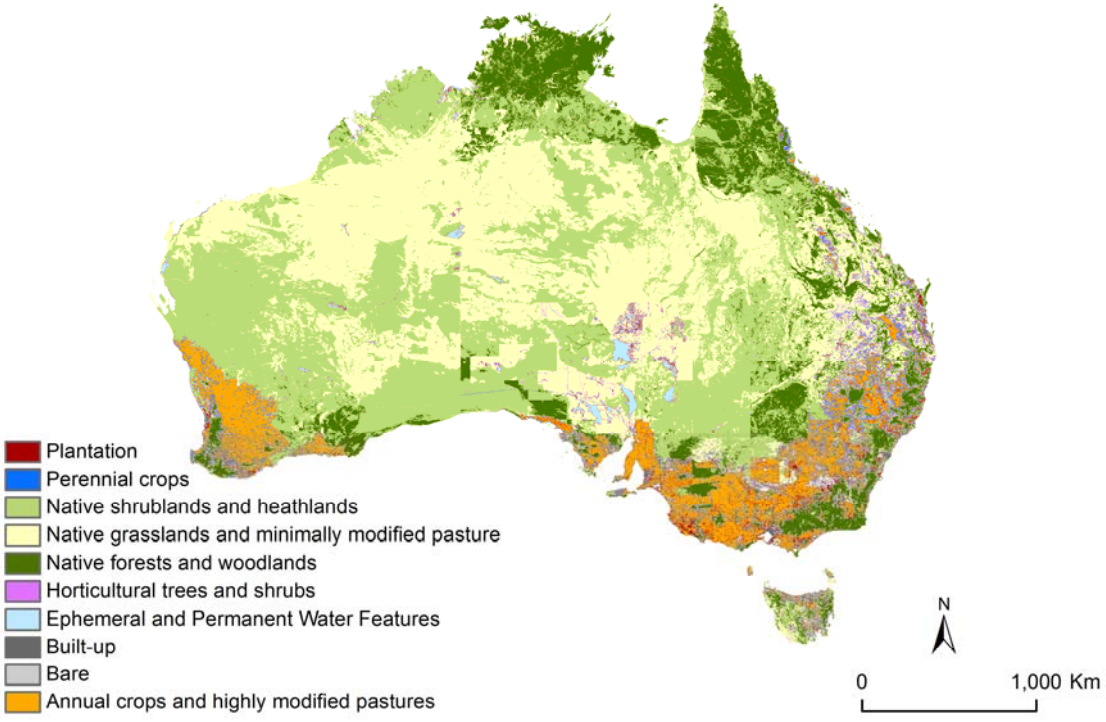

Figure 3-2. Land cover map for Australia (BRS, 2008)

3.2. Historical change in the extent of climate types

Köppen-Geiger climate type maps were derived for various historical periods to assess climate type transitions over the past 70 years. The historical series of Australian Köppen-Geiger climate type maps shows the pattern in climate type changes, estimated for 30-year intervals ending in 1969, 1979, 1989, 1999 and 2009 (Figure 3-3).

The series shows that 78% of Australia did not experience a shift in climate type during the 70 year period, while the remainder of the continent experienced some form of climate type transition. Within this sequence there was a 7.7% increase in BSh, and a 1.5% increase in Aw (Figure 3-4). These changes were offset by a 6.3% decline in BWh, 1.7% decline in BWk, and 0.7% decline in Cfb.

This overall indicates a transition from desert conditions to steppe conditions due to an increase in mean annual precipitation in central and northern Australia. In these regions the increased precipitation has caused a southward shift in the BSh climate type in central-northern Australia and an associated increase in the Aw climate type in the north.

The reduction in the occurrence of the Cfb climate type was attributed to drier summers in south-western Victoria, which resulted in the transition to the Csb climate type. A decline in the occurrence of the Csa climate type is noticeable in south-western Western Australia.

It must be noted that the number and location of climate stations in Australia has varied over the years (Jones et al., 2009) and this has an impact on the accuracy of the derived climate type maps. Generally speaking, more recent climate type maps should be more detailed and accurate due to a more complete set of climate observations. This complicates assessment of climate type change, because some apparent changes in climate type may be related to change in the monitoring network rather than changes in climatic conditions. One likely area of concern is north-western Australia, which contained minimal climate stations during the early part of the 20th century. While error propagation analysis may help to quantify impact, this has not been attempted at this stage.

The results of the analysis provide a historical reference for investigating the effect of projected climates on the occurrence of climate types in Australia.

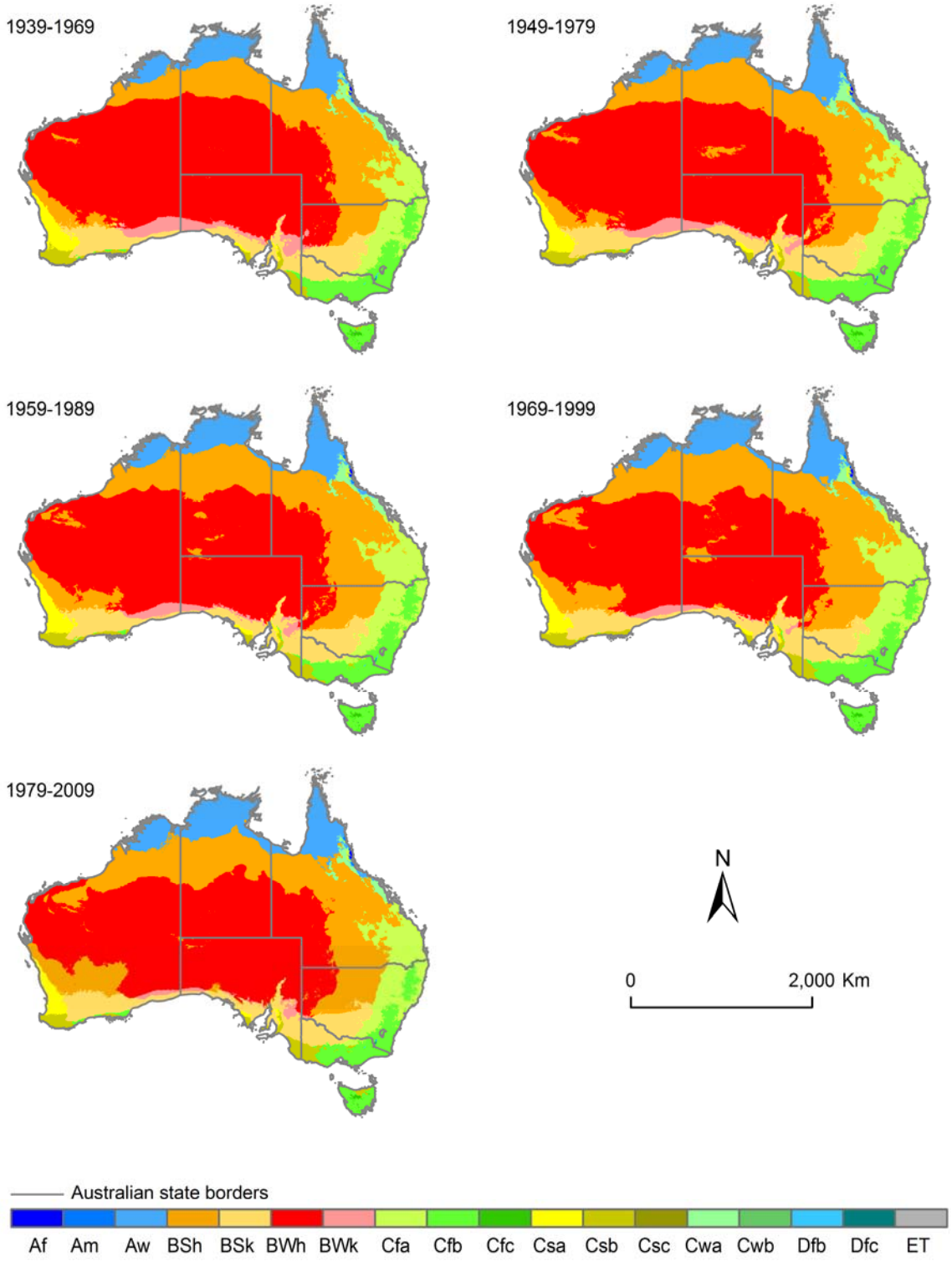

Figure 3-3. Historical series of Australian Köppen-Geiger climate type maps: 1939–1969, 1949–1979, 1959–1989, 1969–1999 and 1979–2009.

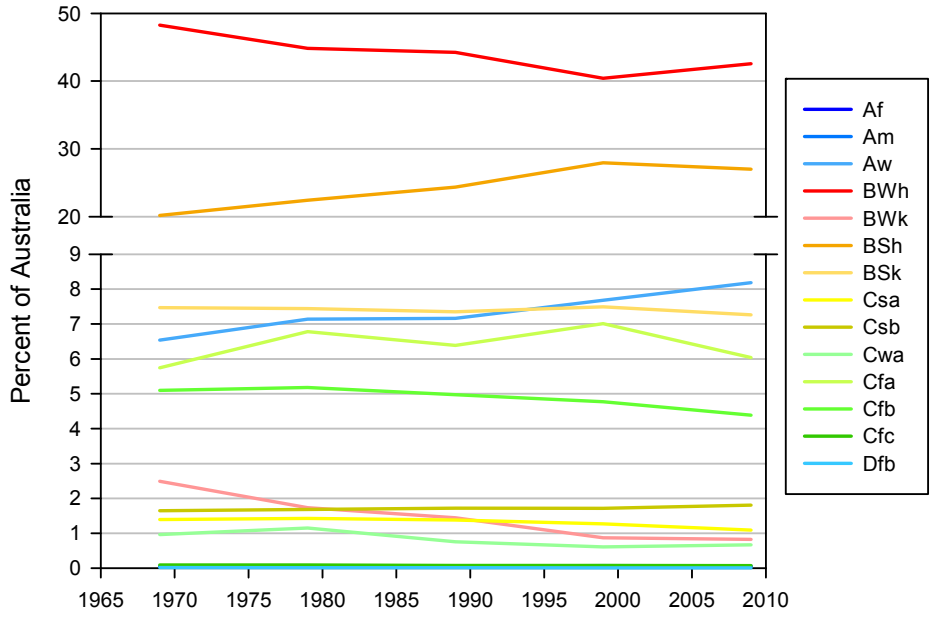

Figure 3-4. Percentage of Australia territory under different climate types

3.3. Projected changes for 2030

Projected 2030 Australian Köppen-Geiger climate type maps were produced for low, medium, and high global warming projections using the projected climate data generated by 17 GCM models. For each of the global warming projections, the 17 projected climate type maps were summarised to produce: a mode climate type map; a frequency map of the mode climate type; a comparison between the baseline climate type and the projected mode climate type; and a count of the number of climate types projected. These results are shown for the 2030 medium global warming projection in Figure 3-6.

Comparison of the mode projected climate types for the three global warming scenarios revealed a fairly linear trend for the impact of global warming on climate type in Australia. The mode climate types for 2030 projected climate type transitions from between 8.5% (low warming projections) and 14.7% (high warming projections) of the Australian continent. Analysis of the mode projected climate type maps for the three warming scenarios showed a 3.6% increase in BWh per degree of global warming (pdw), and a 1.9% (pdw) increase in BSh (Figure 3-5). These shifts were offset by decreases in BSk (3.3% pdw), Cfb (0.8% pdw), and Csb (0.5% pdw).

Analysis of the 2030 medium warming projections allowed comparison against baseline climate types and more detailed assessment of the consistency of the climate types projected for this scenario. Comparing the mode climate type from the 2030 medium global warming projections (Figure 3-6a) to the current baseline (Figure 3-1), showed a 4.6% increase in BWh and a 1.7% increase in BSh (Table 3-1). Conversely, there is a 3.4% decrease in BSk, a 0.8% decrease in Cfb, and a 0.7% decrease in BWk.

Figure 3-6b shows the level of agreement between the 2030 medium warming climate type projections, where the value indicates the number of models that projected the mode climate type with 17 as the highest possible agreement and 5 as the lowest observed agreement. The level of agreement between the climate type projections is lowest on the borders of the

climate types, and there is visibly less agreement in northern Australia than the rest of the continent.

Figure 3-6c indicates where the 2030 medium warming mode climate type projection was different from the baseline climate type, thereby projecting a climate type transition for 11.7% of the continent, with most of the climate transitions trending in the north-south direction.

The consistency of the 2030 medium warming climate type projections is illustrated in Figure 3-6d, where a value of 1 indicates unanimous agreement with the mode climate type projection (79%), a value of 2 indicates one climate type was projected by some GCMs that was not the same as the mode climate type (21%), and values greater that 2 indicate some disagreement between the climate type projections (<1%).

The increased occurrences of the arid climate types, both desert (BWh) and steppe (BSh), is due to a projected decrease in precipitation in central Australia, as well as a projected increase in temperature. The cold arid conditions are also likely to be replaced by hotter arid conditions, and there is a general reduction in occurrence of temperate conditions.

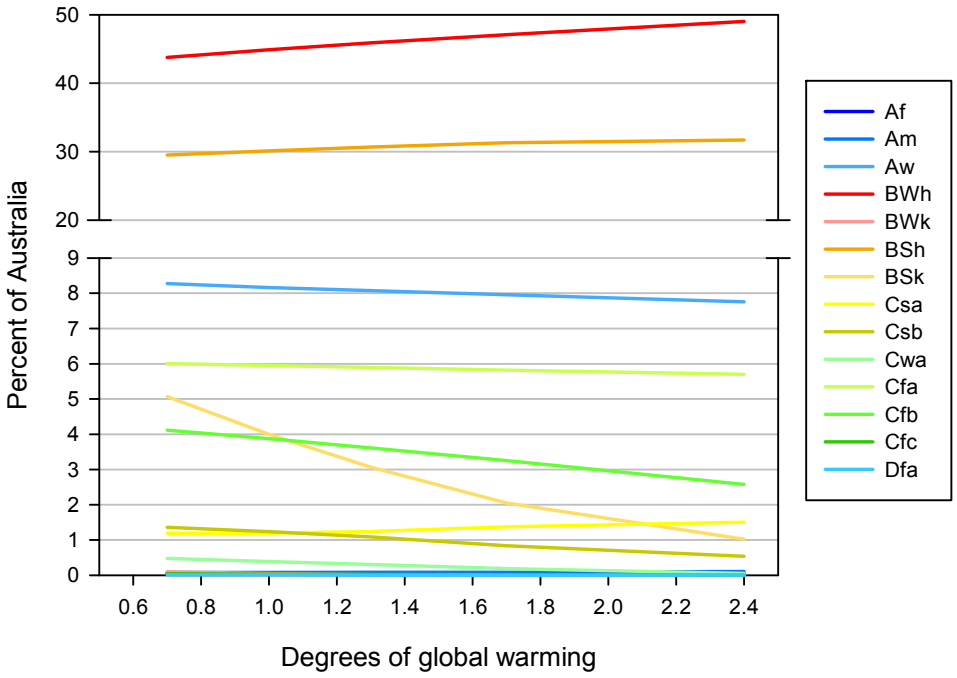

Figure 3-5. Percentage of Australia territory under different climate types, per degree of global warming (low, medium, and high projections for 2030 and 2050)

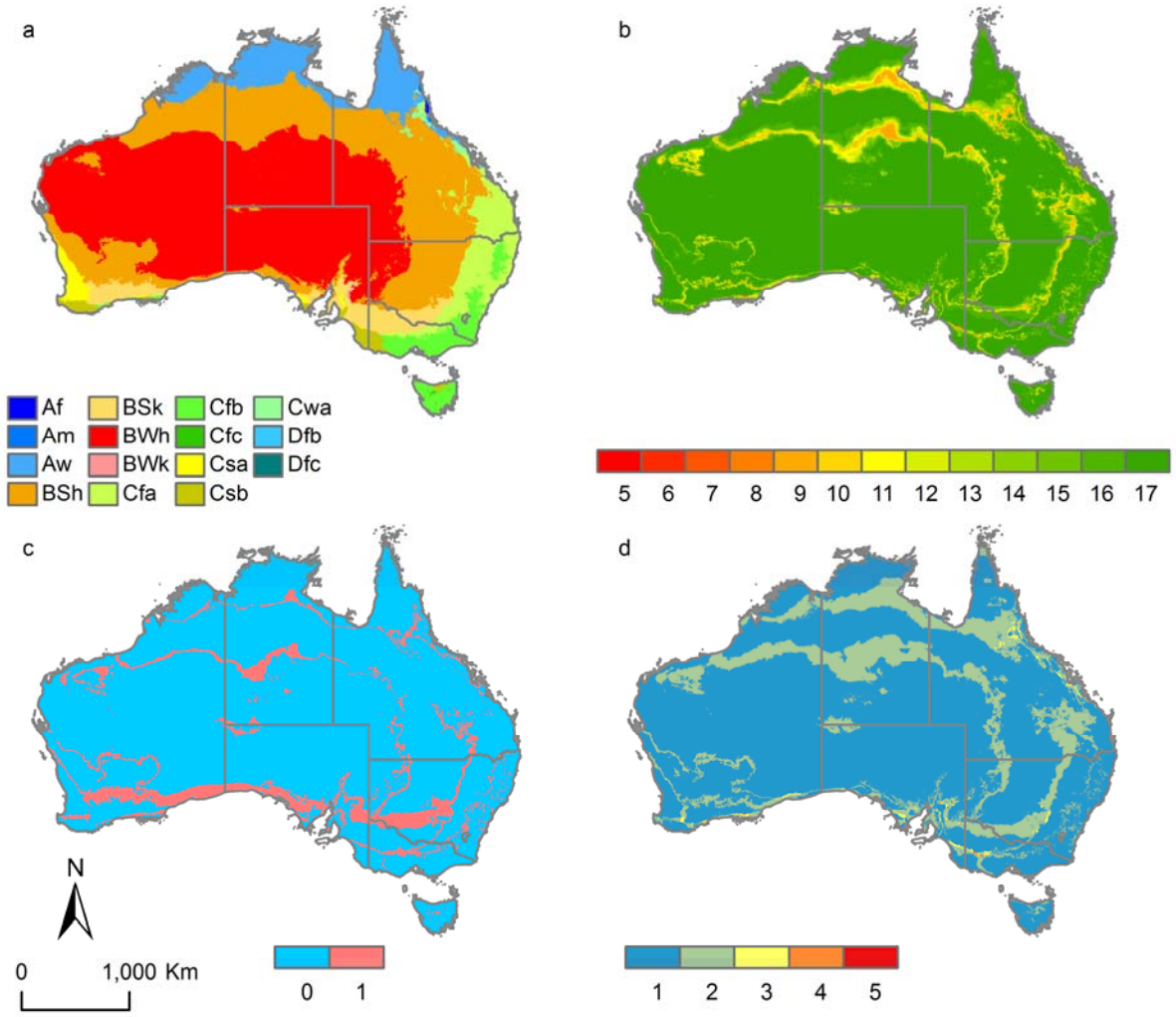

Figure 3-6. 2030 medium global warming projections: (a) mode climate type; (b) frequency of the mode climate type; (c) mode climate type compared to baseline climate type, 0 – no difference, 1 – different; (d) number of different projected climate types

Table 3-1. Change in percentage occurrence from baseline to 2030 (low, medium and high projections)

Climate type	2030 (low)	2030 (medium)	2030 (high)
Aw	-0.3	-0.4	-0.5
BWh	3.5	4.6	5.6
BWk	-0.7	-0.7	-0.8
BSh	1.1	1.7	2.2
BSk	-2.3	-3.4	-4.3
Csa	0.0	0.0	0.1
Csb	-0.3	-0.4	-0.6
Cwa	-0.3	-0.4	-0.4
Cfa	-0.1	-0.2	-0.2
Cfb	-0.5	-0.8	-1.0
Cfc	0.0	0.0	0.0

3.4. Projected changes for 2050

The projected 2050 Australian Köppen-Geiger climate type maps show a continuation of the trends noted for the 2030 projections. The range in projected climate type transition for 2050 is between 14.7% and 23.1% of the Australian continent.

The trend for the 2050 projections shows a 2.8% increase per degree of global warming (pdw) in BWh, 0.9% pdw increase in BSh, and a decrease in BSk of 1.8% pdw (Figure 3-5). Comparing baseline conditions (Figure 3-1) to the 2050 medium global warming mode climate type projection (Figure 3-7a) reveals a 6.8% increase in BWh, 2.9% increase in BSh, and 5.4% decrease in BSk (Table 3-2).

Figure 3-7b shows that the level of agreement between the 2050 medium warming climate type projections has declined in northern Australia visibly more than the rest of the continent. Figure 3-7c shows transitions from baseline climate types for the 2050 medium warming mode climate type, indicating transitions for 18.1% of the continent, with a broadening of the transition zone in southern Australia, when compared to the equivalent 2030 projection. Figure 3-7d shows the number of climate types projected for the 2050 medium warming case, with 67% agreement in climate type projection, while 31% of the continent has two

projected climate types, and less than 1% of the continent has more than two projected climate types.

The 2050 medium warming projection of climate type shows a continuation of the trend away from cold arid to hot arid conditions, and a continued decline in the occurrence of temperate conditions. These patterns are explained by the patterns in the GCM results, which project declines in precipitation in central Australia, and increases in temperature between 0.7 and 3 ºC with a mean of 2 ºC, which is overall above the global mean of 1.7 ºC for this projection.

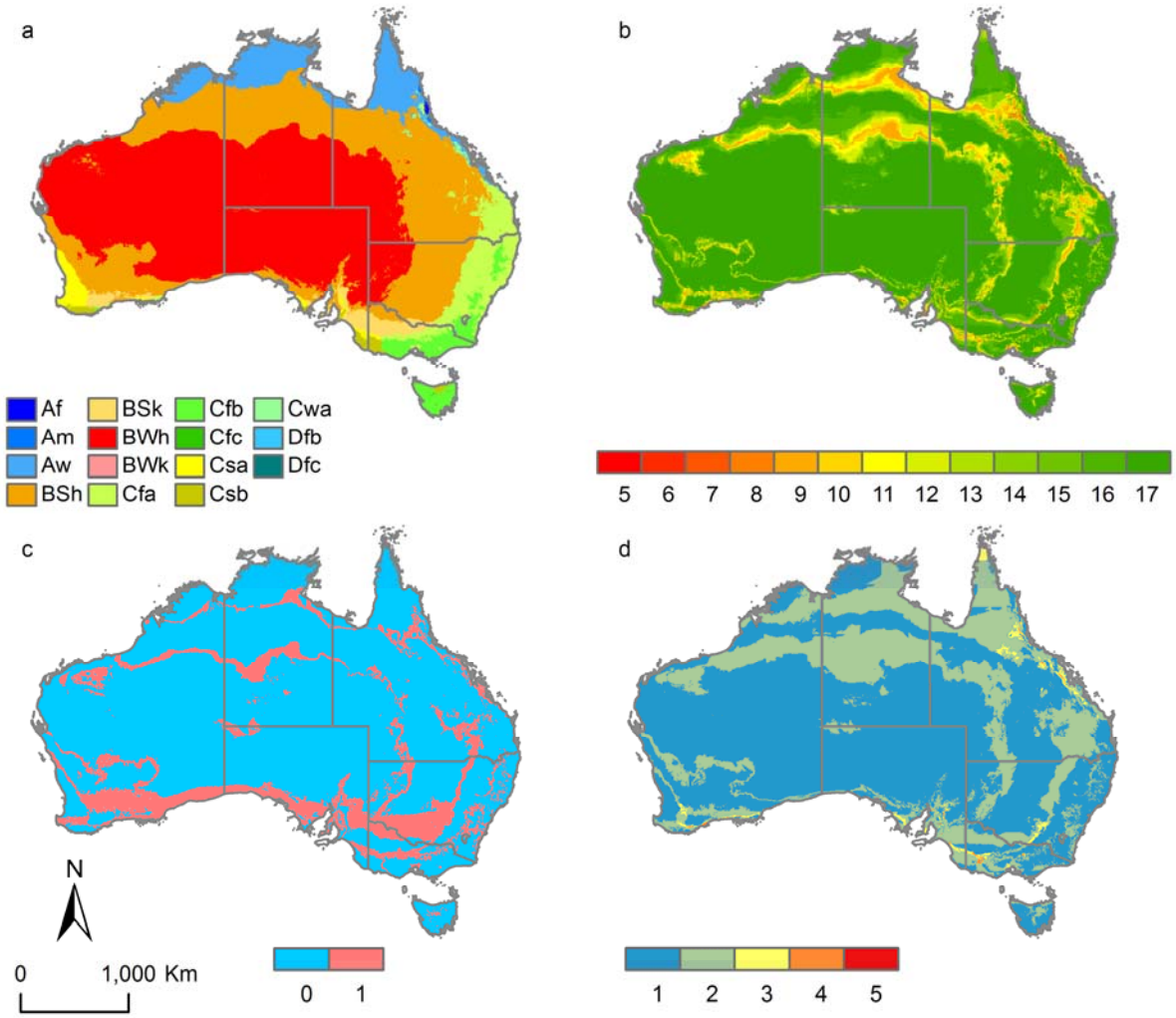

Figure 3-7. 2050 medium global warming projections: (a) mode climate type; (b) frequency of the mode climate type; (c) mode climate type compared to baseline climate type, 0 – no difference, 1 – different; (d) number of different projected climate types

Table 3-2. Change in percentage occurrence from baseline to 2050 (low, medium and high projections)

Climate type	2050 (low)	2050 (medium)	2050 (high)
Aw	-0.5	-0.6	-0.8
BWh	5.6	6.8	8.7
BWk	-0.8	-0.8	-0.8
BSh	2.2	2.9	3.2
BSk	-4.3	-5.4	-6.4
Csa	0.1	0.2	0.4
Csb	-0.6	-0.8	-1.1
Cwa	-0.4	-0.6	-0.7
Cfa	-0.2	-0.3	-0.4
Cfb	-1.0	-1.4	-2.1
Cfc	0.0	-0.1	-0.1

3.5. Potential risk to changes in land cover

Results of the above analyses were used to identify the locations where a potential risk to land cover changes due to the changes in climatic conditions is possible. For 2030 and 2050 these locations are identified in Figure 3-8 and Figure 3-9, respectively. The transition zone is identified from the medium warming projections of mode climate type transitions from baseline conditions (Figure 3-6c and Figure 3-7c), overlain on the vegetation cover (BRS, 2008). The key feature of these maps is the projected transition zone near the fringe of the ‘annual crop’ class in south-east Australia.

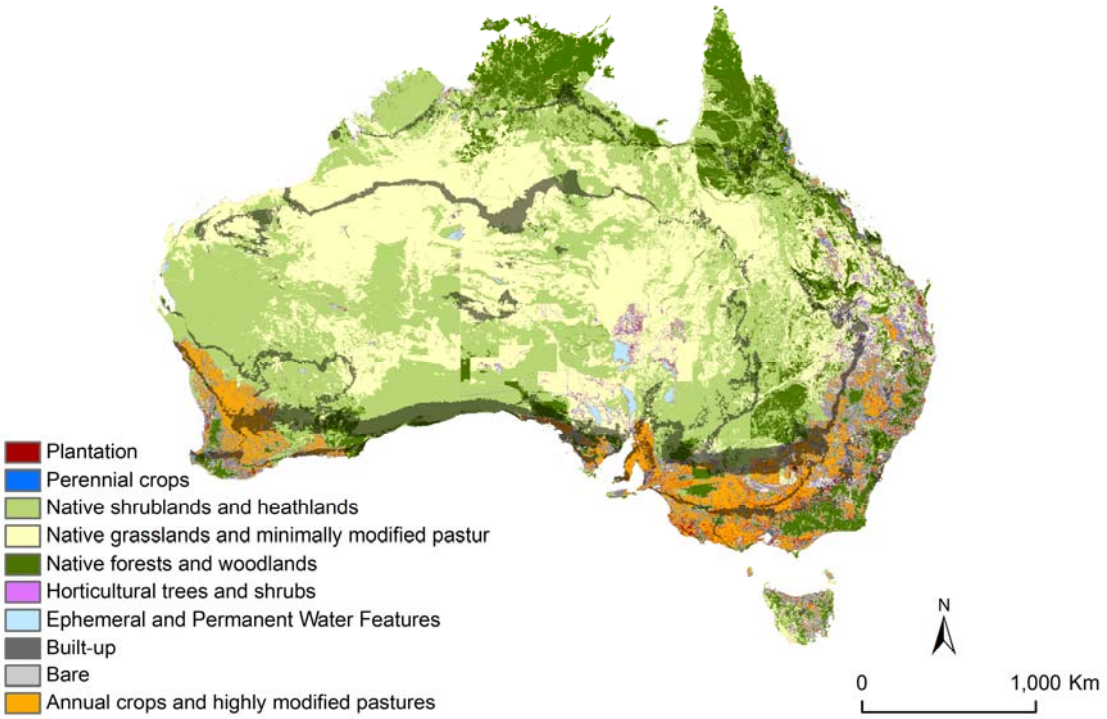

Figure 3-8. Mode projected climate type change (medium projection for 2030) and current land cover (BRS, 2008)

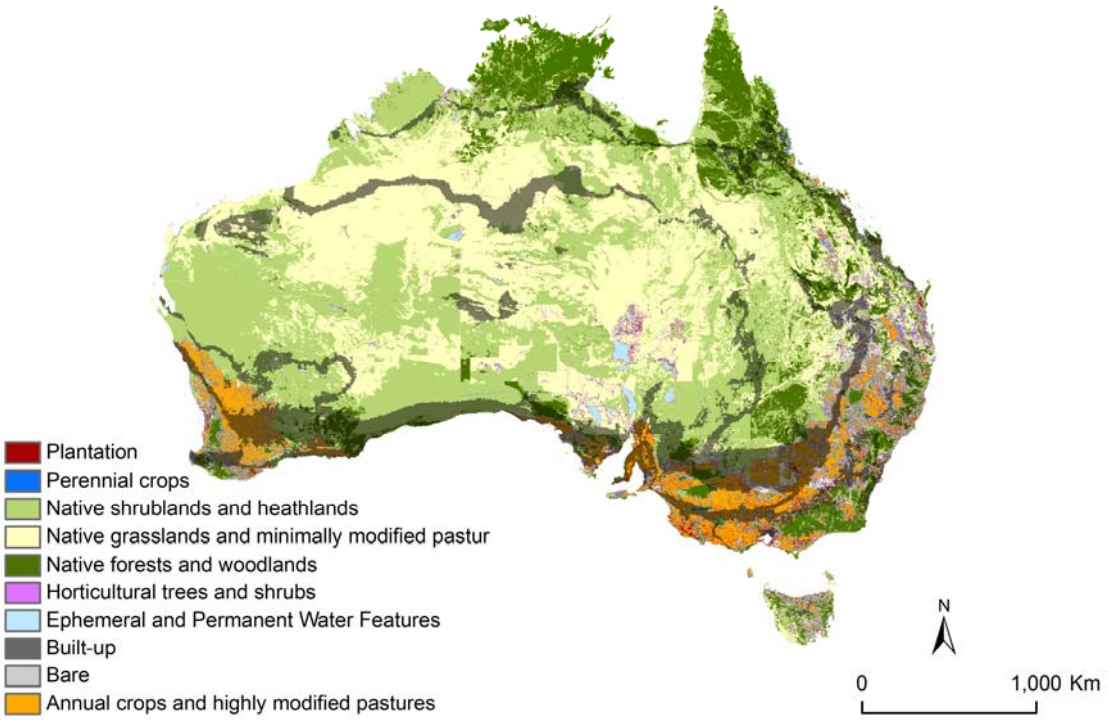

Figure 3-9. Mode projected climate type change (medium projection for 2050) and current land cover (BRS, 2008)

3.6. Conclusions

Analysis of the historical climate type series suggests a transition from desert conditions to steppe conditions that may be attributed to an observed increase in mean annual precipitation in central and northern Australia. This increased precipitation may also explain the increase in savannah conditions in the north. It was also observed that there was a slight shift to drier summers in south-western Victoria. In south-western Western Australia, there is a decline in the occurrence of temperate conditions with hot dry summers.

Projected climates are characterised by a decrease in precipitation in central Australia, as well as an overall increase in temperature. The result of this, with respect to climate type, is an increase in the occurrence of arid conditions (both desert and steppe). Cold arid conditions are projected to be replaced by hotter arid conditions, and there is a general reduction in the occurrence of temperate conditions.

In addition to projected changes in rainfall and temperature across the country (from the GCMs), the changes in the climate types as a combination of both climate parameters may potentially cause changes in vegetation cover. The latter may have an additional impact on groundwater resources, which will be considered in the later stage of the project.

4. EFFECT OF INDIVIDUAL CLIMATE CHARACTERISTICS AND THEIR COMBINATION ON DIFFUSE GROUNDWATER RECHARGE

The objective of the study described in this section is to clarify if diffused groundwater recharge characteristics vary within different climate types. The analysis was based on modelled estimates of a deep drainage below 4 m of the soil profile using the WAVES model (Zhang and Dawes, 1998). As stated in Chapter 2, the modelled recharge was not validated with field data, and therefore the modelled deep drainage estimation is considered as an approximation of the groundwater recharge and comparison between climate types is reported in relative terms.

As described in Chapter 2 the analyses were based on the currently available data, which was obtained under the NASY (Crosbie et al., 2009) and within the MDB (Crosbie et al., 2010b). As these regions fall in five climate types, only those types were considered here. They are tropical (Aw), arid (BWh, BSh and BSk), temperate (Cfa) and cold (Dfc) (Table 4-1). Only one climate type (BSh) was in both regions (MDB and NASY) and further in this chapter this type is referred to as BSh4 for NASY and BSh3 for MDB.

Climate type delineation based on Köppen-Geiger methodology accounts for rainfall and temperature characteristics and their combinations as described in Chapter 2. It is important to mention that the climate types were delineated and largely used for identification of vegetation variability under various rainfall and temperature conditions. They may also influence the agricultural activities which are sustainable under certain combinations of temperature and rainfall. As was shown earlier (Crosbie et al., 2010b), these two factors (native vegetation and agriculture activity type) may have a greater impact on groundwater recharge than changes in climate characteristics. As only three types of vegetation cover (annuals, perennials and trees) were modelled for all climate types, and model parameters related to these vegetation types were assumed constant across the MDB and northern Australia (but different between the two regions), such an approach may limit the reported outcomes.

The analyses results are considered as preliminary and can be reviewed when recharge estimates are available at a national scale.

A number of hypotheses were tested:

- The frequency of estimated annual recharge may be used to define the conditions where episodic recharge dominates.
- The relative importance of rainfall, temperature, solar radiation and vapour pressure deficit in estimations of recharge may vary in various climate types.
- Rainfall characteristics other than a total annual rainfall (such as rainfall intensity or seasonality) may influence recharge to a greater degree than total annual rainfall.
- Analysis of the slope defining the relationship between recharge and climate characteristics is indicative of the sensitivity of recharge to these factors.

The analyses related to the above points are discussed below.

4.1. Selected climate type characterisation

The summary of climate type characteristics are given in Table 4-1, while Figure 4-1 shows a probability of exceedance of annual rainfall for the selected types. The climate types with the higher annual rainfall are Aw and Dfc with 1122 mm and 1644 mm, respectively. Winter rainfall dominates in climate type BSk as well as in the southern part of types Cfa and BWh. The Dfc climate type is the coldest with mean daily temperature of 5.3 ºC. The locations where climate data was extracted for recharge modelling are shown in Figure 4-2. Only one point occurs in climate types BWh and Dfc, and seven sites are in the area with prevailing winter rainfall.

Additionally, the relationship between the climate characteristics within each climate type is illustrated in Appendix A (Figure A-1 to Figure A-7), showing scatter plots for relevant pairs of climate characteristics at each location and their ranges. Though those relationships demonstrate rather weak correlation for all climate types, it appears that rainfall shows negative correlation with temperature, solar radiation and vapour pressure deficit (VPD), while correlation between temperature, solar radiation and VPD is positive.

In climate types Aw and Cfa the climate data, as shown in Figure A-1and Figure A-6, fall into a number of data clusters, suggesting variability of the climate characteristics within the same climate type. Strong positive correlation between temperature, solar radiation and VPD is found for climate type Cfa (Figure A-6). In climate type Dfc, in addition to low annual average temperatures, VPD is also low (Figure A-7).

Table 4-1. Characterisation of the selected climate types

Climate types		Rainfall		Rainfall seasonality: summer rainfall as proportion of annual		Mean temperature	
		Annual (mm)	***Range (mm)***	***Annual***	***Range***	***Annual (ºC)***	***Range (ºC)***
Tropical savannah	**Aw**	1122	752–2032	0.92	0.67–0.96	26.7	22.4–29.5
Arid steppe hot	**BSh**	253	137–419	0.67	0.25–0.90	22.4	18.0–28.1
Arid desert hot	**BWh**	486	223–866	0.76	0.15–0.96	23.5	18.0–29.7
Arid steppe cold	**BSk**	341	236–497	0.43	0.26–0.69	16.9	14.2–18.0
Temperate without dry season with hot summer	**Cfa**	757	438–3452	0.63	0.37–0.79	18.5	14.1–23.4
Cold without dry season with cold summer	**Dfc**	1644	1578–1699	0.45	0.44–0.47	5.3	4.7–5.9

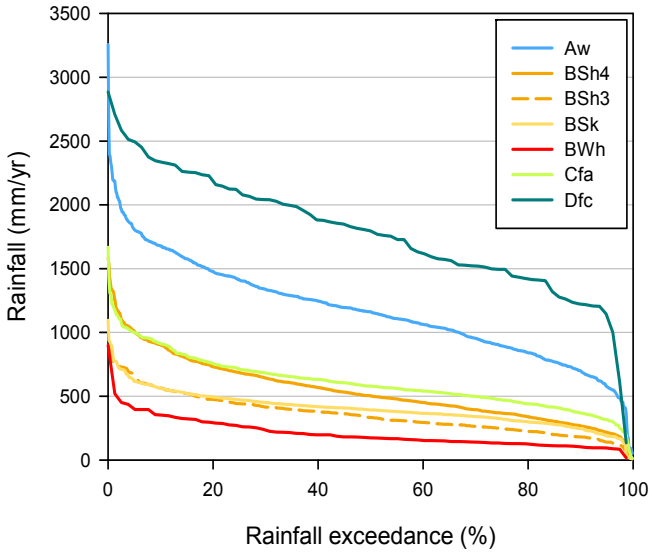

Figure 4-1. Probability of exceedance of annual rainfall for selected climate types

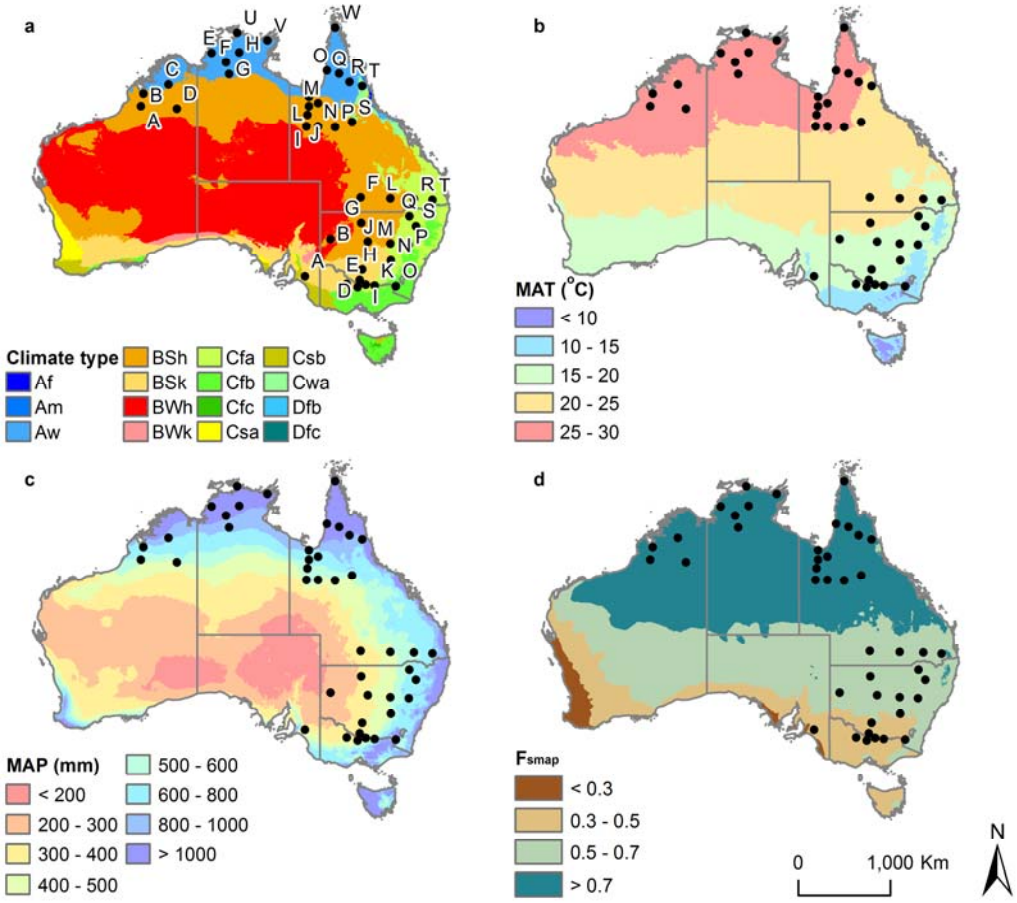

Figure 4-2. Locations where climate data was extracted for recharge modelling shown in relation to (a) climate type, (b) mean annual temperature (MAT, °C), derived from daily maximum and minimum temperature, (c) mean annual precipitation (MAP, mm), and (d) fraction of mean annual precipitation during summer period (F_{smap})

4.2. Recharge frequency

Figure 4-3 (as well as Figure A-8 to Figure A-10 in Appendix A) shows the probability of exceedance of recharge for various soil and vegetation types within various climate types. The plots reflect the frequency of the annual recharge at all points located in each climate type. The conditions which are characterised by a low annual recharge and a small change in an annual recharge for the majority of the years, but a sharp rise in an annual recharge for lowest probability of exceedance are likely to be indicative of an episodic nature of groundwater recharge at those locations. As shown in Figure 4-3, such conditions are most evident for

- soils with lower K
- tree land cover
- in the sequence of climate types BWh>BSk>BSh>Cfa>Dfc.

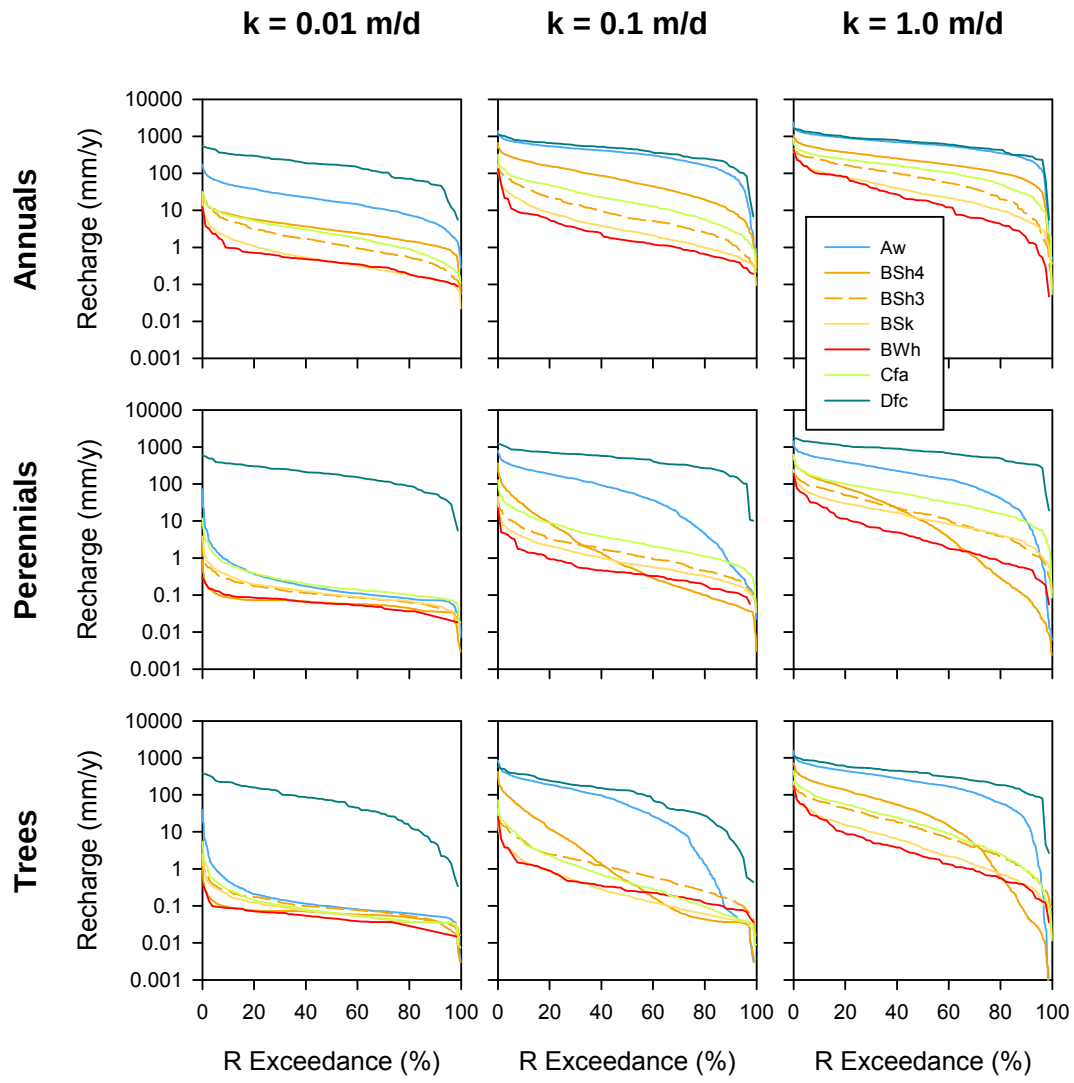

Figure 4-3. Probability of exceedance of annual recharge for various vegetation, climate types and soil types

4.3. Relative importance of climate characteristics in recharge estimation

Previous analysis of modelled recharge sensitivity to various climate characteristics was undertaken by changing an individual climate characteristic as an input to the WAVES model, while other characteristics remained unchanged (McCallum et al., 2010). Within the current analysis, an observed combination of climate characteristics which were used for recharge modelling was considered. The reason for using such an approach was based on the assumption that it allows accounting for interdependency of climate characteristics, when changes in one characteristic may be associated with changes in others.

As described in Chapter 2, analysis of relative importance was undertaken for modelled recharge and climate data of the historical observation for the period from 1930 to 2009. Figure 4-4 shows the relative importance of the climate characteristics estimated based on multivariate regression analysis between recharge and annual rainfall as well as annual mean temperature, solar radiation and VPD. Only three soil types are shown, as it was identified that the annual modelled recharge under the soils with hydraulic conductivity K greater than 1 m/day show low variability (see Chapter 2).

For all climate types, the overall importance of climate characteristics in recharge estimation increases for more permeable soils. Within the same soil type, the importance of all considered climate characteristics is greatest for annuals and lowest for trees.

4.3.1. Total annual rainfall

As expected the annual rainfall is identified as a major factor influencing recharge. The exception is related to soils with particularly low hydraulic properties, where other climate characteristics play a more important role. However, in such cases overall correlation between recharge and climate characteristics is weak, while the estimated recharge is commonly low.

The relative importance of total annual rainfall is particularly low for clay-rich soil in climate type Aw followed by types Cfa, BSh and BSk, and is somewhat greater in types Dfc and BWh. Despite considerable difference in climatic conditions the two climate types Dfc and BWh show a similarity in the pattern of relationships between recharge and climatic characteristics. In both climate types there is a relatively small difference in relative importance of various climate characteristics for various soils and vegetation. However, the overall importance of climate characteristics in recharge estimation is lesser for climate type BWh than for Dfc.

4.3.2. Other climate characteristics

For the majority of cases the importance of temperature, VPD and solar radiation in recharge estimation is relatively higher under soils with a lower hydraulic conductivity (Figure 4-5). The importance of these climate characteristics is overall greater for annuals with the exception of the climate type Dfc. The combined contribution of these climate characteristics (temperature, VPD and solar radiation) to overall R^2 reduces in sequence from the greatest in Aw and lowest in BSk as Aw≥Dfc>BSh3>BWh>BSh4>Cfa>BSk (Figure 4-6).

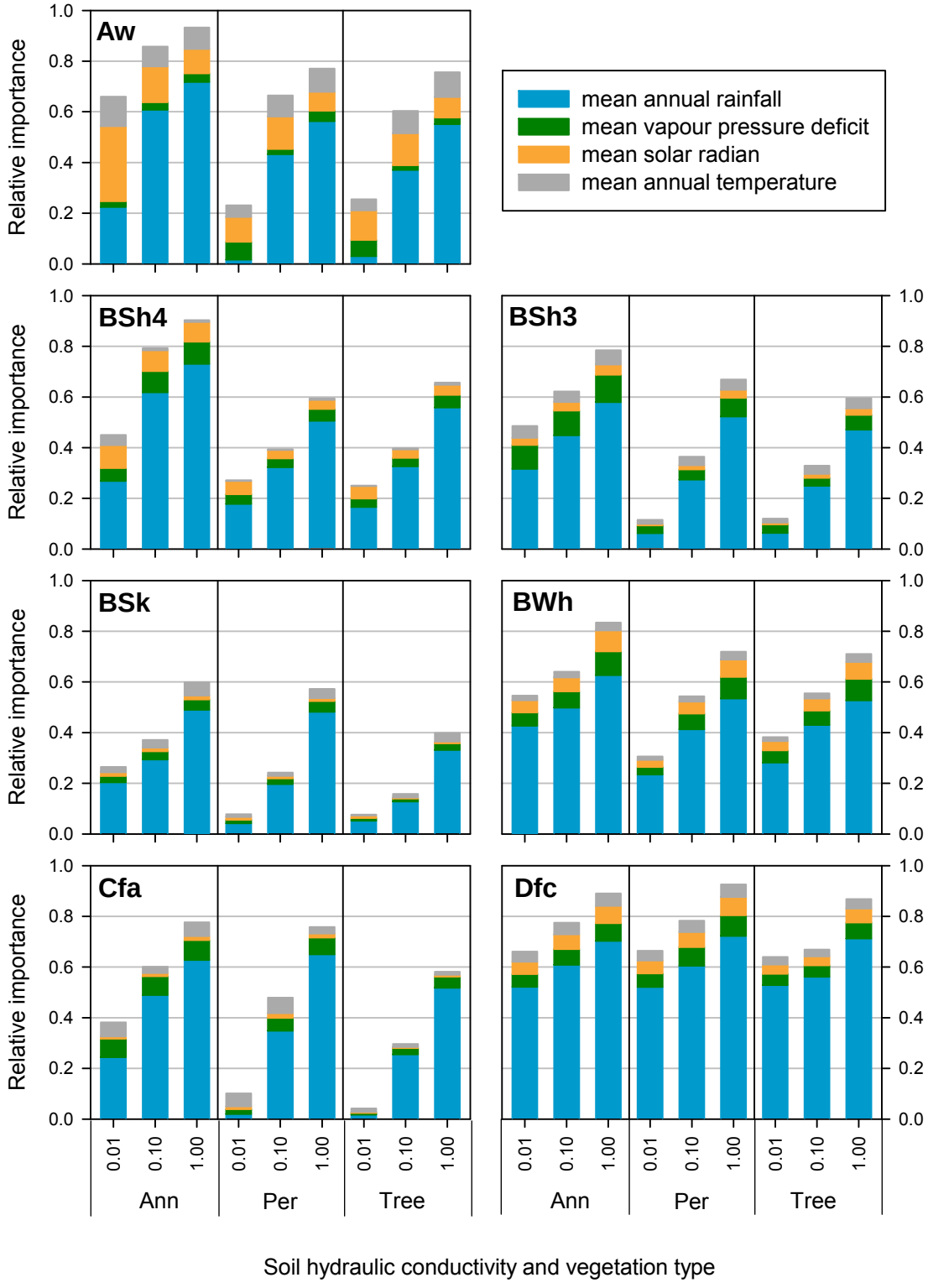

Figure 4-4. Relative importance of all considered climate characteristics

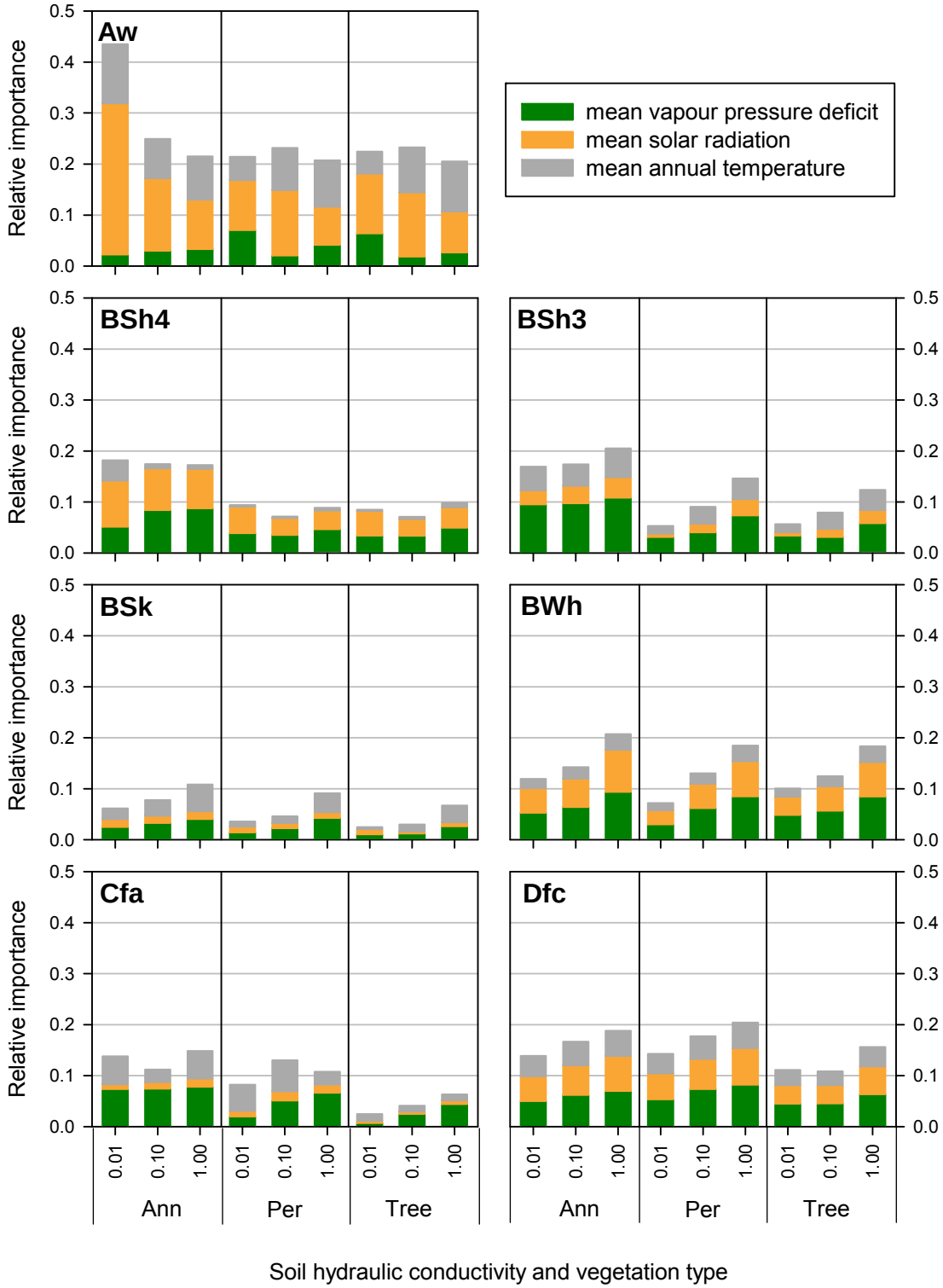

Figure 4-5. Relative importance of the considered climate characteristics other than annual rainfall

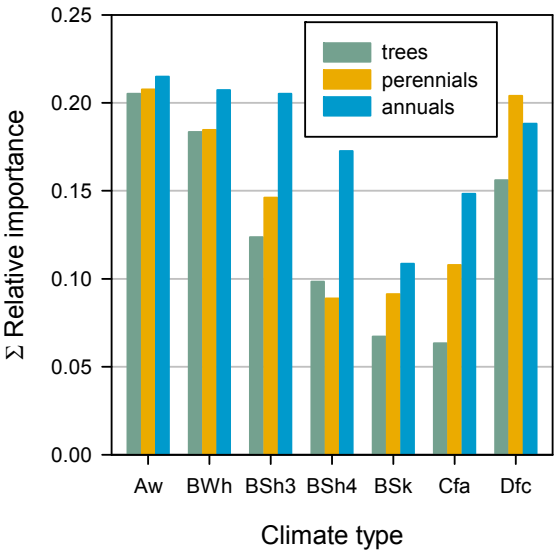

Figure 4-6. Relative importance of climate characteristics (all but rainfall) in recharge estimation for three vegetation types and soil K > 1 m/d

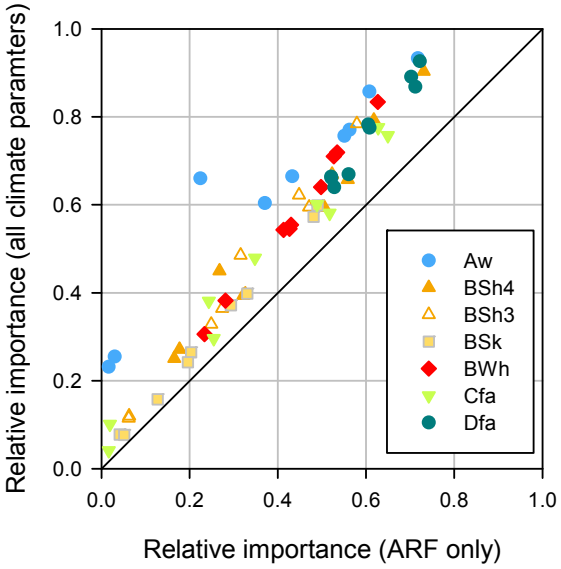

Figure 4-7. Average increase in relative importance when selected climate characteristics are considered in addition to annual rainfall

In the Aw and Dfc climate types, solar radiation and temperature show a relatively higher importance in recharge estimation. On the other hand, in BWh and BSh climate types, VPD has a relatively higher importance when compared with other characteristics (Figure 4-6).

As shown in Figure 4-7 the variability of annual recharge estimation is likely to be predicted more accurately when, in addition to total annual rainfall, other climate characteristics are included. Figure 4-7 shows the increase in R^2 when a set of climate characteristics are included in regression analysis in addition to rainfall only.

4.4. Effect of rainfall characteristics on estimated recharge

A set of various rainfall characteristics combined over individual years was considered in addition to total annual rainfall to investigate the effect of daily rainfall intensity on recharge (see Chapter 2). The coefficient of correlation between the total annual rainfall (or other annual rainfall characteristics) and recharge was used to identify the best fit of the recharge and rainfall relationship at each of the considered sites.

It appears that for the majority of the considered climate types the total annual rainfall does not produce the strongest correlation with recharge, with the exception of climate type Dfc. The correlation between recharge and derived rainfall characteristics was particularly strong in the BWh and BSh4 climate types, where R^2 increased from 0.4–0.6 estimated for the total annual rainfall to 0.7–0.9 when other rainfall characteristics are included in addition to rainfall (Figure 4-8). The BSk and Cfa climate types also showed significant improvements in correlation between recharge and rainfall, when other rainfall characteristics in addition to total annual rainfall were considered. As a number of annual rainfall variables were analysed, the correlation between them and recharge was further explored.

For all data, R^2 of the relationship between the total annual rainfall and recharge was plotted against the R^2 estimated for the relationship between other rainfall characteristics and recharge (Figure 4-9). The increase in R^2 was the greatest for relationships between:

- recharge and total daily rainfall with higher intensity (as threshold >10 mm and >20 mm)
- recharge and a sum of moving averages daily rainfall (as described in Table 2-3).

For some scenarios, such as band 20 to 40 mm or 95th and 99th percentile, an increase in R^2 was also evident but in those cases the increase in R^2 was less than that for the best fit scenarios for the same site.

When the correlation between total annual rainfall and recharge is high (R^2>0.9) or particularly low (R^2<0.3) the consideration for other rainfall characteristics does not produce any better fit with recharge. This is commonly the case for the climate types with particularly high rainfall and high R^2 (Aw and Dfc) and for soils with low hydraulic conductivity.

Overall the best scenarios (or the scenarios with the highest R^2) are associated with a moving average over 14 and 21-day periods with a daily rainfall threshold of 5 mm/day. Table 4-2 shows results, summarised for the individual climate types. As an annually cumulated moving average value reflects either particularly high daily rainfall (see Table 2-3) or a series of a smaller events, the larger period of the moving average calculation is a better fit for recharge estimation in the regions where:

- episodic recharge is likely
- recharge is associated with a prolonged rainfall periods.

For the MDB region, the results indicate that the best fit between rainfall and recharge is for the moving average, while for the NASY region a sum of rainfall greater than defined daily thresholds produces a better fit.

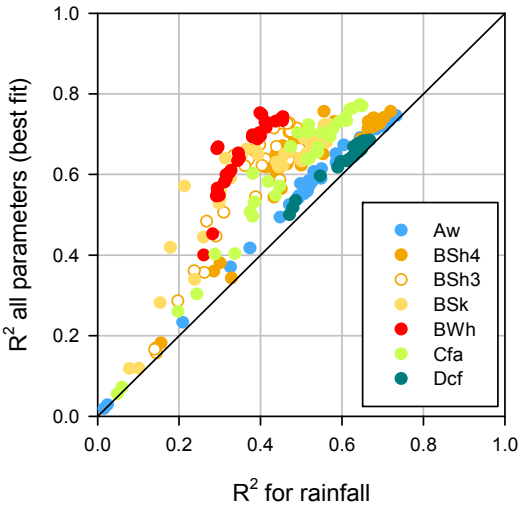

Figure 4-8. Comparison of the correlation coefficients (R^2) for the recharge and rainfall relationship: (X-axis) with total annual rainfall and (Y-axis) derived annual rainfall characteristics which reflect intra-annual rainfall patterns (as a best fit for considered range)

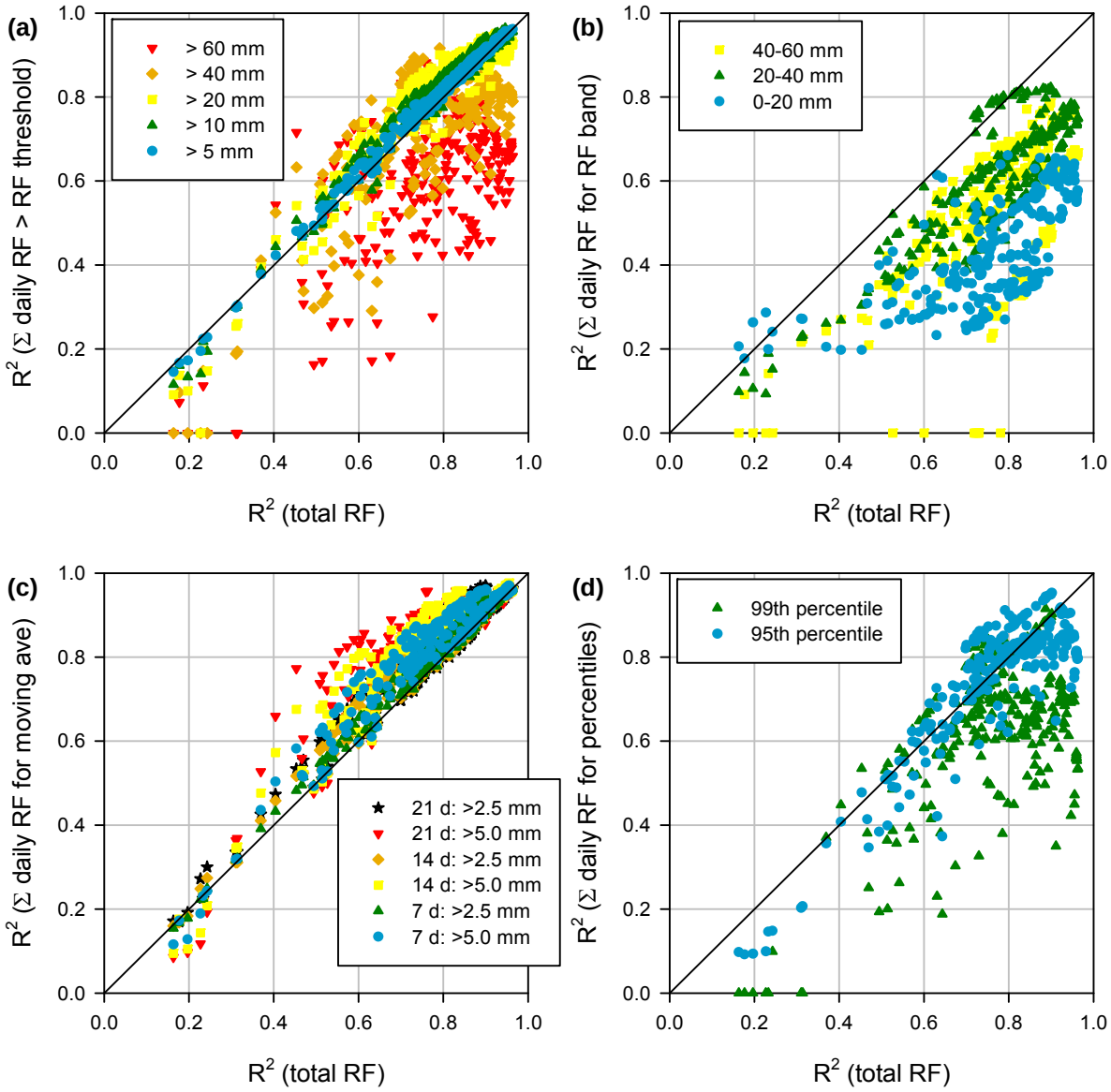

Figure 4-9. Comparison of the correlation coefficients (R^2) for the recharge and rainfall relationship: (X-axis) with total annual rainfall and (Y-axis) derived annual rainfall characteristics: (a) sum of the daily rainfall above the identified thresholds; (b) sum of the daily rainfall within the identified bands; (c) sum of the daily rainfall as moving average with identified intervals and daily thresholds; and (d) sum of 95th and 99th percentile daily rainfall

Table 4-2. Annual rainfall characteristics with highest R^2 for recharge estimation

Climate type	Vegetation type	Total rainfall	Band	Threshold	Moving average
Aw	All	For clays only		Most >20 n	
BWh	Perennials and trees				14 days with a daily rainfall of 5 mm as threshold
	Annuals				21 days with a daily rainfall of 5 mm as threshold
BSh4	Savannah	For clays only		>40 mm	
	Perennials	For clays only		>40 mm	
	Annuals	For clays only		>10 mm	
BSh3	Trees	For clays only			21 days with a daily rainfall of 5 mm as threshold
	Perennials	For clays only			21 days with a daily rainfall of 5 mm as threshold
	Annuals	For clays only			7 days with a daily rainfall of 5 mm as threshold
BSk	Trees				21 days with a daily rainfall of 5 mm as threshold
	Perennials		0-20 for clays only		21 days with a daily rainfall of 5 mm as threshold
	Annuals				21 days with a daily rainfall of 5 mm as threshold
Cfa	Trees		0-20 for clays only		21 days with a daily rainfall of 5 mm as threshold
	Perennials		0-20 for clays only		14 days with a daily rainfall of 5 mm as threshold
	Annuals				14 days with a daily rainfall of 5 mm as threshold
Dfc	Trees				14 days with a daily rainfall of 5 mm as threshold
	Perennials				14 days with a daily rainfall of 5 mm as threshold
	Annuals				14 days with a daily rainfall of 5 mm as threshold

4.5. Recharge sensitivity to rainfall and its intensity

The recharge (R) sensitivity to rainfall (P) changes was assessed based on the slope analysis of the relationship $R = aP + b$ assuming a greater sensitivity of the recharge when similar changes in absolute values of rainfall cause greater changes in absolute estimated recharge under a larger a. This approach could not be directly used for analysis of relative changes in rainfall and recharge.

The relationship between a and annual average rainfall for all considered scenarios and site locations is given in Figure 4-10, which shows an overall a increase in the area with a higher annual average rainfall. Slopes are also greater under annual vegetation. However, a significant scatter of data is apparent for the area with annual average rainfall less than 800 mm. It appears that under the same scenario of soil and vegetation cover, similar slopes exist at the locations with different annual rainfall or different slopes are associated with the regions of equal annual average rainfalls. To assist the interpretation of results, these two scenarios were further analysed.

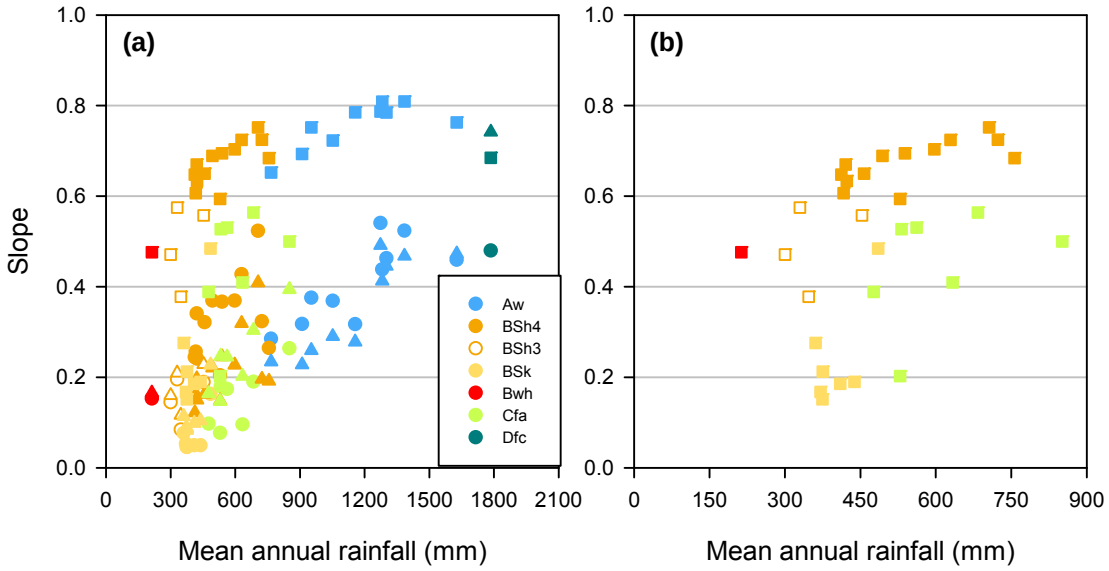

Figure 4-10. Slope of the R and RF relation at individual sites and the mean annual rainfall at the same site for all locations (a) and for annual vegetation only (b); square symbols are used for annuals, circles for perennials and triangular symbols for trees

As an example, Figure 4-11a shows that at three selected locations ('P' in NASY and 'L' and 'J' in MDB, see Figure 4-2) with a similar annual rainfall of 430–450 mm, the slope a of the relationship between annual recharge and annual rainfall varies from 0.60 to 0.19. Further analysis of the rainfall data showed that at each location the amount of rainfall associated with events >20 mm composed 56% at site 'P', 39% at site 'L' and 22% at site 'J' (Figure 4-11b). Consequently, the annual average recharge was found to be smaller for the locations where low-intensity rainfall prevails (site 'J', Figure 4-11c).

Therefore the different slopes under similar annual average rainfall are likely to indicate the effect of rainfall intensity. For such cases a correlation between the recharge and the annual rainfall characteristics, reflecting rainfall intensity, is likely to be stronger.

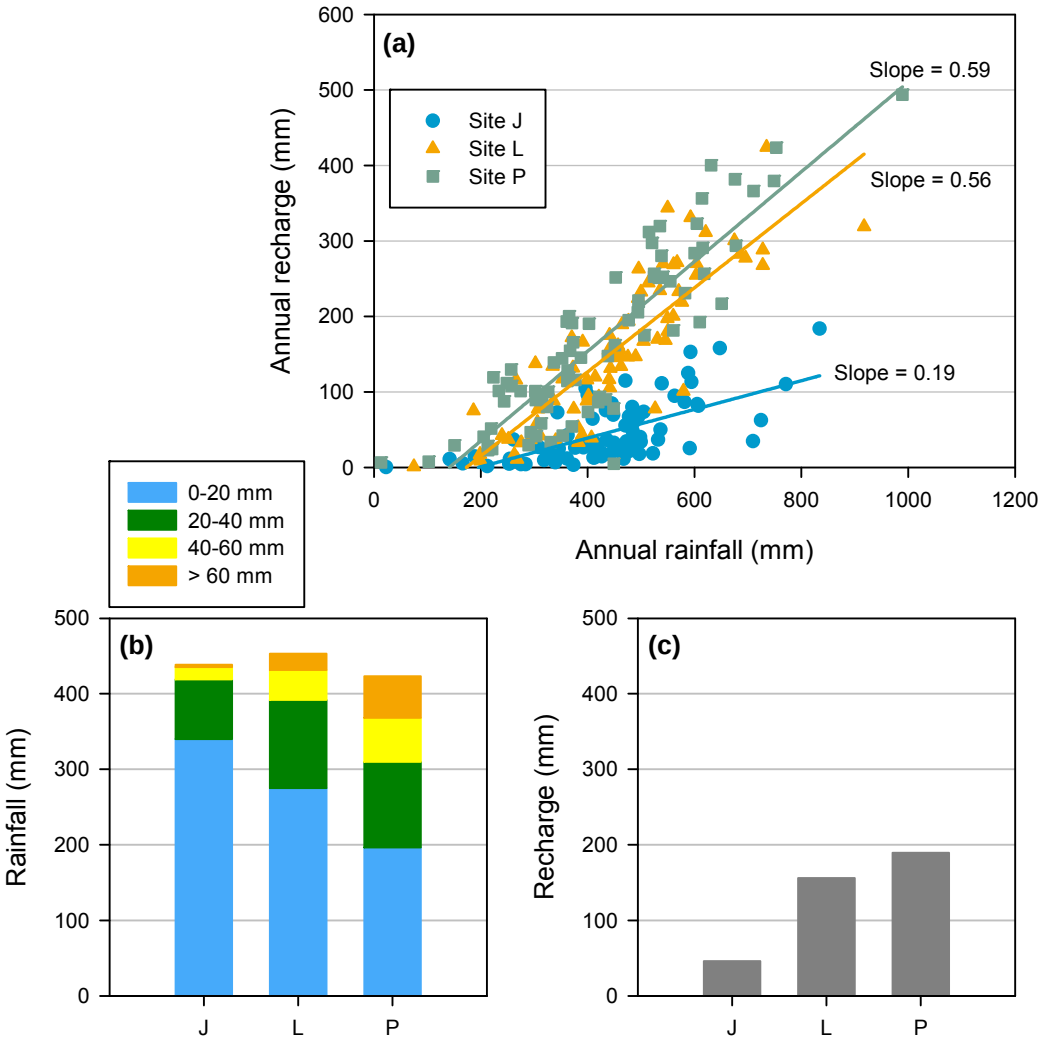

Figure 4-11. Annual rainfall and recharge relationship (a) contribution of high intensity daily rainfall to total annual average rainfall, (b) the annual average recharge, and (c) at three selected locations under soil with K > 1m/d

On the other hand, there are also cases when a similar slope a in the relationship between recharge and rainfall was identified for sites with different annual average rainfall, as illustrated in Figure 4-12. This figure shows that within a certain range of annual rainfall, higher annual recharge could be estimated for a site with overall smaller annual average rainfall. This is yet another indication of the effect of rainfall intensity on estimated recharge. As Figure 4-13 shows, the high annual rainfall at site 'L' is characterised by a greater contribution of high daily rainfall to the total annual rainfall. As a result, at two sites with annual average rainfall of 330 and 860 mm (F and Q, respectively; see Figure 4-12), in the range of annual rainfall between 450 and 700 mm the groundwater recharge is higher for the site F, which on a long-term basis is characterised by the smaller annual average rainfall (330 mm). This is due to the higher contribution of daily rainfall greater than 20 mm/day, which comprised 46% and 36% of annual rainfall within the range of 450 mm to 700 mm. Long-term average annual recharge at the F and Q sites was 110 mm and 229 mm, respectively.

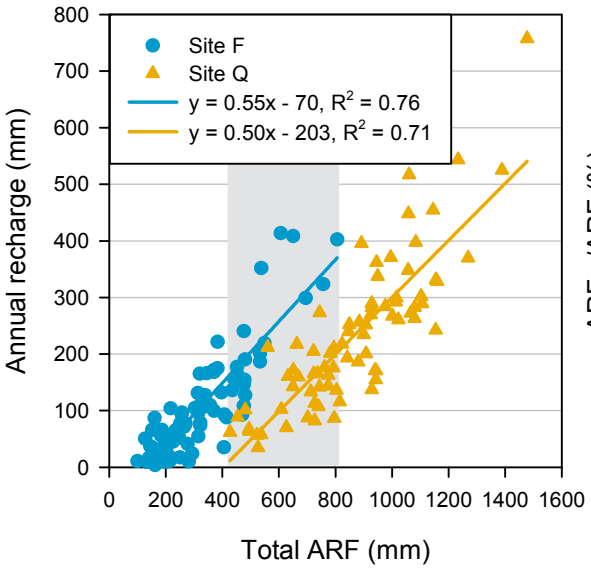

Figure 4-12. Annual rainfall and recharge relationship at two selected locations

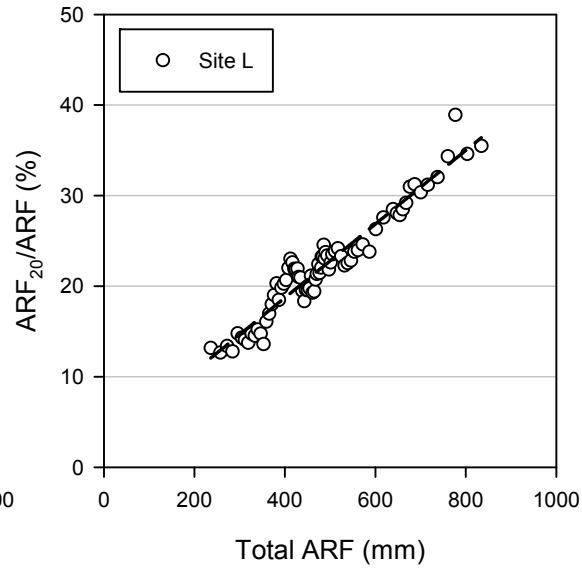

Figure 4-13. Relationship between annual rainfall (ARF) and percent of rainfall greater than 20 mm (ARF_{20}/ARF): example is given for site 'L'

The recharge and the slope of the recharge and rainfall relationship are shown in Figure 4-14 and Figure 4-15 under soil with K ~ 1 m/day. For the regions with similar rainfall zones (Figure 4-14) both characteristics reduce in the southern regions of the country. It was reported previously (Fu et al., 2010) that daily rainfall events in the north are generally of greater intensity as they are associated with monsoons and cyclones. In the southern part of the country, winter rainfall (Figure 4-15) is largely associated with southern frontal weather systems with relatively lower daily rainfalls. Therefore the recharge sensitivity to absolute changes in annual rainfall is likely to be less in the south, although overall recharge is also smaller in these areas. In these regions the sensitivity to rainfall intensity is particularly important. Similar trends can be observed for other vegetation scenarios.

This is further illustrated in Figure 4-16 and Figure 4-17 which shows slopes a in a linear regression of recharge and rainfall relationship for all considered climate types, soil types and vegetation, and also their changes for best fit rainfall characteristics. In the arid climate types (BSh3, BSh4, BSk, BWh) and the Cfa climate type, the sensitivity, defined by a greater a, is higher when high intensity annual rainfall characteristics are considered. For instance, within the desert and arid climate types in the MDB region, the slope a is greater (nearly two-fold) for the relationship between high internsity rainfall and recharge than for total annual rainfall and recharge.

At the same time, in climate types Aw, BSh4 and Dfc there is no significant difference when total annual rainfall or high intensity annual rainfall characteristics are considered.

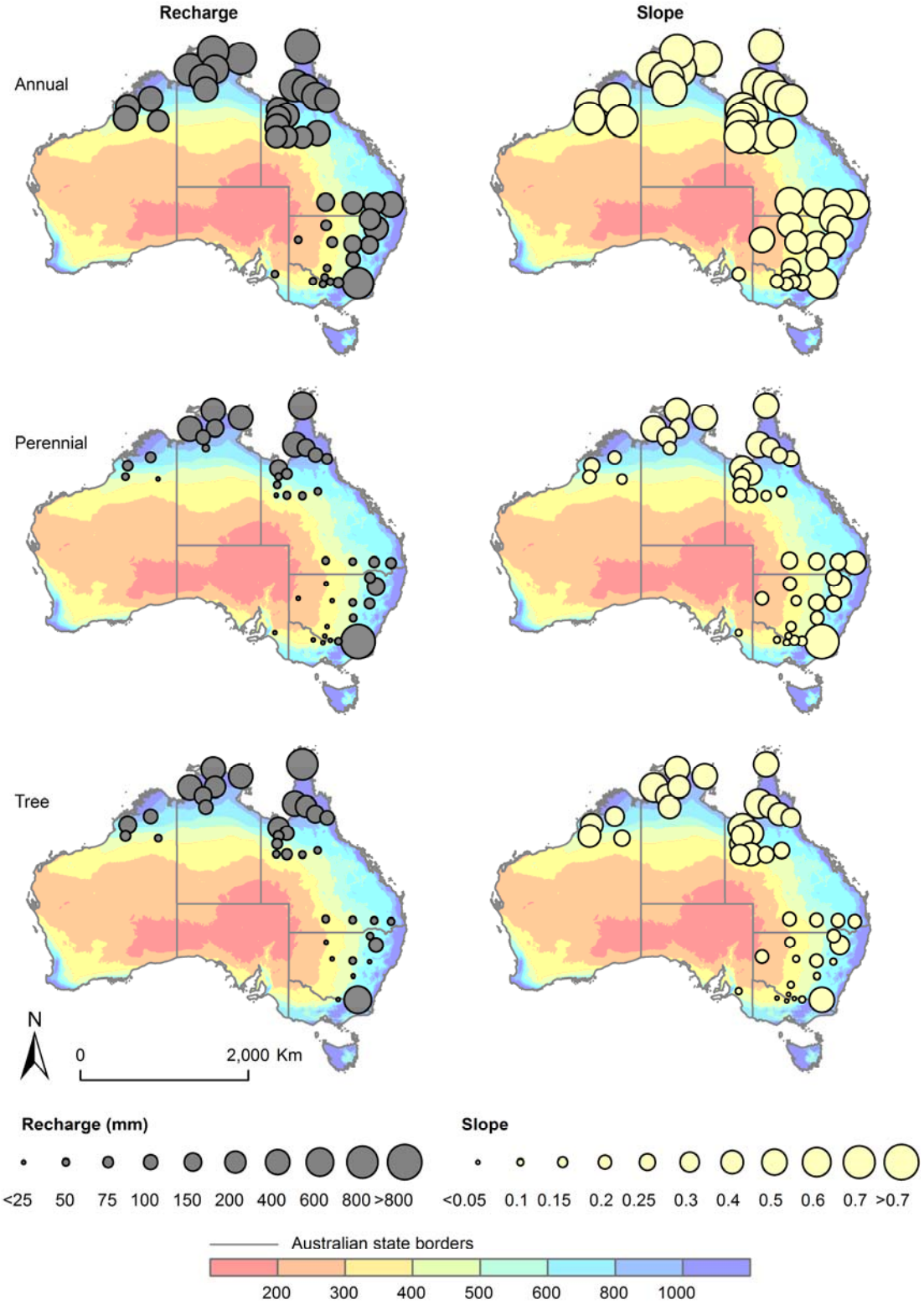

Figure 4-14. Annual average recharge and a (slope) of the relationship between recharge and annual average rainfall for annual, perennial vegetation and trees under soil with high hydraulic conductivity, plotted over annual average rainfall

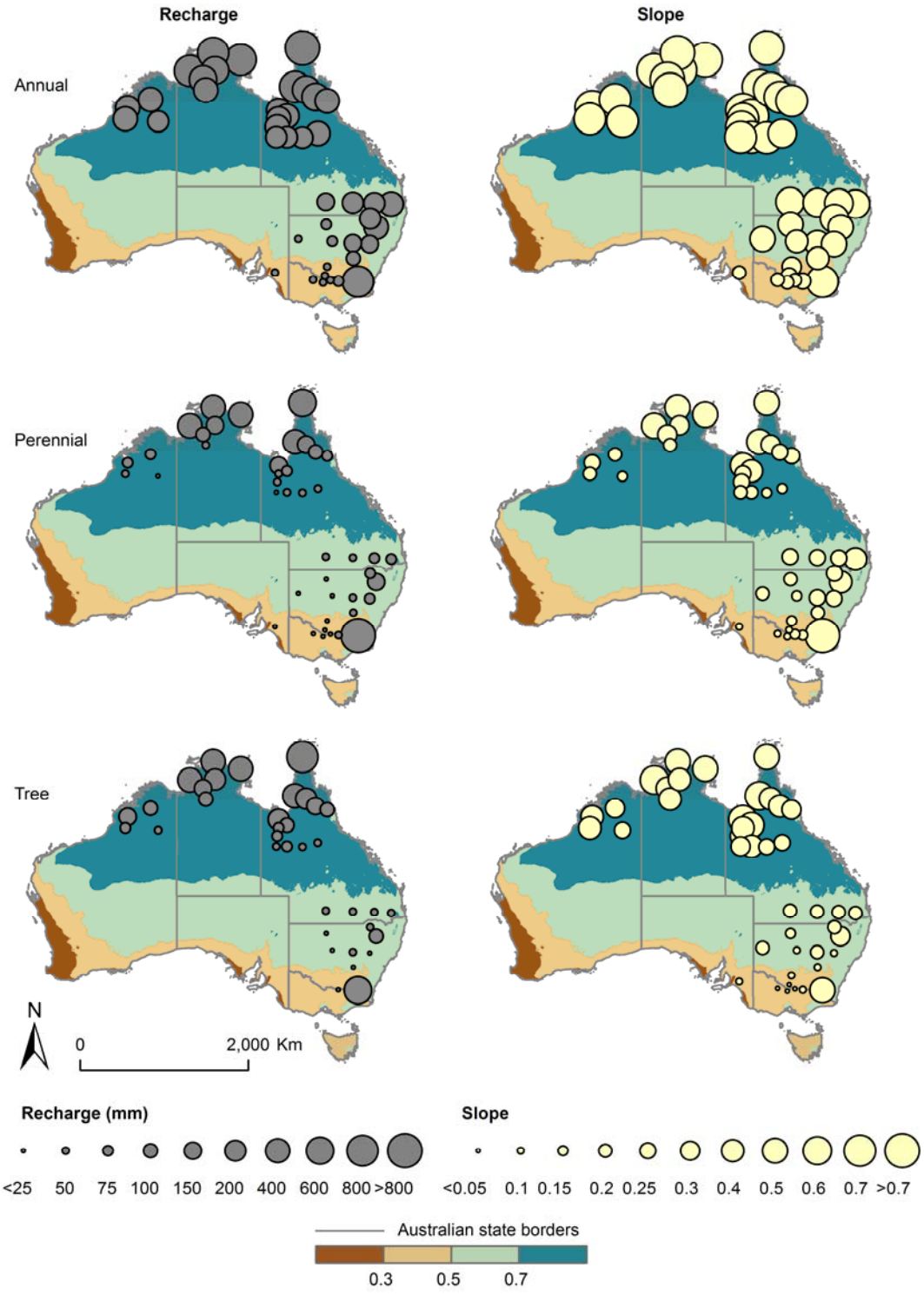

Figure 4-15. Annual average recharge and a (slope) of the relationship between recharge and annual average rainfall for annual, perennial vegetation and trees under soil with high hydraulic conductivity, plotted over annual average rainfall, plotted over the map of summer rainfall as proportion of total annual rainfall

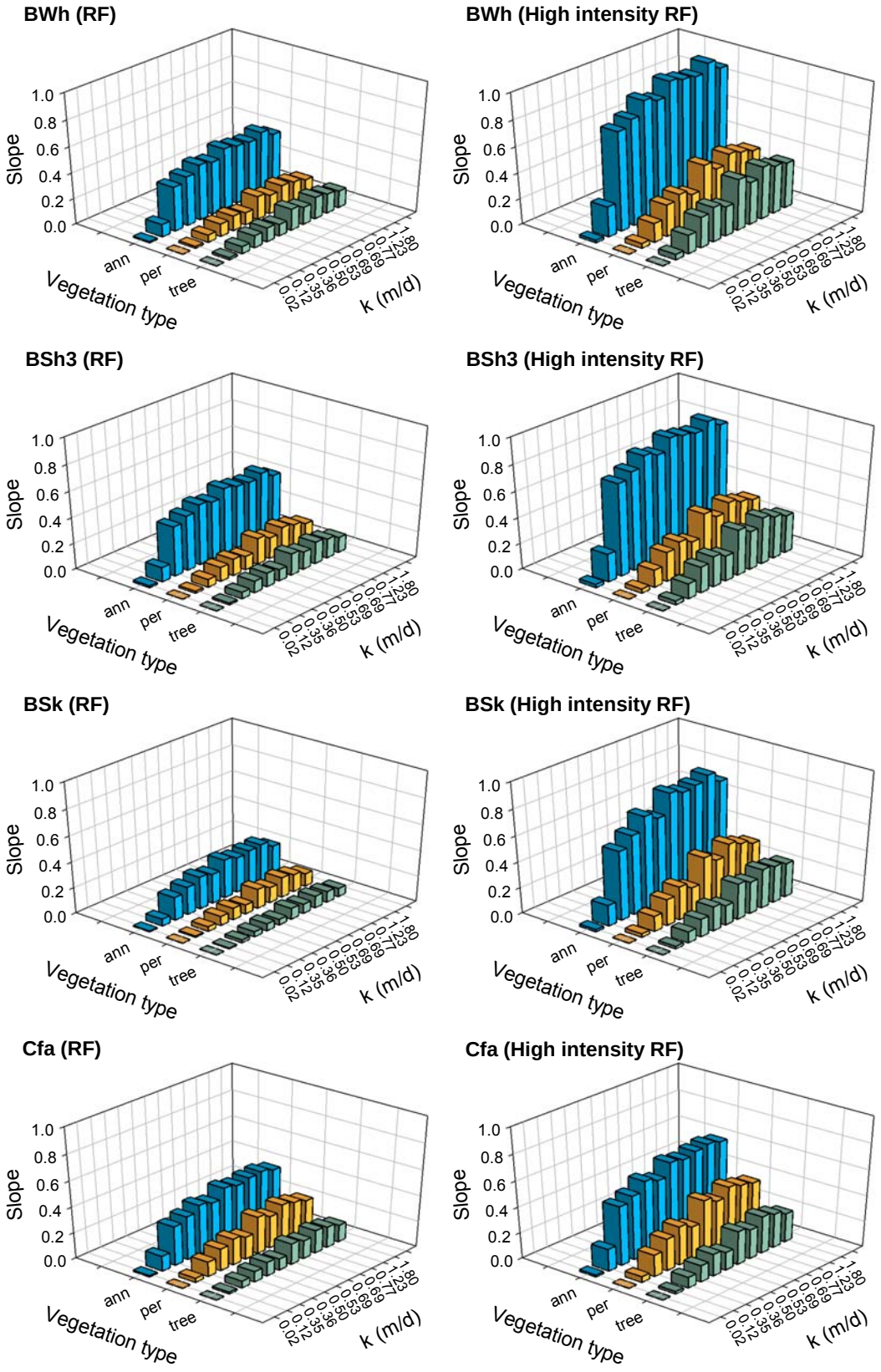

Figure 4-16. Slopes of the recharge and rainfall relationship, when the total annual (left column) and only rainfall of high intensity (right column) were considered for combination of soils and vegetations under BSh3, BSk, BWh and Cfa climate types

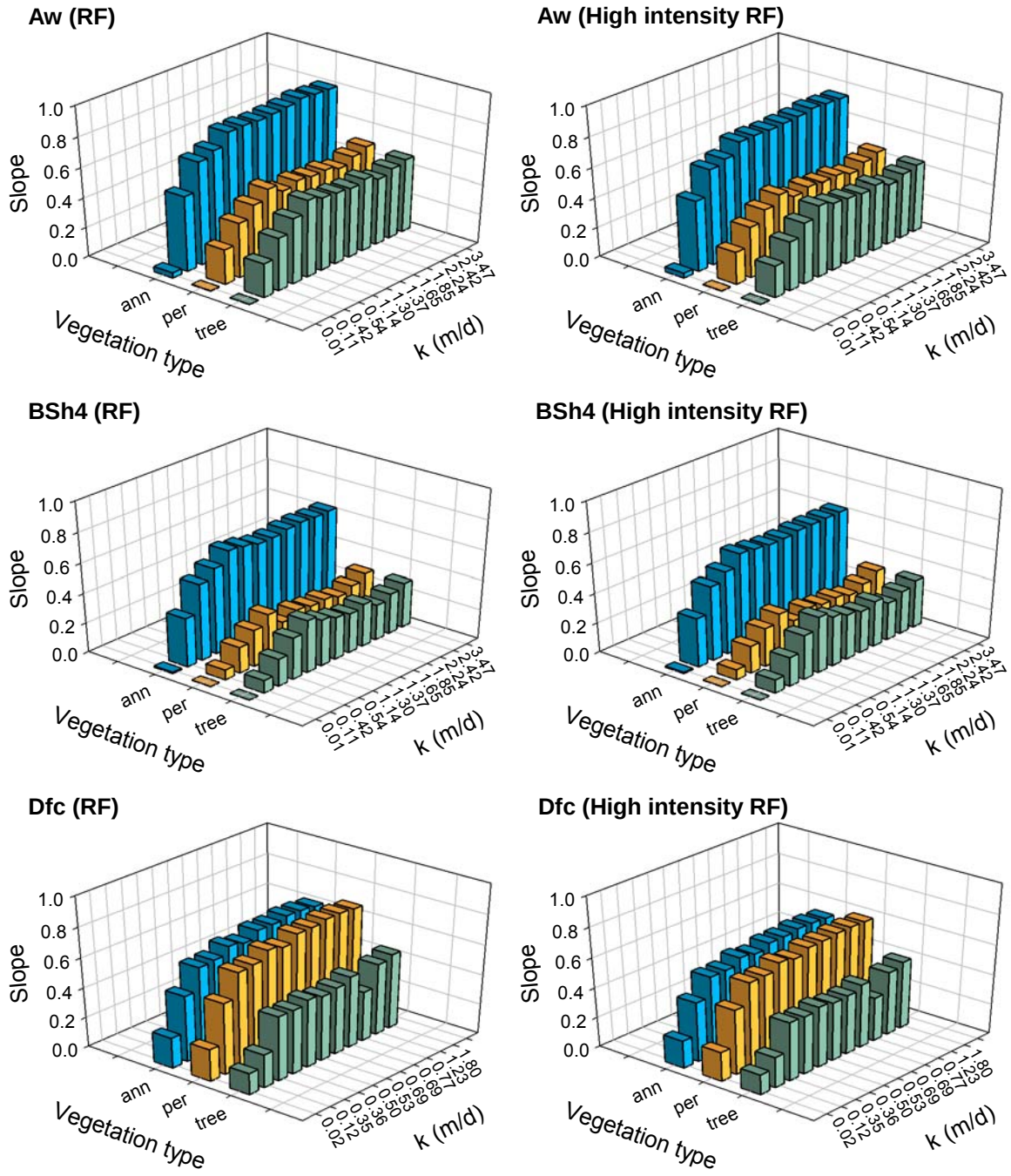

Figure 4-17. Slopes of the recharge and rainfall relationship, when the total annual (left column) and only rainfall of high intensity (right column) was considered for combination of soils and vegetations under Aw, BSh4 and Dfc climate types

4.6. Conclusions

The results of the analyses indicate that the estimated recharge within the selected climate types shows variable relationships with annual rainfall, its intensity and seasonality as well as with other climate characteristics. The specifics of climatic conditions in Australia indicate that the northern regions are greatly influenced by monsoons and tropical cyclones, both of which bring heavy rains during summer months. In the south, frontal weather systems and east coast lows during winter in combination with localised troughs (western and eastern) during summer bring occasional heavy rains with prolonged periods of lower intensity rainfall, mainly during winter. The sub-tropical ridge brings dry and stable conditions to large parts of middle Australia. To some extent, the approximate position of the ridge separates the area of summer-dominated or winter-dominated rainfall in the eastern part of the country. These circumstances influence the estimated recharge.

In the tropical savannah climate type (Aw), recharge shows a strong correlation with total annual rainfall and appears to have higher overall sensitivity to total annual rainfall. The daily rainfall above 20 mm summed on an annual basis shows only a slightly better correlation with recharge. Episodic recharge is only related to soils with low hydraulic conductivity under land cover of perennial vegetation and trees. It was also shown that in recharge estimation the relative importance of climate characteristics other than rainfall is high; this is particularly evident for annual average mean daily temperature and solar radiation.

In the arid steppe hot climate type (BSh), some differences in the recharge in the NASY and MDB regions were found. This difference was attributed to the reduction in the influence of the monsoon/cyclone-related rainfall on meteorological conditions in southern regions (which have an equi-seasonal rainfall distribution) compared to conditions found in northern regions.

In climate type BSh4 (NASY), the recharge shows some similarity in relationship with rainfall characteristics as in the Aw climate type. The daily rainfall above 40 mm summarised on an annual basis provides only a slightly better correlation with recharge than the total annual rainfall. For the same annual rainfall, the recharge in climate type BSh4 is greater than that estimated in climate type BSh3, which is due to the greater proportion of high daily rainfall events in the total annual rainfall in BSh4. Climate characteristics other than rainfall provide cumulatively a similar input to recharge prediction in both regions. However, solar radiation has higher relative importance in recharge estimation in the BSh4 climate type and VPD in the BSh3 climate type.

In the arid steppe cold climate type (BSk), recharge shows the weakest correlation with total annual rainfall among all considered zones. This correlation improves when the moving average over a 21-day interval is summarised on an annual basis with a daily threshold of 5 mm. This indicates the importance of particularly high rainfall events (as a single daily rainfall event greater than 100 mm/day) but more likely it identifies the importance of a prolonged series of daily rainfalls. The relative importance of other climate characteristics is also the lowest in this zone, though the relative importance of VPD seems to prevail.

In the temperate without dry season with hot summer climate type (Cfa), there is a particularly low correlation between estimated recharge under clays (low conductivity soils) and also a relatively higher importance of VPD compared to other climate characteristics. As in the case of the BSk climate type, the better correlation between rainfall and recharge is related to some of the moving averages, but over a shorter period of time (14-day interval) with a daily threshold of 5 mm. This indicates the importance of rare high rainfall events (as a single daily rainfall event greater than 70 mm/day) but also of a prolonged series of daily rainfalls.

Only one location was available for analysis of recharge relationship with climate characteristics in the arid desert hot climate type (BWh) and the cold without dry season with cold summer climate type (Dfc). Based on the limited data, it was concluded that the recharge/rainfall relationship is reasonably strong in the BWh climate type which also shows the greatest improvement when characteristics other than total annual rainfall are considered (moving average). The relative importance of other climate characteristics is higher compared to other climate types; particularly for VPD.

In the Dfc climate type, high annual rainfall and particularly low temperatures make this climate type quite unique. It has the strongest correlation between recharge and rainfall.

Table 4-3 provides a summary of the analyses for the most common land cover (perennials) and soil with high hydraulic conductivity (K > 1 m/day), which allows for some quantitative comparison of recharge characteristics between various climate types.

Table 4-3. Summary for perennial vegetation and K ≥ 1.0 m/d

Climate types	**Relative importance (R^2)**					**Rainfall characteristics**	**Sensitivity to rainfall change** a (slope)
	Total rainfall	***Best fit rainfall***	***T mean***	***Solar radiation***	***VPD***		
Aw	0.55	0.61	0.09	0.08	0.04	High daily rainfall events	0.36
BSh4	0.47	0.70	0.01	0.04	0.05		0.21
BSh3	0.49	0.71	0.04	0.03	0.07	High daily rainfall events and prolonged period rain	0.18
BWh	0.40	0.75	0.03	0.07	0.09		0.17
BSk	0.52	0.71	0.04	0.01	0.04		0.12
Cfa	0.62	0.76	0.03	0.02	0.07		0.24
Dfc	0.66	0.68	0.05	0.07	0.08	High daily rainfall events	0.94

The analyses were undertaken for the NASY and MBD regions where recharge estimation was available to the project. It was identified that:

- Annual rainfall is a major factor influencing recharge. However, for the majority of the climate types the total annual rainfall has a weaker correlation with recharge than the rainfall characteristics reflecting rainfall intensity.
- Annual recharge is more sensitive to daily rainfall intensity in regions with winter-dominated rainfall, where it is also less sensitive to absolute changes in annual rainfall.
- In regions with winter-dominated rainfall, the annual recharge under the same annual rainfall, soils and vegetation conditions is lower than in regions with summer-dominated rainfall. This was attributed to the differences between rainfall patterns associated with monsoons/cyclones of predominately heavy rains in the north and

frontal weather systems with prolonged periods of smaller daily rainfall events in the south.

- The relative importance of climate characteristics other than rainfall is higher for recharge under annual vegetation, but overall is highest in the tropical climate type. Solar radiation and VPD show greater relative importance than average annual daily mean temperature. Climate characteristics have lowest relative importance in arid (with cold winters) and temperate climate types.
- Episodic recharge is more likely associated with the desert climate type, with the probability of episodic recharge reducing in the sequence: arid > temporal > cold. However, episodic recharge may also occur in an area with overall high annual rainfall but under less conductive soils (such as vertosol) and with trees as a land cover.

The results of the analyses highlight the importance of the rainfall intensity projection under future climate scenarios, particularly in the southern regions of the country

5. EFFECT OF GCMS, DOWNSCALING METHODS AND SELECTION OF HYDROLOGICAL MODELS ON RECHARGE PROJECTION UNDER FUTURE CLIMATE

This section of the report describes the results of the modelling undertaken to evaluate the differences in GCMs, downscaling methods and hydrological models for projecting future recharge at three locations.

Investigations of climate impact on groundwater recharge in the Murray-Darling Basin Sustainable Yields (MDBSY) and Northern Australia Sustainable Yields (NASY) Projects used daily downscaling of 15 GCMs and a single recharge model (WAVES). The sustainable yields results indicated a greater variability of climate projection between the GCMs than variability of an individual GCM for different global warming scenarios. Recently, in addition to daily downscaling, statistical and dynamical downscaling methods were tested in Australia using various rainfall/runoff models to investigate the variability in runoff projections (Chiew et al., 2010). Similar analyses have not been undertaken for recharge estimation.

Within the current project we consider a single global warming scenario and estimate recharge using future climate derived from five GCMs (CSIRO Mk3.5, GFDL 2.0, GFDL 2.1, MIROC 3.2 midres, and MPI-ECHAM5) in their projections under the A2 scenario for 2050, using three downscaling methods (daily scaling (daily), stochastic downscaling model (ST), and daily scaling using dynamical downscaling model Cubic Conformal Atmospheric Model (CCAM) results (CCAM-scaled)), with four hydrological models (WAVES with and without plant growth, HELP, and SIMHYD). However, at this stage of the project development the analysis is not aiming to provide a conclusion on a best GCM, downscaling method or hydrological model for the assessment of future climate impacts on groundwater resources. Also, this chapter does not report on an evaluation of the recharge models' ability to simulate the effect of future climate on recharge as only a comparison of the water balance outputs was undertaken at this stage.

5.1. Climate data

5.1.1. Observed historical data

The three sites chosen for analysis (described in Chapter 2) have differing rainfall regimes (Figure 5-1). Gnangara (Wanneroo, Western Australia) had an annual average rainfall for the period 1981–2000 of 767 mm/year, Moorook (South Australia) had an average of 252 mm/year and Livingston Creek (Wagga Wagga, New South Wales) had an average of 599 mm/year.

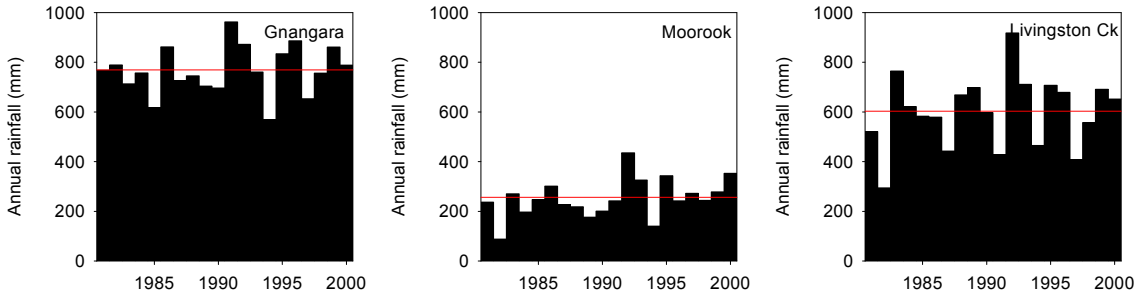

Figure 5-1. Observed annual series of rainfall at each site for the historical period (red line shows the average).

5.1.2. GCM outputs

The need for the downscaling of GCM rainfall outputs is highlighted in Figure 5-2. This shows that all five selected GCMs failed to reproduce the observed rainfall at Gnangara within 250 mm/year for the period 1981–2000. At the other two sites at least some GCMs get close to the observed average annual rainfall. Four of the five GCMs projected a decrease in rainfall for Gnangara and Moorook, with the CSIRO GCM showing a small increase at Gnangara and ECHAM showing a small increase for Moorook. At Livingston Creek, two (GFDL 2.1 and MIROC) of the five GCMs projected an increase in rainfall for the future climate period.

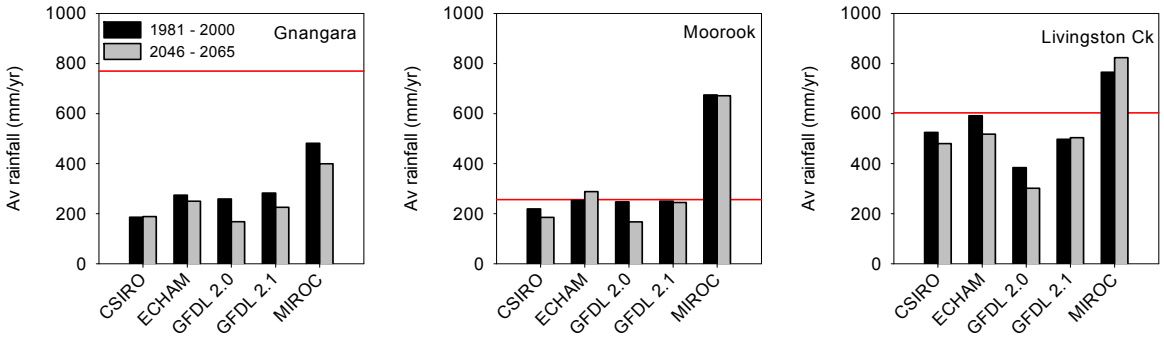

Figure 5-2. Average annual rainfall from the GCMs without downscaling for each of the three sites showing the current climate period (black), future climate period (grey) and the observed annual average for comparison (red line)

5.1.3. Downscaling

Three downscaling methods – a daily scaling approach (daily), a stochastic downscaling model (ST) and daily scaling based on dynamical downscaling model (Cubic Conformal Atmospheric Model (CCAM)) results (CCAM-scaled) – were used here with each of the five GCMs, giving a total of 15 future climate sequences for each field site (Figure 5-3).

For Gnangara, the range across the three downscaling methods for each GCM is less than the range across the five GCMs for each downscaling method with one exception (that being the range across the three downscaling methods for MIROC, which is greater than the range across the five GCMs for the CCAM-scaled and stochastic downscaling methods). For Moorook, the range across the three downscaling methods for each GCM is greater than the

range across the five GCMs for the CCAM-scaled and stochastic downscaling methods. The range across the five GCMs for the daily scaling is greater than the range across the three downscaling methods for each GCM. Likewise for Livingston Creek, the range across the three downscaling methods for each GCM is greater than the range across the five GCMs for the CCAM-scaled and stochastic downscaling methods. The range across the five GCMs for the daily scaling is greater than the range across the three downscaling methods for three out of five GCMs.

For each location there is one individual GCM that produces a much larger range across the three downscaling methods than the other four GCMs, but it is a different GCM for each region (MIROC for Gnangara, ECHAM for Moorook, and GFDL 2.0 for Livingston Creek).

There is often consistency in the relative changes across the three downscaling methods, e.g. for Moorook GFDL 2.0 is the driest GCM for all three downscaling methods, ECHAM is the wettest GCM for the daily and stochastic methods and the ranked order of the five GCMs (from driest to wettest) is the same for the daily and stochastic methods. For Livingston Creek the two driest GCMs (CSIRO and GFDL 2.0) are in common for daily and stochastic downscaling, and the driest CCAM-scaled downscaling is CSIRO. MIROC is the wettest for the daily and CCAM-scaled methods. For Gnangara, CSIRO is the wettest GCM for the daily and stochastic methods (this is surprising, given CSIRO was the driest GCM in the SWWASY project).

There is also consistency between the range of changes from the five GCMs for the CCAM-scaled and stochastic methods. For Moorook, the range across the five GCMs is 12% for CCAM-scaled (11% reduction to 1% increase) and 11% for stochastic (28% reduction to 17% reduction). For Livingston Creek, the range is 13% for CCAM-scaled (5% reduction to 8% increase) and 14% for stochastic (31% decrease to 17% decrease). For Gnangara, the range is 25% for CCAM-scaled (25% decrease to 0% change) and 26% for stochastic (32% decrease to 6% decrease). The daily range across the GCMs is largest for Moorook (53%, 35% decrease to 18% increase) which has the smallest CCAM-scaled and stochastic range.

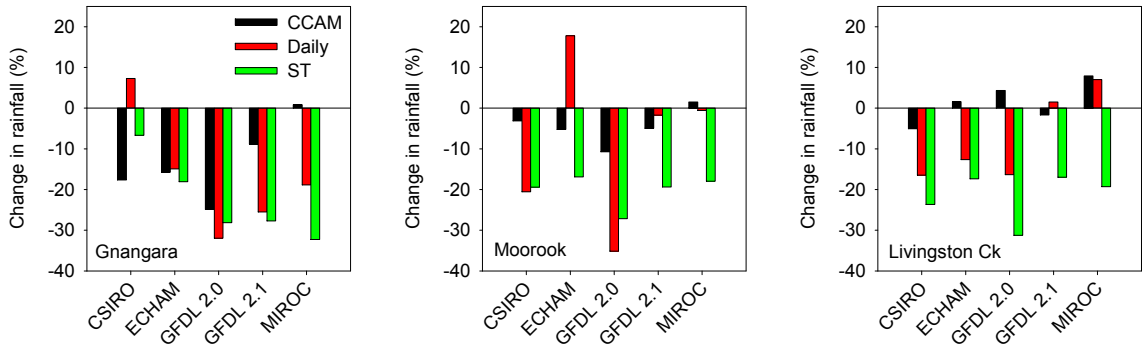

Figure 5-3. Comparison of change in rainfall for the downscaling methods for each GCM and site

A paired t-test was used to compare the means of the change in rainfall projected by the different GCMs after being downscaled. A significance level of 0.05 was used. The mean change in rainfall is displayed in Figure 5-4 as a red line in the boxplots. Across all sites, in 23 out of 30 comparisons the changes in rainfall projected by the GCMs are different from each other. Across all sites, in seven out of nine comparisons the changes in rainfall projected by the downscaling methods are different from each other.

At Gnangara, the GFDL 2.0 GCM is significantly different with overall lower rainfall to every other GCM. The CSIRO GCM is significantly different (higher) from all the other GCMs except MIROC. The stochastic downscaling was significantly different (lower) from the other two methods of downscaling and the CCAM-scaled and daily scaling were not significantly different from each other.

At Moorook, the only combination of GCMs that is not significantly different is MIROC and ECHAM. The stochastic downscaling was significantly different (lower) from the other two methods of downscaling and the CCAM-scaled and daily scaling were not significantly different from each other.

At Livingston Creek, the only combinations of GCMs that were not significantly different were CSIRO–GFDL 2.0 and ECHAM–GFDL 2.1. All downscaling methods were significantly different from each other; the daily scaling was the highest and the stochastic downscaling the lowest.

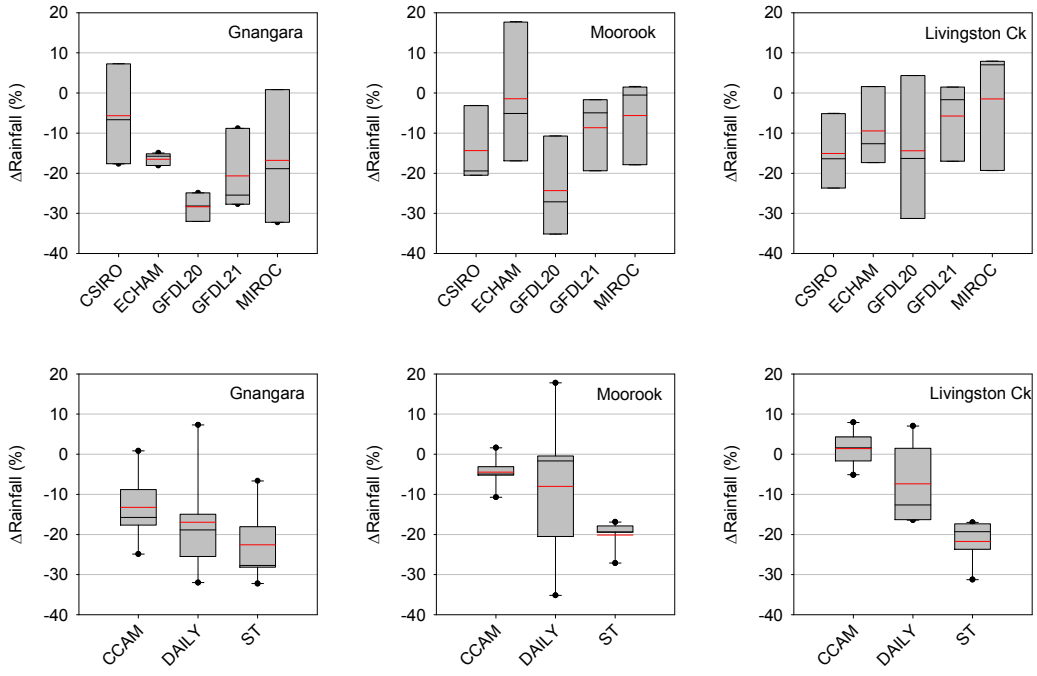

Figure 5-4. Boxplots of the change in rainfall at the three sites comparing the differences in GCMs and downscaling methods. The red line in the box represents the mean.

The rainfall under a future climate is projected to have changes in intensity as well as changes in magnitude; this means the distribution of rainfall will change rather than just having a change in the mean. This can be displayed as a probability of exceedance curve (Figure 5-5, Figure 5-6 and Figure 5-7). The percentage of total rainfall that occurs on the highest 1% of days has been used as the metric of rainfall intensity. This shows that in the majority of cases (40/45) that the proportion of rainfall on the highest 1% of days is projected to increase.

At Gnangara, the greatest increase in intensity of rainfall is from the MIROC/ST10 climate with an increase from 22.3% of rainfall occurring on the highest 1% of days to 31.1% of rainfall occurring on the highest 1% of days. The greatest decrease is from the CSIRO/ST90

climate from 24.9% down to 23.3% of total rainfall occurring on the highest 1% of days (Figure 5-5).

At Moorook, the greatest increase in intensity of rainfall is from the GFDL 2.0/ST90 climate with an increase from 31.4% of rainfall occurring on the highest 1% of days to 42.6% of rainfall occurring on the highest 1% of days. The greatest decrease is from the MIROC/ST90 climate from 34.1% down to 33.3% of total rainfall occurring on the highest 1% of days (Figure 5-6).

At Livingston Creek, the greatest increase in intensity of rainfall is also from the GFDL 2.0/ST90 climate with an increase from 25.9% of rainfall occurring on the highest 1% of days to 32.8% of rainfall occurring on the highest 1% of days. The greatest decrease is from the ECHAM/CCAM-scaled climate from 24.0% down to 22.9% of total rainfall occurring on the highest 1% of days (Figure 5-7).

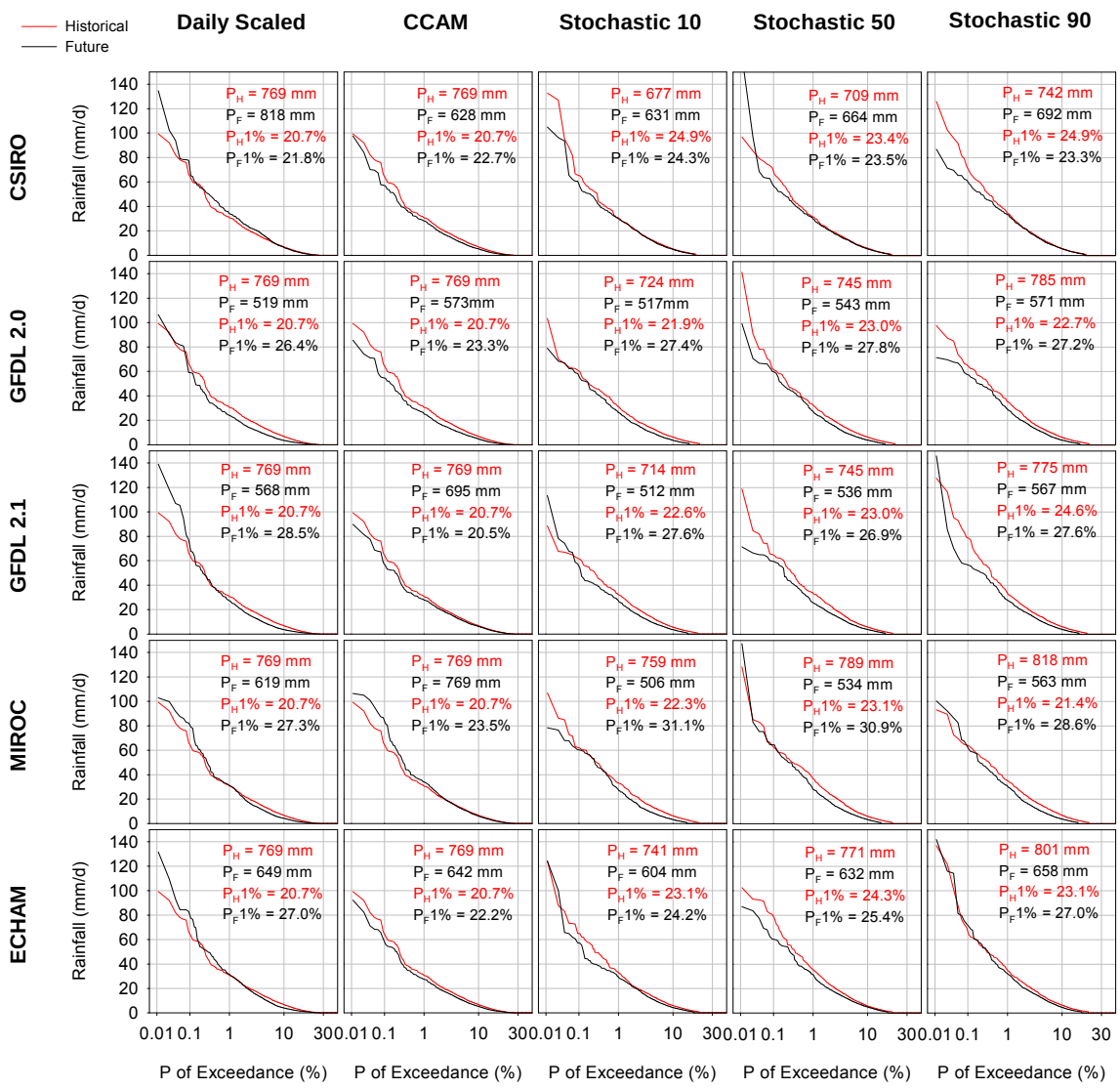

Figure 5-5. Probability of exceedances of daily rainfall for the current and future climates for Gnangara. 'Stochastic 10', 'Stochastic 50', and 'Stochastic 90' refer to the 10th, 50th and 90th percentile replicates (in terms of mean annual rainfall change) extracted from 100 stochastic replicates. P_H refers to the historical rainfall and P_F refers to the future rainfall.

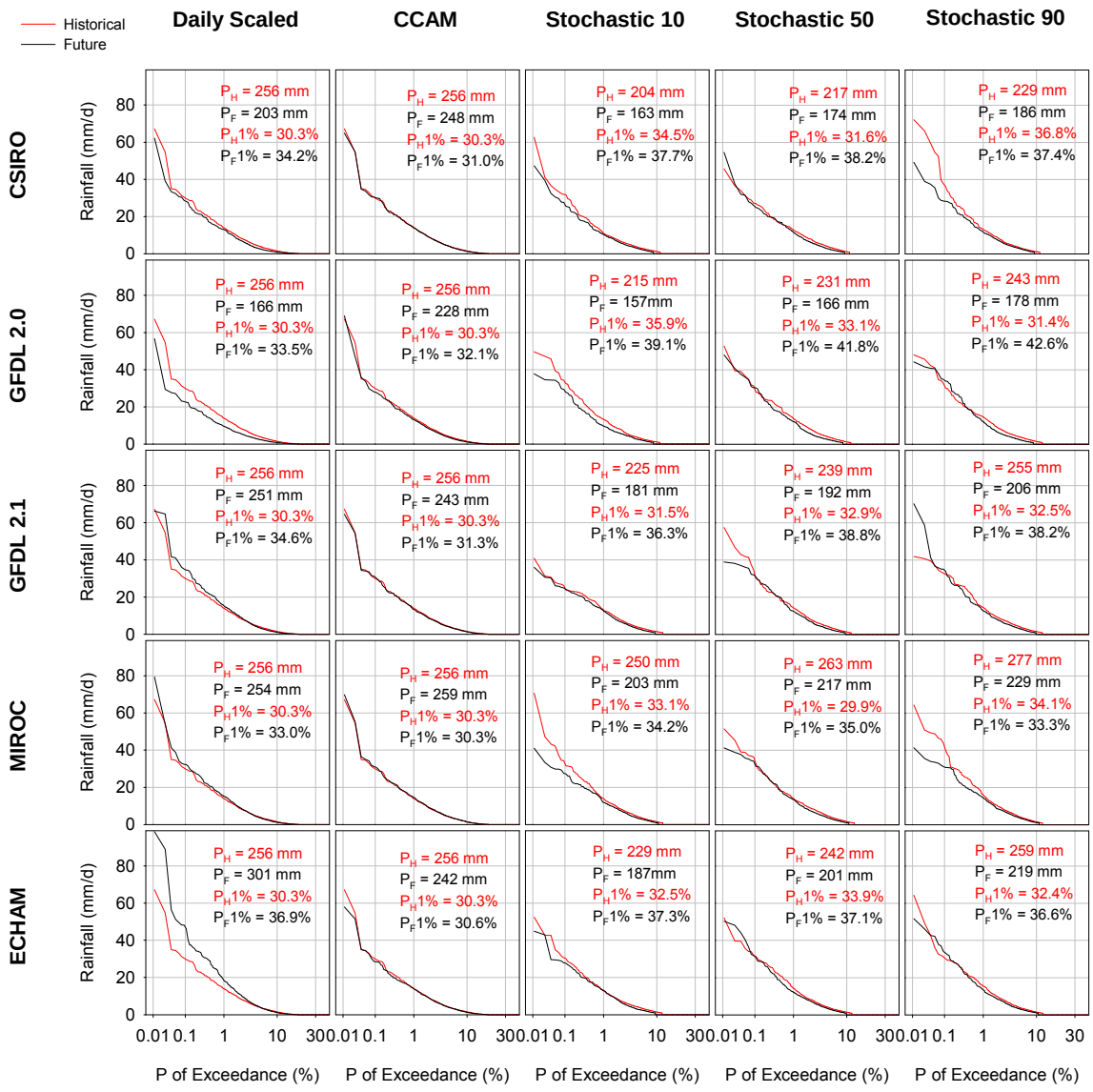

Figure 5-6. Probability of exceedances of daily rainfall for the current and future climates for Moorook. 'Stochastic 10', 'Stochastic 50', and 'Stochastic 90' refer to the 10th, 50th and 90th percentile replicates (in terms of mean annual rainfall change) extracted from 100 stochastic replicates. P_H refers to the historical rainfall and P_F refers to the future rainfall.

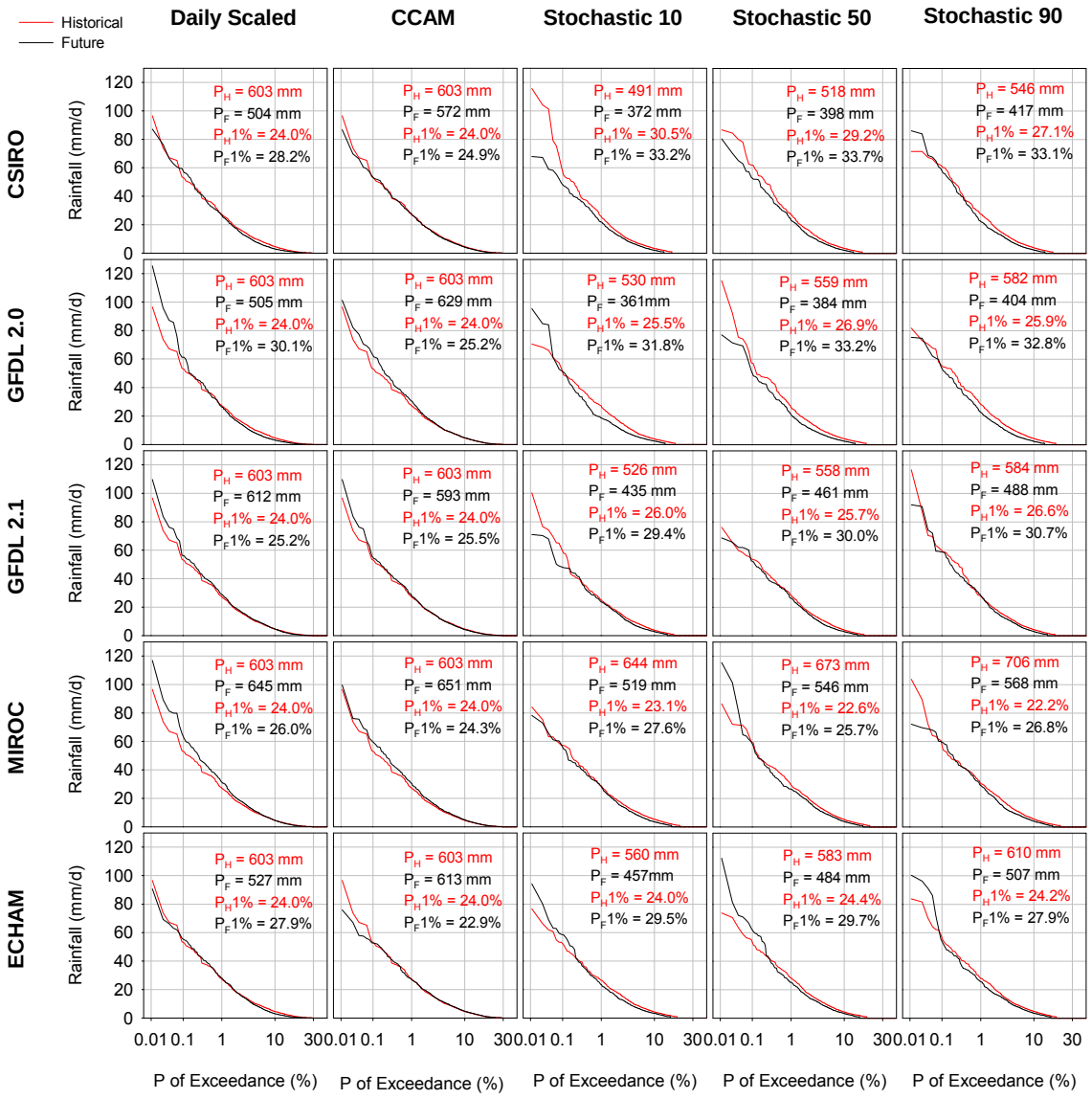

Figure 5-7. Probability of exceedances of daily rainfall for the current and future climates for Livingston Creek. 'Stochastic 10', 'Stochastic 50', and 'Stochastic 90' refer to the 10th, 50th and 90th percentile replicates (in terms of mean annual rainfall change) extracted from 100 stochastic replicates. P_H refers to the historical rainfall and P_F refers to the future rainfall.

5.2. Calibration of hydrological models

Gnangara

At Gnangara, four hydrological models were calibrated to the recharge estimates made by Sharma et al. (1991) (which were approximately 50% of rainfall). The results of the baseline historical scenario are presented in Table 5-1.

Table 5-1. Summary of the annual averages of the water balance terms from the calibrated hydrological models at Gnangara

	Rain (mm)	ET (mm)	Recharge (mm)	Runoff (mm)	Recharge (% P)
HELP	762	400	363	0	48
SIMHYD	762	360	343	59	45
WAVES-C	762	387	376	0	49
WAVES-G	762	385	378	0	50

Moorook

At Moorook, four hydrological models were calibrated to the recharge estimates made by Cook et al. (2004) (which were approximately 5% of rainfall). The results of the baseline historical scenario are presented in Table 5-2.

Table 5-2. Summary of the annual averages of the water balance terms from the calibrated hydrological models at Moorook

	Rain (mm)	ET (mm)	Recharge (mm)	Runoff (mm)	Recharge (% P)
HELP	256	252	2	0	0.9
SIMHYD	256	242	13	1	5
WAVES-C	256	249	11	0	4
WAVES-G	256	249	10	0	4

Livingston Creek

At Moorook, HELP and two WAVES models were calibrated to the volume of streamflow with a relative split between recharge and runoff based upon an interpretation of the site data by Summerell (2004). SIMHYD is generally calibrated to a time series of streamflow and the same has been done here in line with common practice for this type of model. Figure 5-8

shows the scatter plot of monthly modelled and simulated runoffs achieved in the calibration for the Livingstone Creek catchment showing an R^2 of 0.6. Although calibrated for a relatively short duration, the result gives some degree of confidence in model performance for predicting future runoff using future climate scenario data. The results of the baseline historical scenario for all models are presented in Table 5-3.

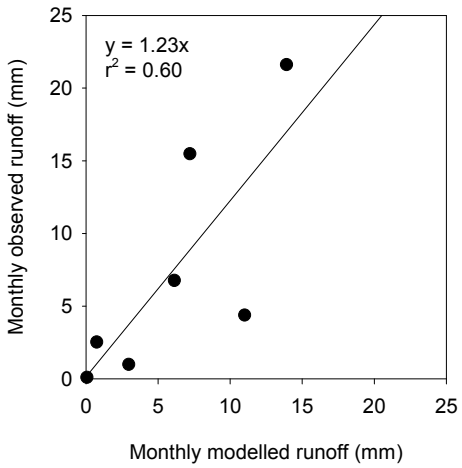

Figure 5-8. Scatter plot of monthly modelled and simulated runoff for the Livingstone Creek catchment

Table 5-3. Summary of the annual averages of the water balance terms from the calibrated hydrological models at Livingston Creek

	Rain (mm)	ET (mm)	Recharge (mm)	Runoff (mm)	Recharge (% P)
HELP	603	509	21	72	4
SIMHYD	603	504	93	6	15
WAVES-C	603	532	22	54	4
WAVES-G	603	524	26	58	4

5.3. Recharge under a future climate

A summary of the change in recharge between the future climate and the historical climate scenarios modelled for each of the sites using every combination of GCM, downscaling method and hydrological model is displayed in Figure 5-9. When this is compared to Figure 5-3 it can be seen that in 75% of cases where rainfall is projected to increase, recharge is also projected to increase. Similarly, in 92% of cases where rainfall is projected to decrease, recharge is also projected to decrease.

At Gnangara the range of recharge projections is from +17% to –55% with a median of –31%. Both extremes come from the HELP model with the high recharge estimated from the CSIRO/daily climate and low recharge estimated from the MIROC/ST climate. At Moorook, the range of recharge projections is from +553% to –80% with a median of –37%. Both extremes come from the HELP model with the high recharge estimated from the ECHAM/daily climate and the low recharge estimated from the MIROC/ST climate. At Livingston Creek, the range of recharge projections is from +101% to –68% with a median of –7%. The extremes come from the WAVES-C model with the high recharge from the MIROC/CCAM-scaled climate and low recharge estimated from the GFDL 2.0/ST climate.

At Gnangara, the maximum range of recharge projections from a given climate sequence generated from a combination of a GCM and a downscaling method and the different hydrological models is 13% from GFDL 2.0/ST and the minimum range is 3% from MIROC/daily. At Moorook, the maximum range of recharge projections from a given climate sequence and the different hydrological models is 595% from ECHAM/daily and the minimum range is 12% from GFDL 2.0/daily. At Livingston Creek the maximum range of recharge projections from a given climate sequence and the different hydrological models is 86% from MIROC/CCAM-scaled and the minimum range is 7% from MIROC/ST.

Across all sites, HELP was the most frequent model to produce the lowest recharge (56%) and WAVES-G was the least frequent model to produce the lowest recharge (2%). SIMHYD and WAVES-G were equally the most frequent model to produce the highest recharge (29% each) and HELP was the least frequent model to produce the highest recharge (18%).

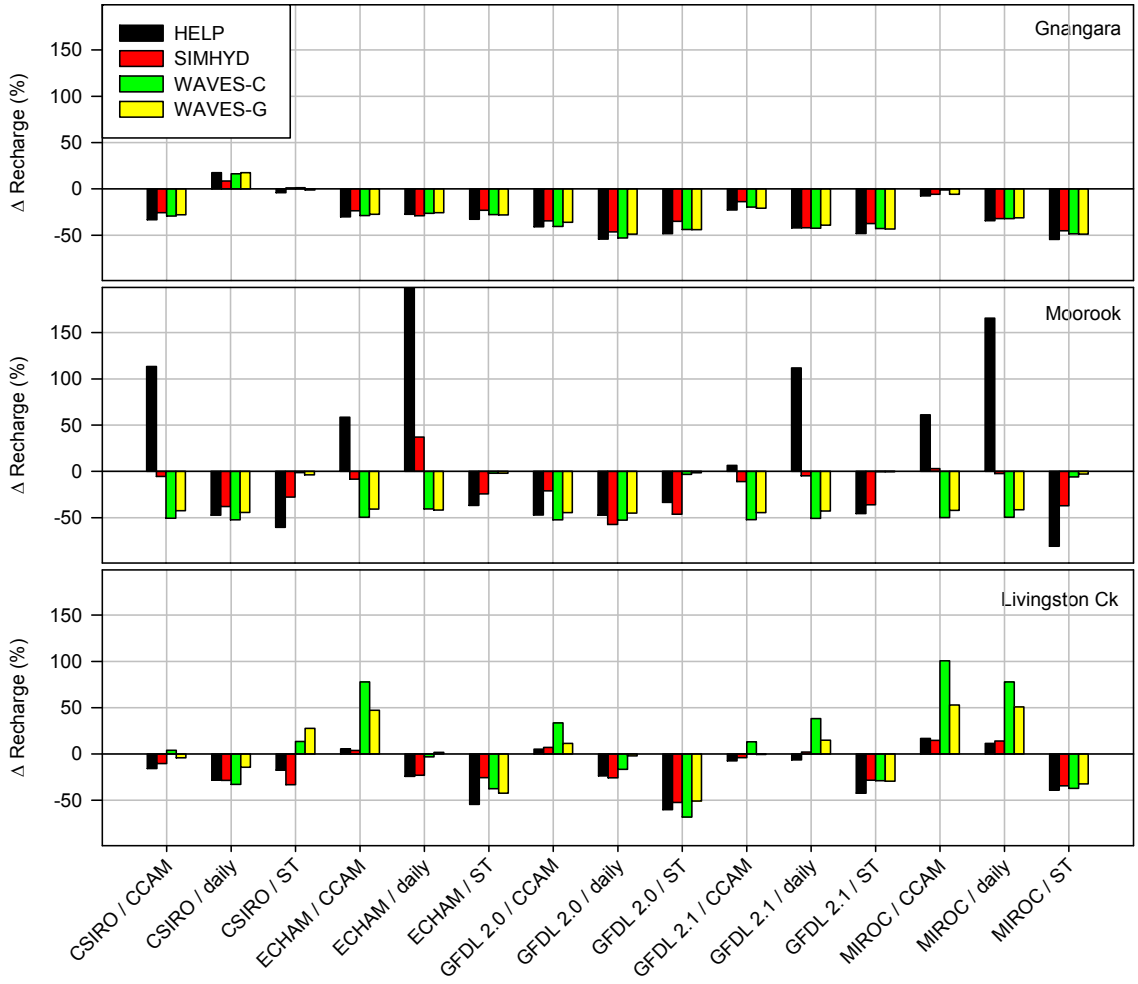

Figure 5-9. The change in recharge estimated from each hydrological model for every combination of future climate projected by the GCMs and downscaling methods

5.3.1. Comparison of GCMs

A paired t-test was used to compare the mean change in recharge estimated from the climate sequences derived from the different GCMs. A significance level of 0.05 was used. The paired t-test is not assessing how close to the line the points are in Figure 5-10, it is assessing whether the points fall on one side of the line. Across all sites, in 11 out of 30 comparisons the changes in recharge estimated from the GCMs are different from each other (Figure 5-11).

At Gnangara, the GFDL 2.0 and CSIRO GCMs are significantly different to every other GCM. At Moorook, there were no combinations of GCMs where significantly different recharge was projected. At Livingston Creek, MIROC was significantly different to all GCMs except CSIRO, and the only other combination that was significantly different was ECHAM-GFDL 2.0.

When the relationship between the change in rainfall and the change in recharge is compared for each GCM there are no patterns that emerge across the sites (Figure 5-12).

At Gnangara, the GFDL 2.0 and CSIRO, GFDL 2.1 and MIROC GCMs appear to have a similar relationship. The ECHAM GCM is quite different, but this is mainly because of the small spread in change in rainfall from the different downscaling methods. The curves fitted at Gnangara have the least difference between them of all the sites.

At Moorook, none of the GCMs appear to have a similar relationship between the change in rainfall and change in recharge. Of the three sites, Moorook has the greatest spread in the curves fitted.

At Livingston Creek, there is more spread in the curves than at Gnangara but less than at Moorook. None of the GCMs appear to follow the same relationship between change in rainfall and change in recharge, with the CSIRO GCM not fitting the same trend as the other GCMs.

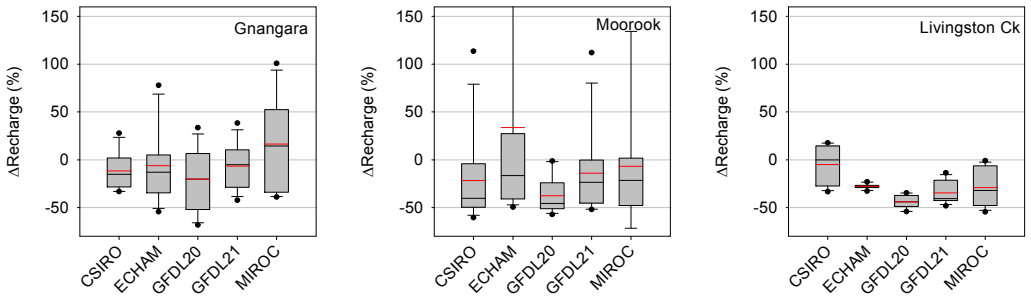

Figure 5-10. Comparison of the change in recharge at each site aggregated by GCM. The red line in the box represents the mean

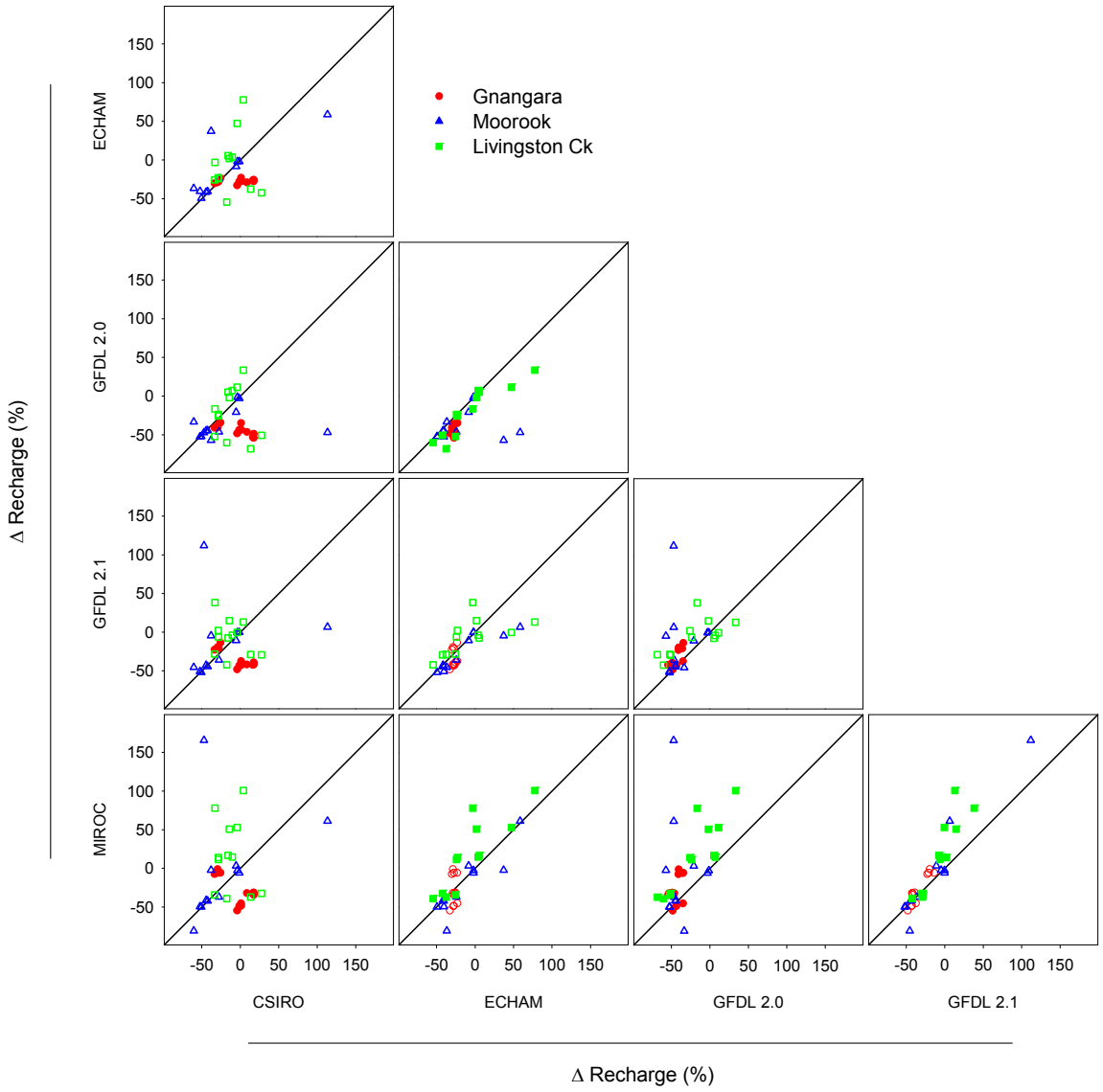

Figure 5-11. Comparison between the change in recharge for the different GCMs at the different sites. The colour filled symbols indicate that the recharge from the two GCMs are different according to a paired t-test.

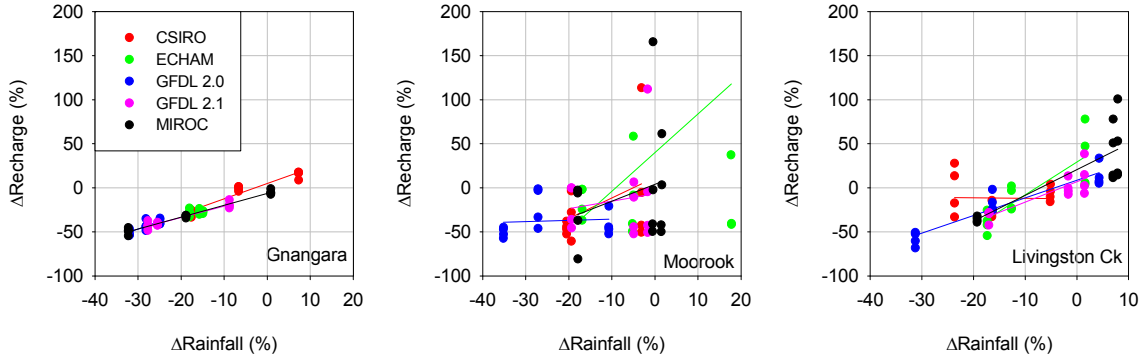

Figure 5-12. The relationship between the change in rainfall and the change in recharge for the different GCMs at the different sites

5.3.2. Comparison of downscaling methods

A paired t-test was used to compare the mean change in recharge estimated from the different downscaling methods (Figure 5-13). A significance level of 0.05 was used. Across all sites, in four out of nine comparisons the changes in recharge estimated by the different downscaling methods are different from each other (

Figure 5-14).

At Gnangara, the daily scaling was significantly different (higher) from the stochastic downscaling, CCAM-scaled was not significantly different from either of the other two downscaling methods. At Moorook, none of the downscaling methods were significantly different from each other for recharge. At Livingston Creek, all of the downscaling methods were significantly different from each other; the daily scaling was the highest and the stochastic downscaling the lowest.

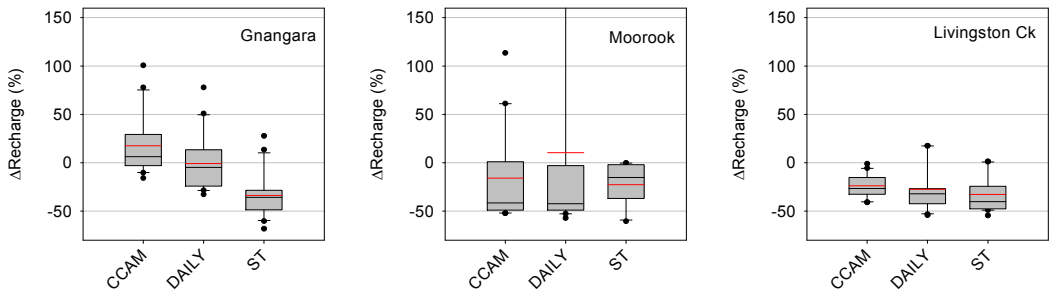

Figure 5-13. Comparison of the change in recharge at each site aggregated by downscaling method. The red line in the box represents the mean.

When the relationship between the change in rainfall and change in recharge is compared for each downscaling method there are no patterns that emerge across the sites (Figure 5-15).

At Gnangara, the three downscaling methods have little spread in the relationship between the change in rainfall and the change in recharge. The stochastic downscaling has the steepest slope (1.9) and CCAM-scaled has the flattest slope (1.3).

At Moorook, the daily scaling and CCAM-scaled relationships between change in rainfall and change in recharge have a similar slope but different intercepts, for no change in rainfall the CCAM-scaled relationship would predict a 1% decrease in recharge but the daily scaling relationship would predict an increase in recharge of 36%. The stochastic downscaling results do not have a relationship between the change in rainfall and change in recharge.

At Livingston Creek, the three downscaling methods produce different relationships between change in rainfall and change in recharge. CCAM-scaled has the steepest slope in the relationship between the change in rainfall and the change in recharge and the stochastic downscaling has the flattest slope.

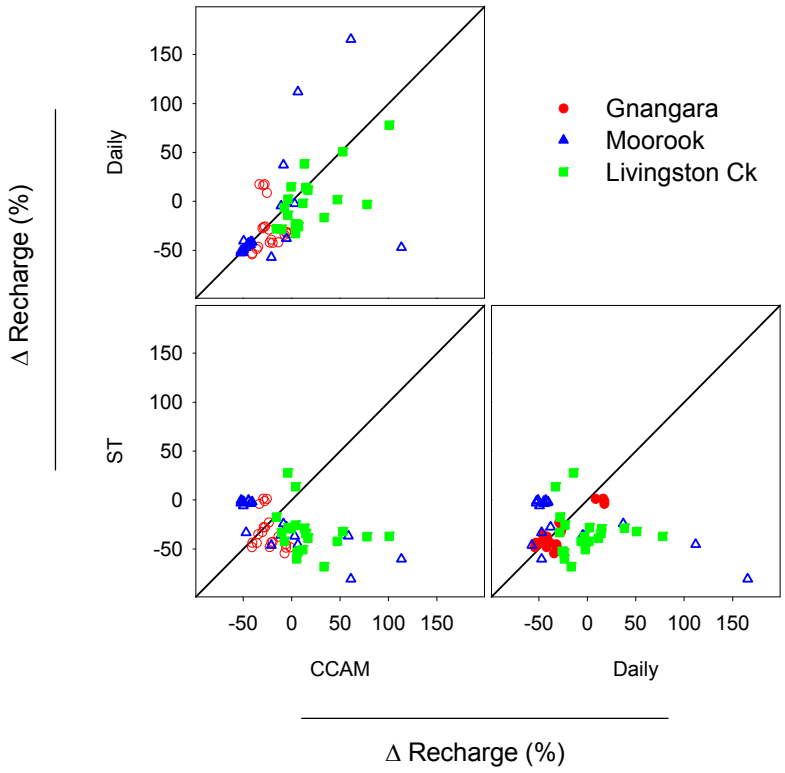

Figure 5-14. Comparison between the change in rainfall and the change in recharge for the different downscaling methods at the different sites. The colour filled symbols indicate that the rainfall or recharge from the two downscaling methods are different according to a paired t-test.

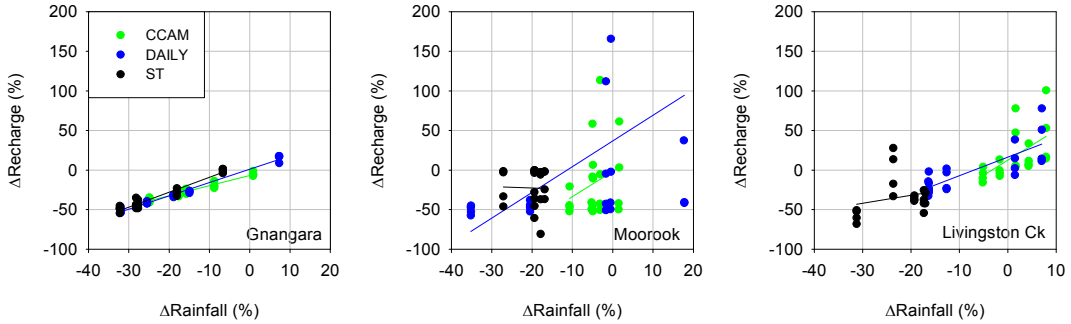

Figure 5-15. The relationship between the change in rainfall and the change in recharge for the different downscaling methods at the different sites

5.3.3. Comparison of hydrological models

A paired t-test was used to compare the mean change in recharge estimated from the different hydrological models (Figure 5-16). A significance level of 0.05 was used. Across all sites, in eight out of 18 comparisons the changes in recharge projected by the hydrological models are different from each other (Figure 5-17).

At Gnangara, recharge from the HELP model is significantly different (lower) from all the other models. The other models are not significantly different from one another. At Moorook, only the WAVES-C and WAVES-G models are significantly different from each other with WAVES-G giving a slightly higher recharge. At Livingston Creek, the HELP model is significantly different (lower) than both WAVES models; the SIMHYD model is also significantly different (lower) than both WAVES models. HELP and SIMHYD are not significantly different from each other and neither are the two WAVES models.

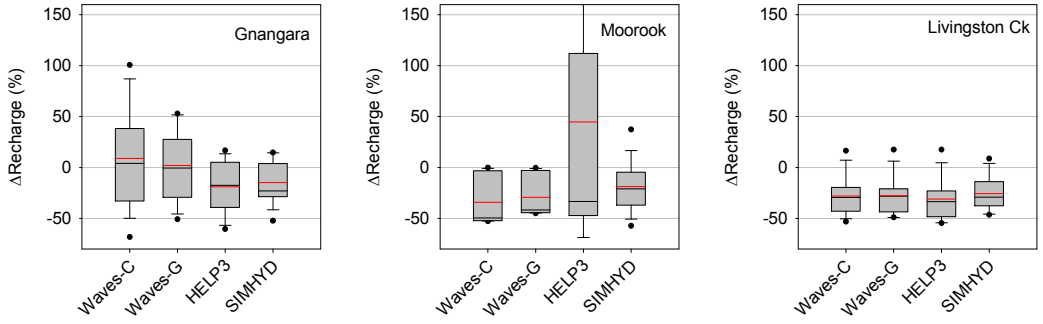

Figure 5-16. Comparison of the change in recharge at each site as aggregated by hydrological model. The red line in the box represents the mean.

When the relationship between the change in rainfall and change in recharge is compared for each hydrological model there are no patterns that emerge across the sites (Figure 5-18).

At Gnangara, the four models are tightly grouped in their relationship between the change in rainfall and the change in recharge. The HELP model has the greatest slope (1.7) and the SIMHYD model has the flattest slope (1.4).

At Moorook, the four models are very different in their relationships between the change in rainfall and the change in recharge. The two WAVES models have a negative slope, implying that recharge decreases with an increase in rainfall; however, in both cases the slope of this line is not statistically significant. This is likely to be indicative of the deep unsaturated zone not having come into equilibrium within the 20-year model run. The HELP model has a slope of 9.8, one reason why it may be so much greater than the other models is related to the calibrations; the HELP model has a baseline recharge for Moorook of one-fifth of the other models. The SIMHYD model has much less scatter in its relationship between change in

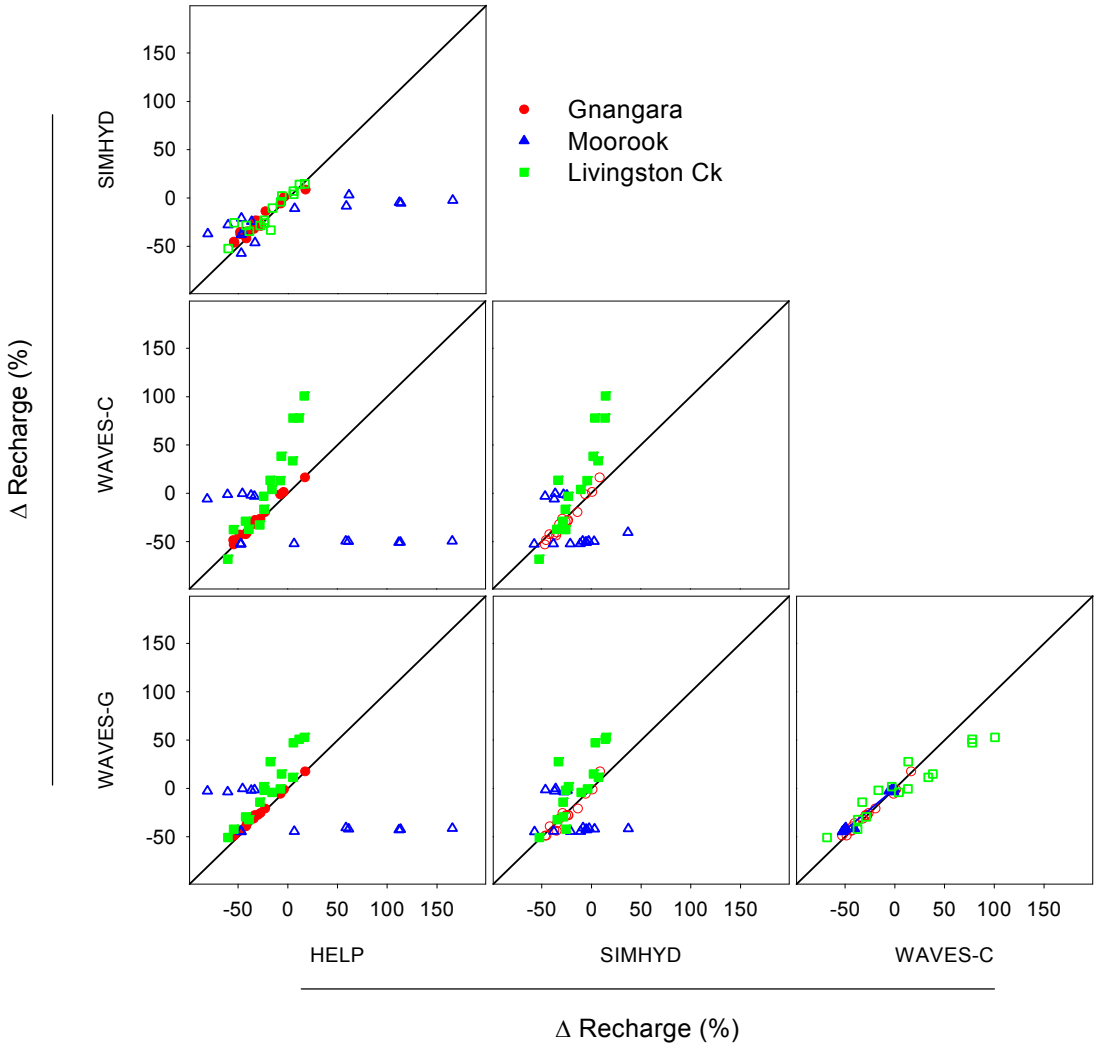

Figure 5-17. Comparison between the change in recharge for the different hydrological models at the different sites. The colour filled symbols indicate that the recharge from the two hydrological models are different according to a paired t-test.

rainfall and change in recharge when compared to the other models at this site; it has an r^2 of 0.98 between the change in rainfall and the change in recharge. This means that that 98% of the variance in change in recharge estimates is explained by the change in rainfall. This would suggest that the change in recharge estimated from SIMHYD is only sensitive to the total change in rainfall; the other climate variables, rainfall intensity and seasonality do not

have an effect (this is similar across all three sites for SIMHYD, with an r^2 of 0.92 at Gnangara and 0.99 at Livingston Creek).

At Livingston Creek, HELP and SIMHYD have similar slopes (1.7) in the relationship between the change in rainfall and the change in recharge but SIMHYD has a greater intercept. The WAVES-G model has a slightly higher slope (2.0) than SIMHYD and HELP and also a greater intercept, this means that it predicts more recharge. The WAVES-C model has a much greater slope (3.5) than the other three models.

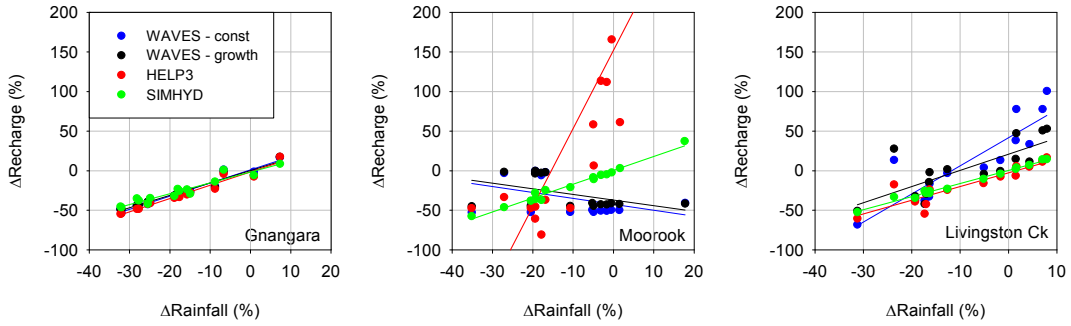

Figure 5-18. The relationship between the change in rainfall and the change in recharge for the different hydrological models at the different sites

5.3.4. Comparison of change in rainfall and change in runoff at Livingston Creek

A comparison of the change in recharge and change in runoff (Figure 5-19) shows that in 53 out of 60 cases the direction of the change is consistent. There is a tendency for increases in recharge to be proportionally greater than increases in runoff and also for decreases in recharge to be proportionally greater than changes in runoff. This suggests that at this site recharge is more sensitive to climate change than runoff.

There are six cases where the change in recharge is positive and the change in runoff is negative. These occur with both WAVES models, all three downscaling methods and two of the five GCMs (CSIRO and ECHAM).

There is one case where runoff increases where recharge decreases, this occurred with the WAVES-G model for the GFDL 2.1/CCAM-scaled climate.

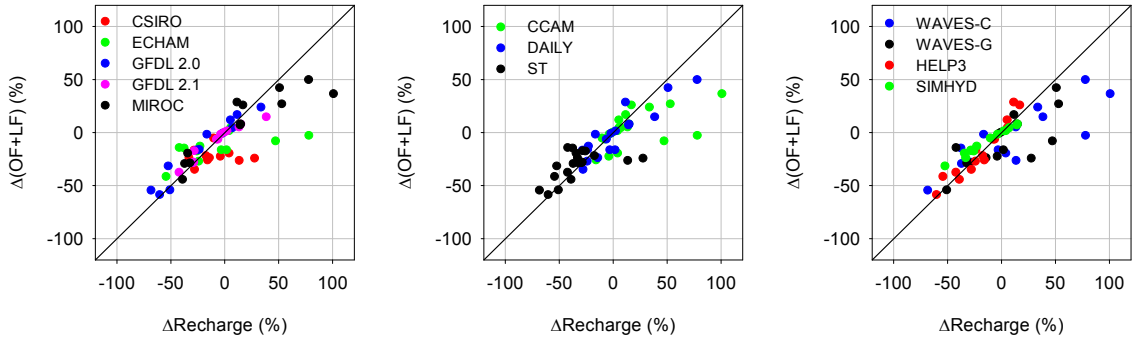

Figure 5-19. Comparison between the change in recharge and change in runoff at Livingston Creek where runoff is the sum of overland flow (OF) and lateral flow (LF)

5.4. Conclusions

This comparison was not aimed at providing a best GCM, downscaling method or hydrological model, it only sought to highlight the differences between them. The five GCMs chosen here are amongst the best-performing GCMs available when considering their ability to simulate the historical climate. However, there is considerable uncertainty in their projections of rainfall with no site having all GCMs projecting changes in rainfall in the same direction.

There was a trend in the downscaling methods where CCAM-scaled would project the highest rainfall, followed by the daily scaling and the stochastic downscaling projecting the least rainfall. Daily downscaling resulted in the greatest range of projected changes in rainfall. There has been no attempt to rank the downscaled results based on GCM or downscaling method performance for the current climate period. For example, relative biases in GCM rainfall are generally larger than biases in the atmospheric predictors used by the stochastic downscaling model and GCM rainfall seasonality is generally poor (not shown), so confidence in scaling factors derived from GCM-projected changes in seasonal rainfall may be low. Therefore there could be support for more confidence in the stochastic downscaled results relative to the daily scaled results; however, thorough testing of this hypothesis is beyond the scope of the current research.

The four hydrological models were all successfully calibrated using sensible parameters to match the recharge estimated from field measurements demonstrating that they could be used for impact studies. Each model differs considerably in its conceptualisation and therefore in its ability to simulate physical processes. Though sensitivity of the modelling to changes in those processes will be undertaken in a later stage of this project, an observation from the modelling is that at two of three sites HELP projected significantly lower recharge than both WAVES models.

There were considerable differences in the change in recharge projected by the different combinations of GCM, downscaling method and hydrological model at each site:

- At Gnangara where the historical recharge was the highest of all three sites (~360 mm) the range of recharge projections was the most consistent and ranged from +17% to –55% with a median of –31% from –18% projected change in rainfall. Only

one combination of GCM/downscaling (CSIRO/daily) resulted in an increase in recharge at this site from all the models. All other combinations projected a reduction in future recharge except for CSIRO/ST with the SIMHYD and WAVES-C models.

- At Moorook where the recharge and rainfall was particularly low, the range of recharge projections is from +553% to –80% with a median of –37% from –18% projected change in rainfall. The largest change in recharge projections were from the HELP model.
- At Livingston Creek with predominately clay-rich soils, the range of recharge projections is from +101% to –68% with a median of –7% from –2% projected change in rainfall. At this site increases in recharge were consistently projected when recharge modelling was based on CCAM-scaled downscaling for the majority of GCMs.

This range of projections across the sites highlights the uncertainty in making projections of recharge under a future climate and as such indicates that the application of a single GCM, downscaling method and hydrological model could be inadequate for future groundwater resources projection (see Chapter 1).

APPENDIX A

This appendix contains a series of plots which are used for illustration of the results and discussion in Chapter 4. It includes:

- relationships between annual rainfalls, temperature solar radiation and vapour pressure deficit for all considered climate types (Figures A-1 to A-7)
- probabilities of exceedance of annual recharge for various vegetation, climate types and soil types (Figures A-8 to A-10)
- The climate types maps showing annual average recharge and a(slope) of the relationship between recharge and annual average rainfall for annual, perennial vegetation and trees under soil with high hydraulic conductivity, plotted over annual average rainfall (Figure A-11).

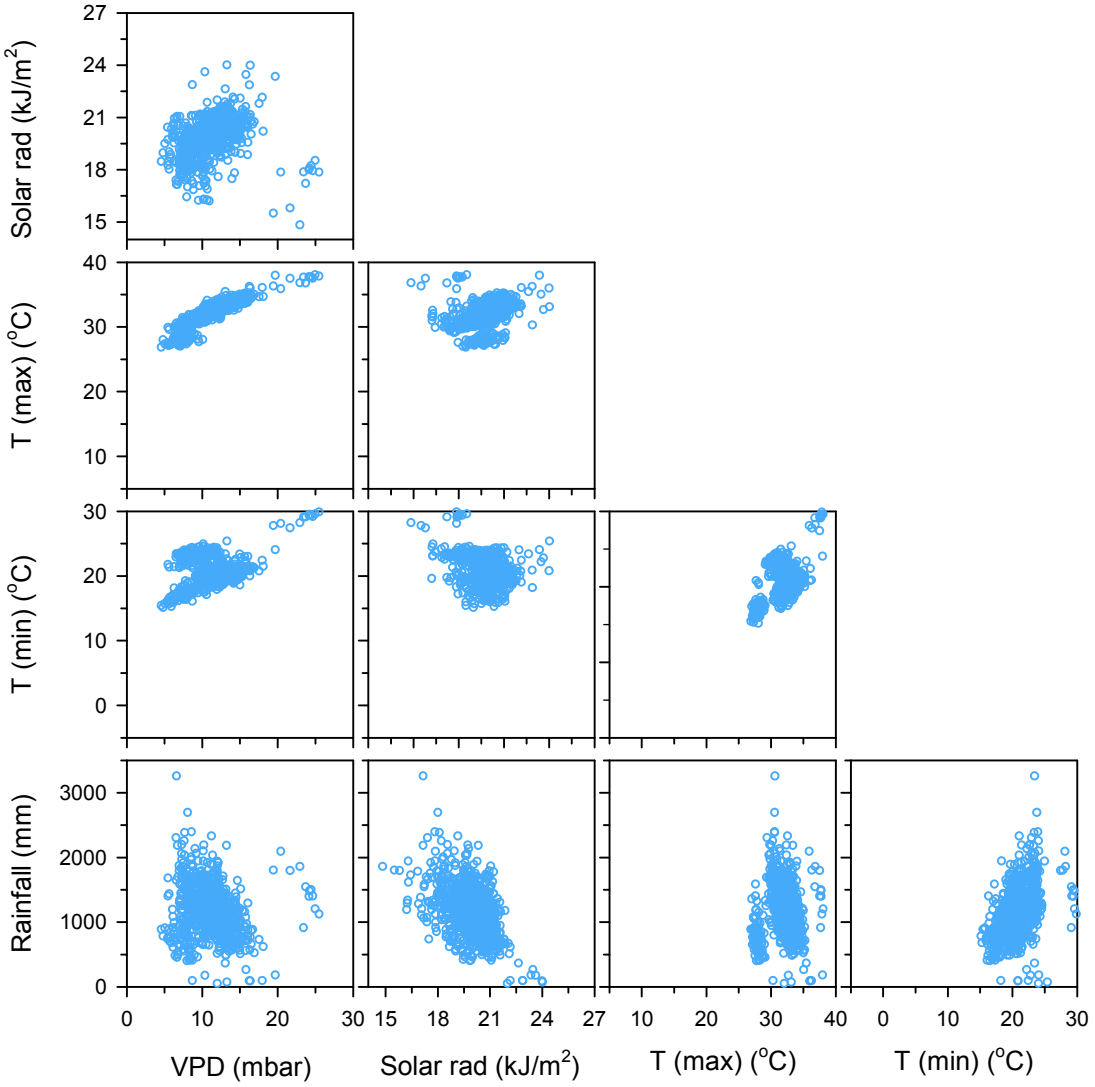

Figure A-1. Relationship between annual rainfalls, temperature solar radiation and vapour pressure deficit for Aw climate type

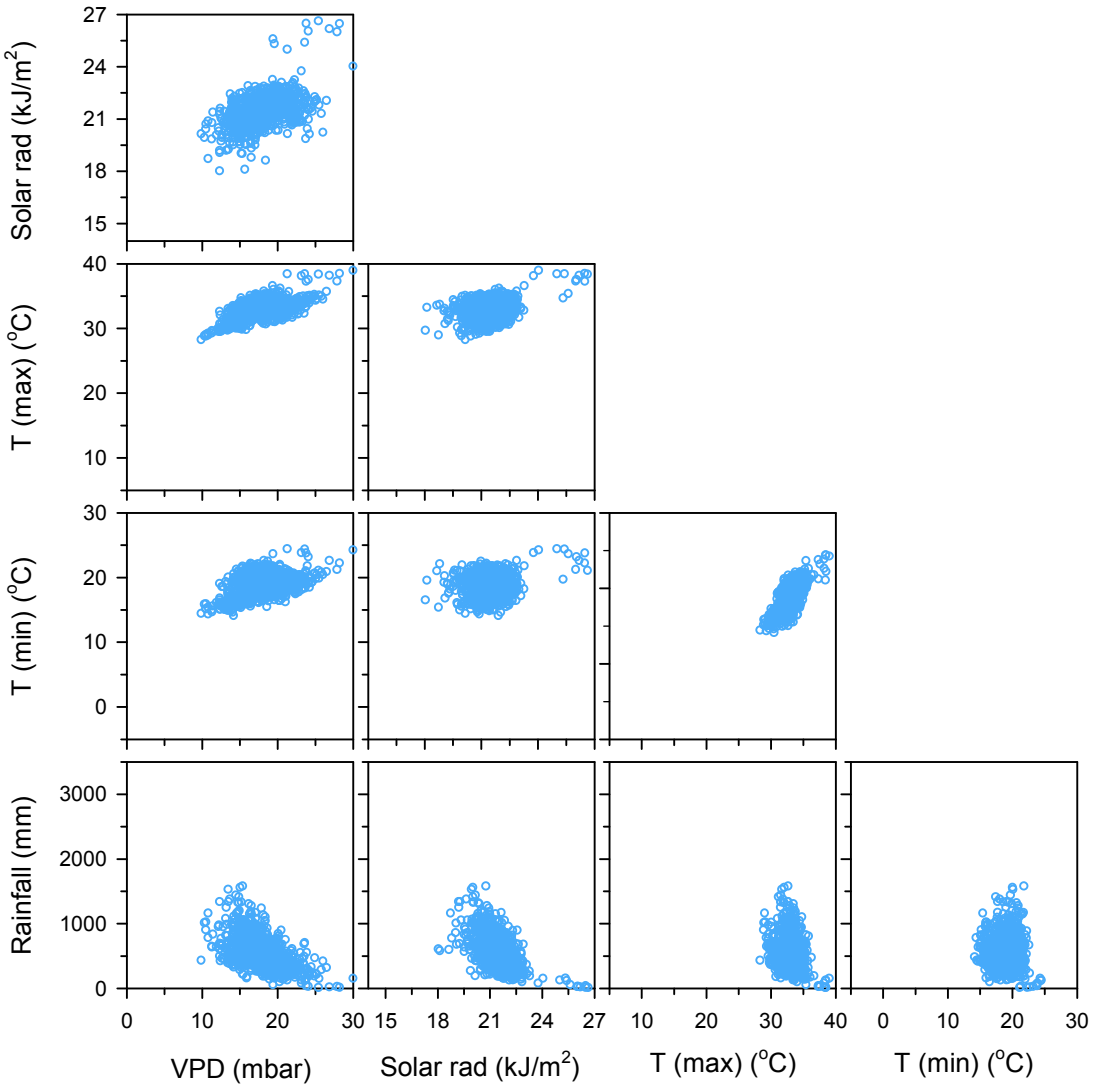

Figure A-2. Relationship between annual rainfalls, temperature solar radiation and vapour pressure deficit for BSh4 climate type

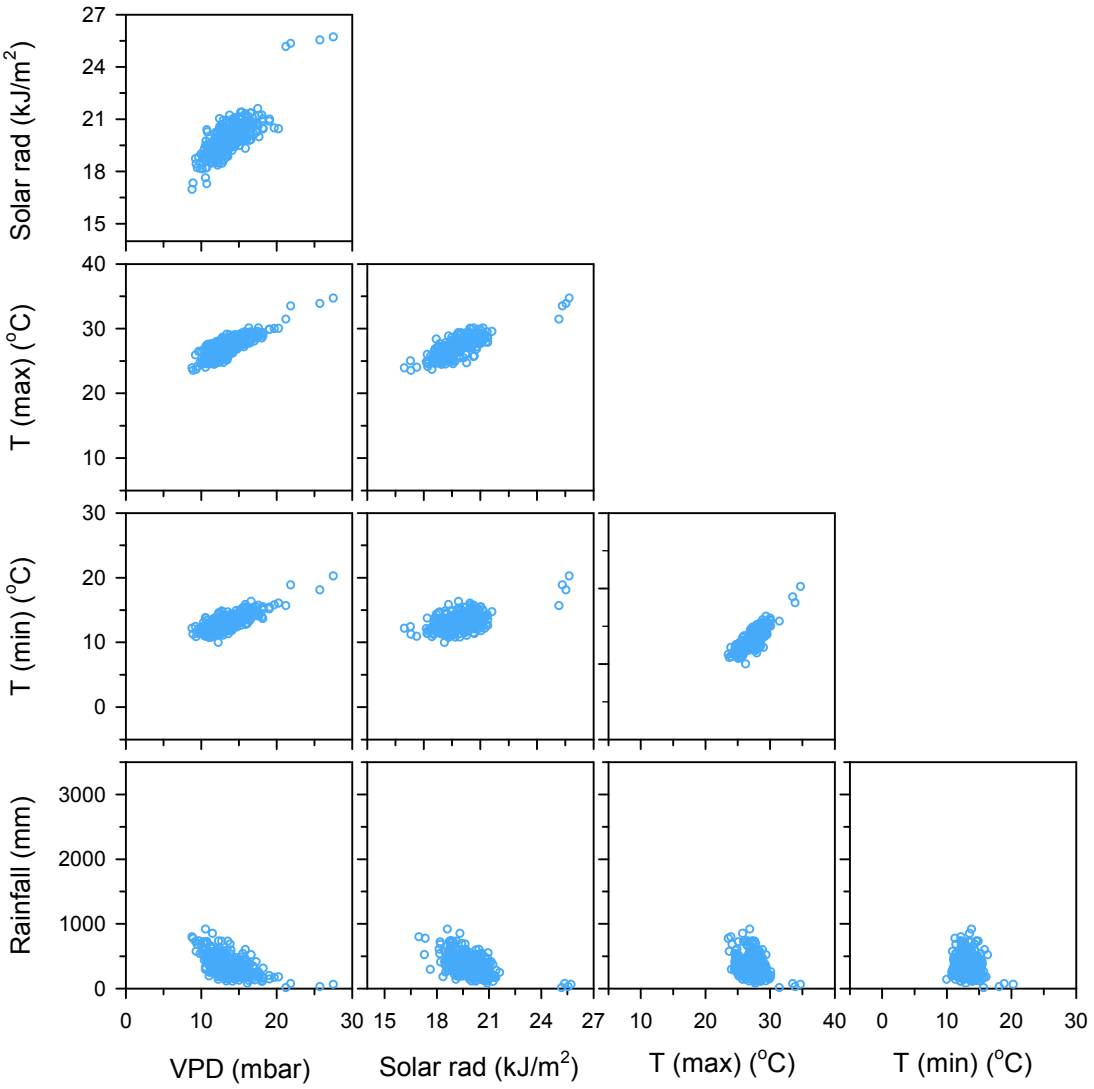

Figure A-3. Relationship between annual rainfalls, temperature solar radiation and vapour pressure deficit for BSh3 climate type

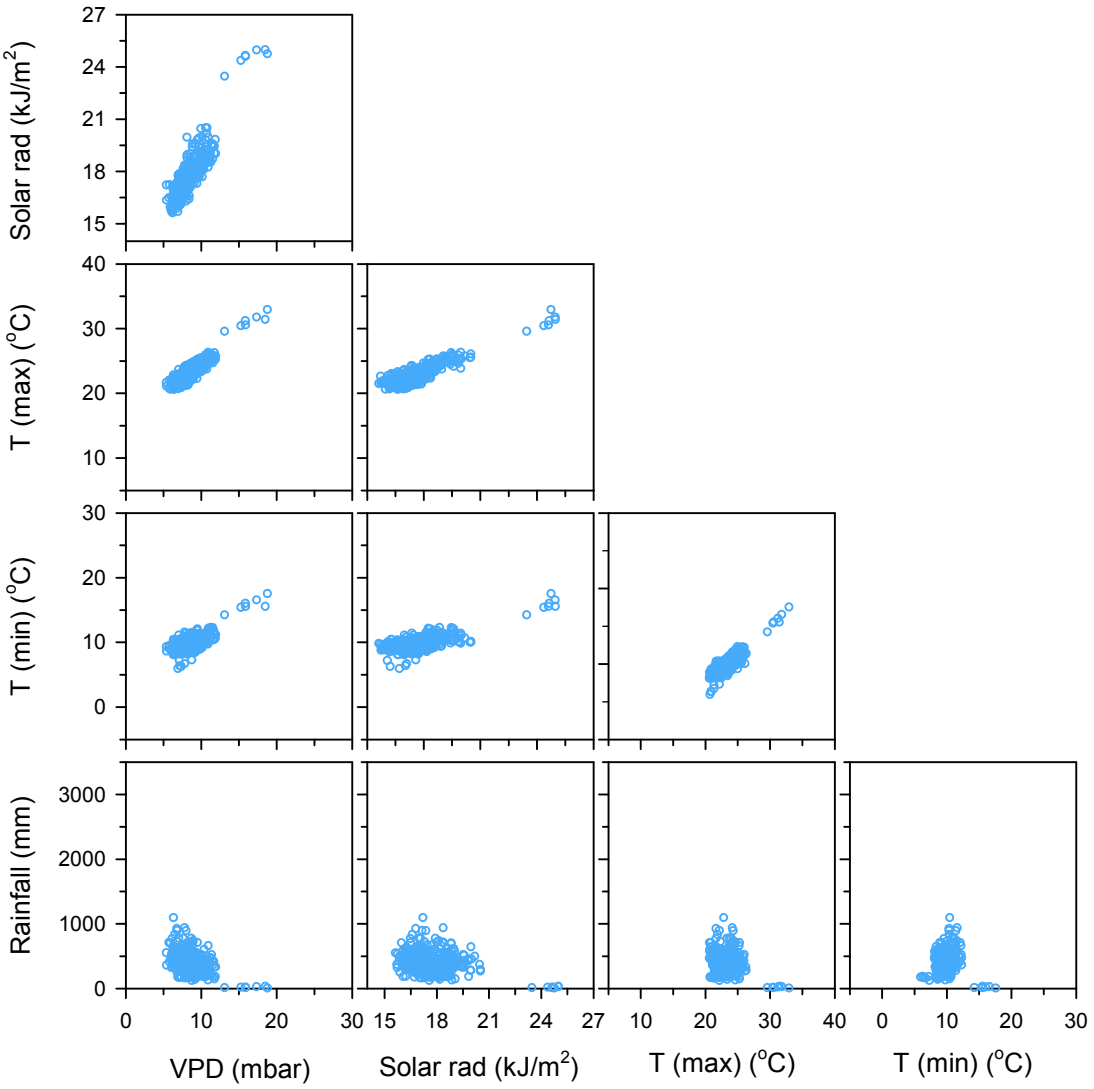

Figure A-4. Relationship between annual rainfalls, temperature solar radiation and vapour pressure deficit for BSk climate type

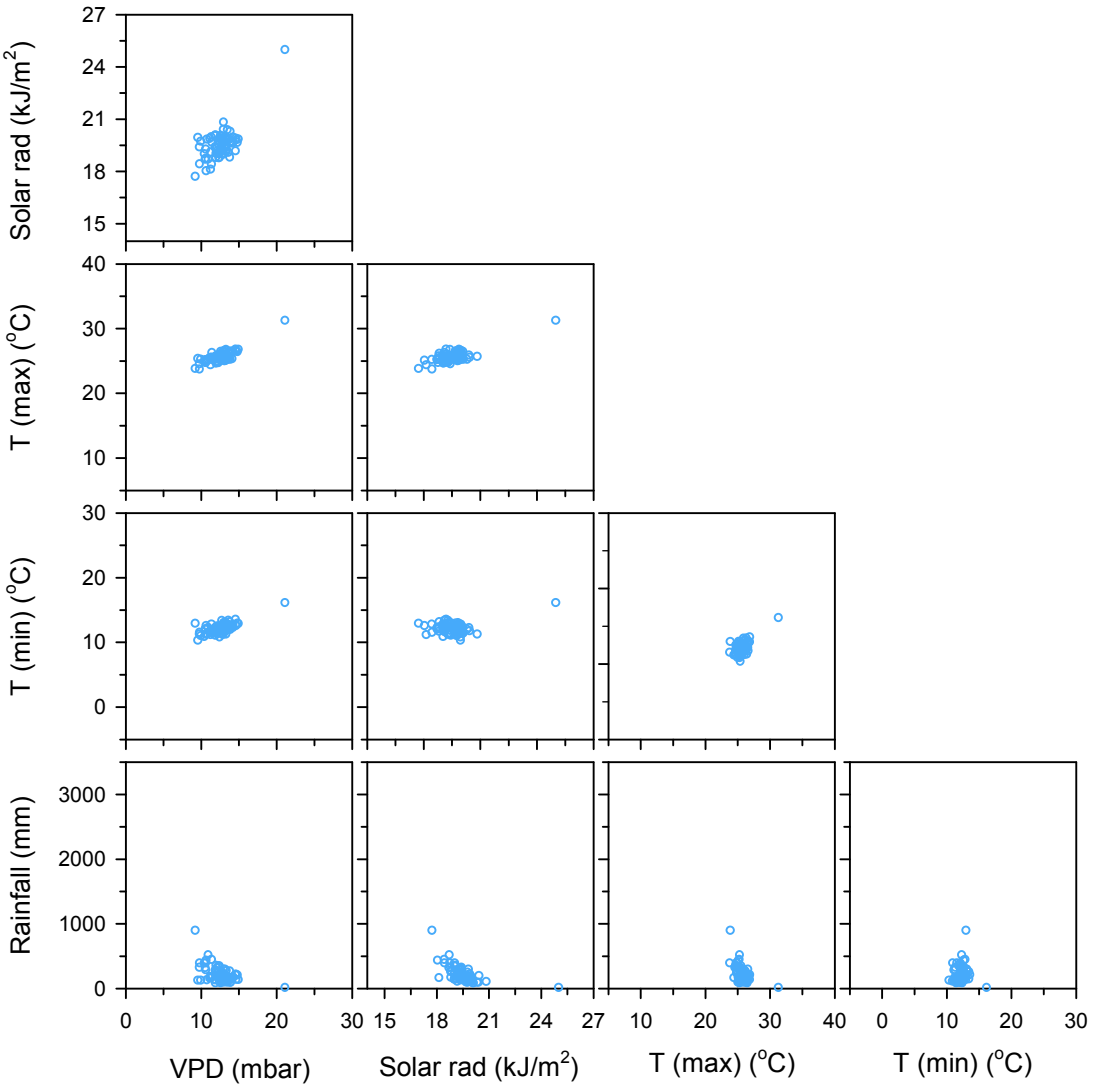

Figure A-5. Relationship between annual rainfalls, temperature solar radiation and vapour pressure deficit for BWh climate type

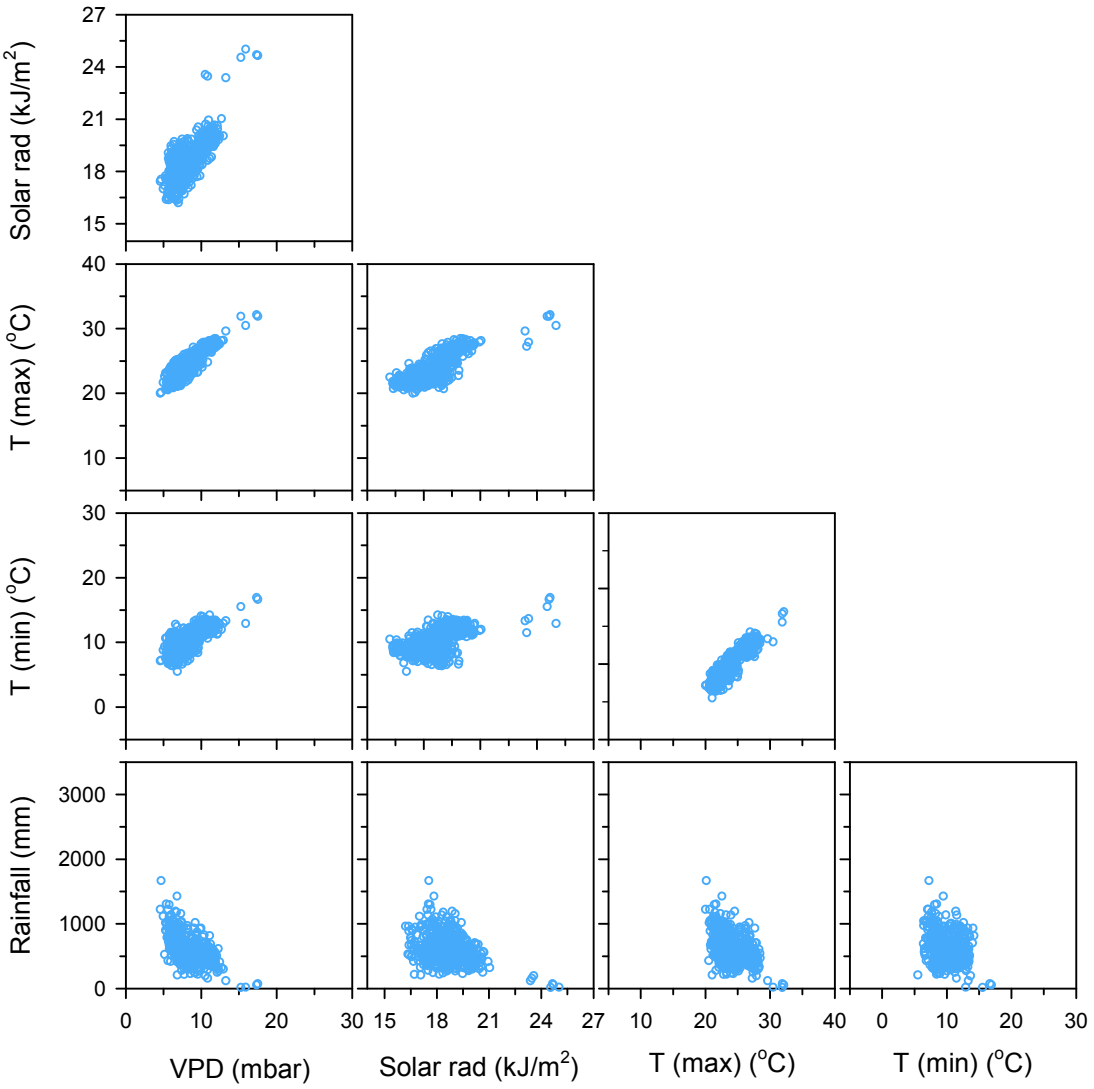

Figure A-6. Relationship between annual rainfalls, temperature solar radiation and vapour pressure deficit for Cfa climate type

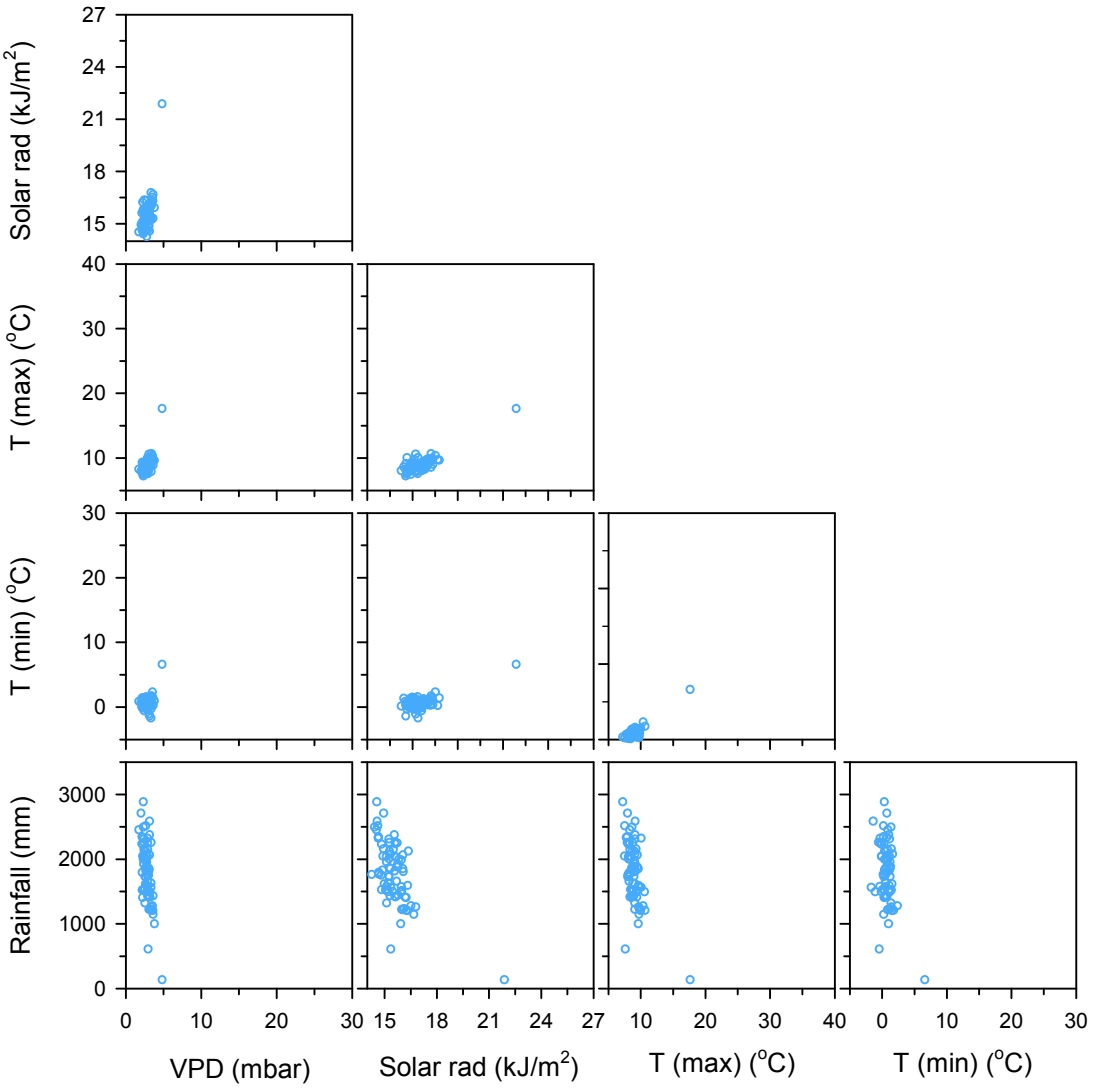

Figure A-7. Relationship between annual rainfalls, temperature solar radiation and vapour pressure deficit for Dfc climate type

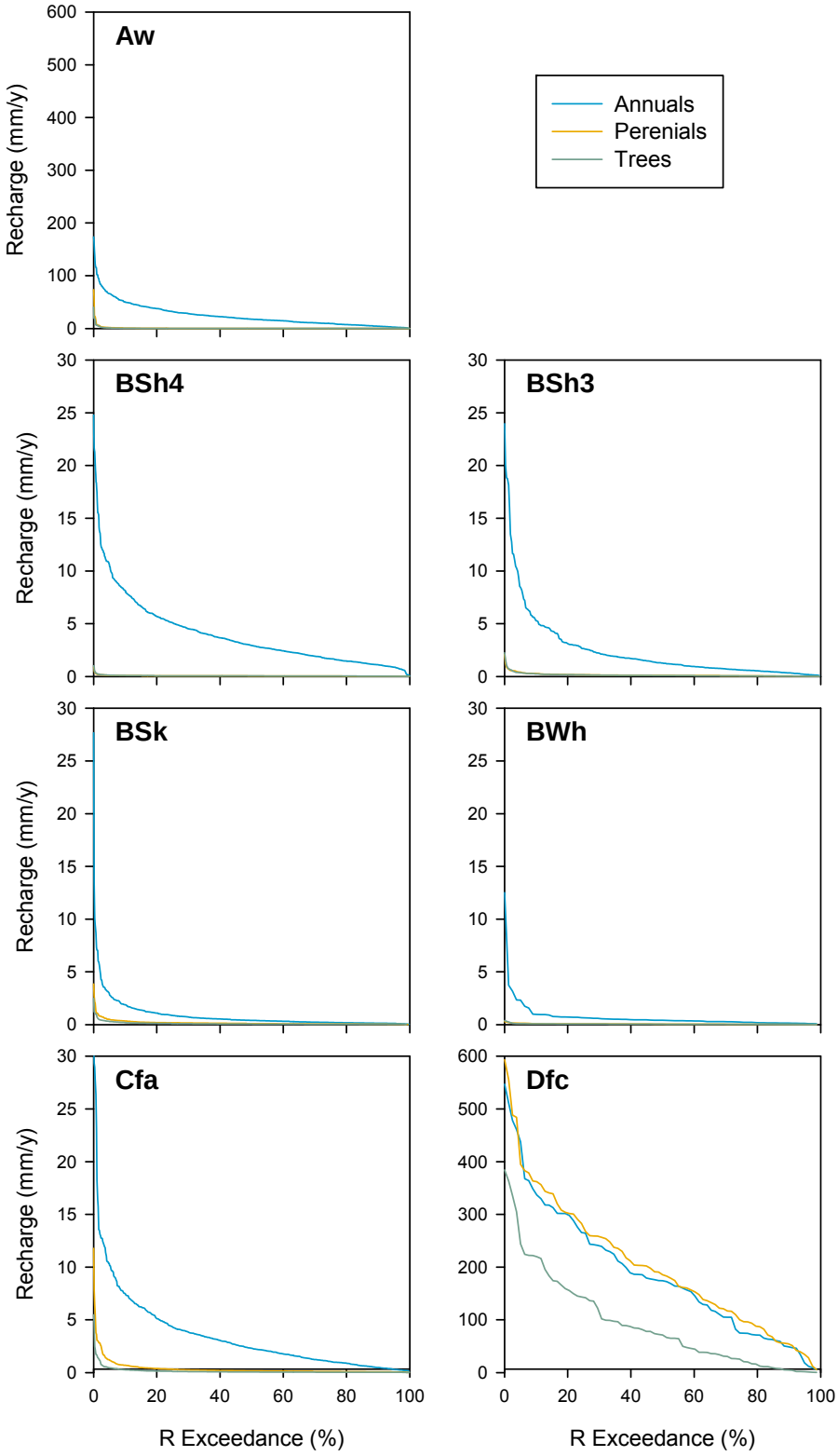

Figure A-8. Probability of exceedance of annual recharge for various vegetation, climate types and clay soil (K=0.01m/d)

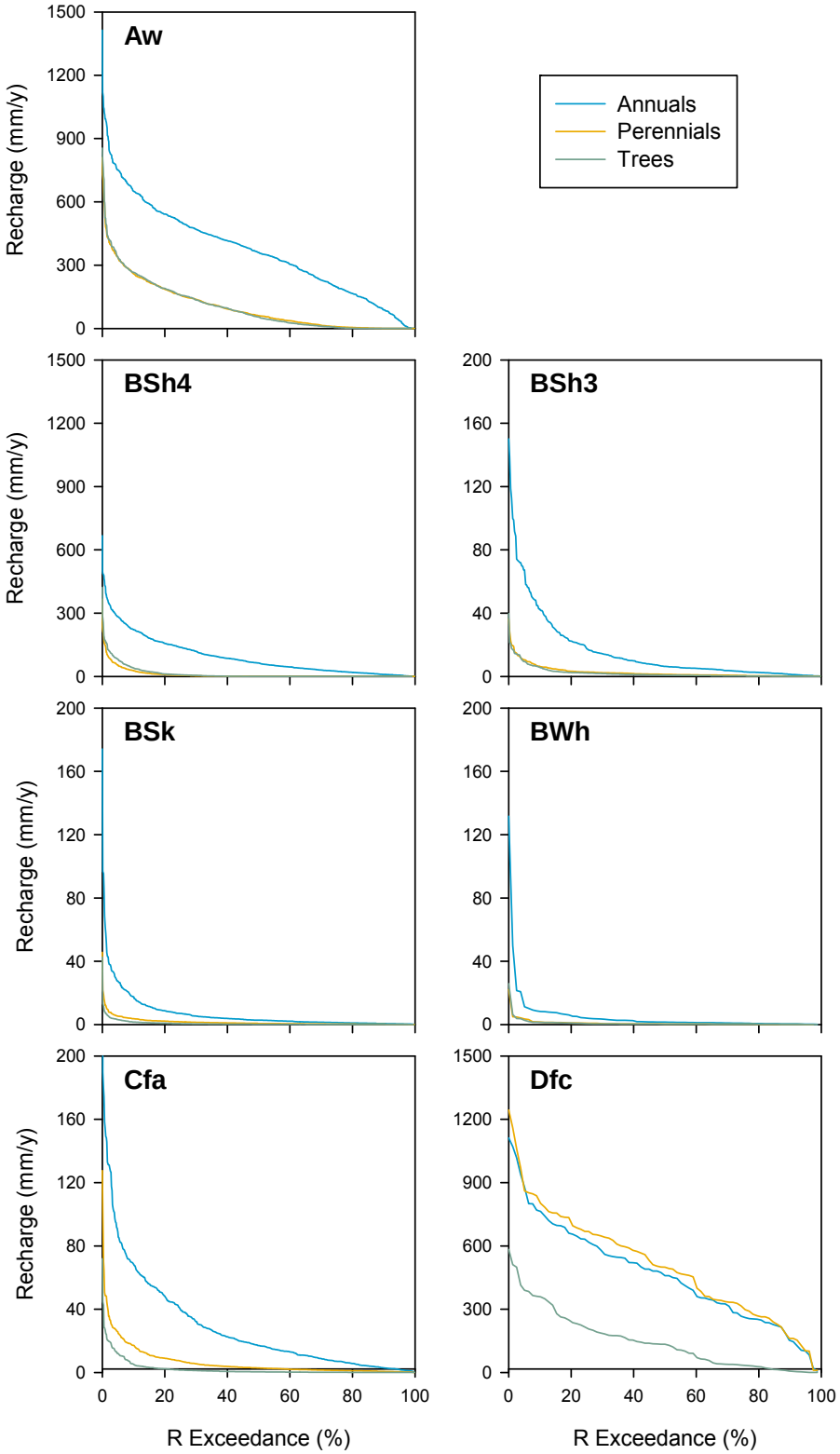

Figure A-9. Probability of exceedance of annual recharge for various vegetation, climate types and light soil (K=0.1m/d)

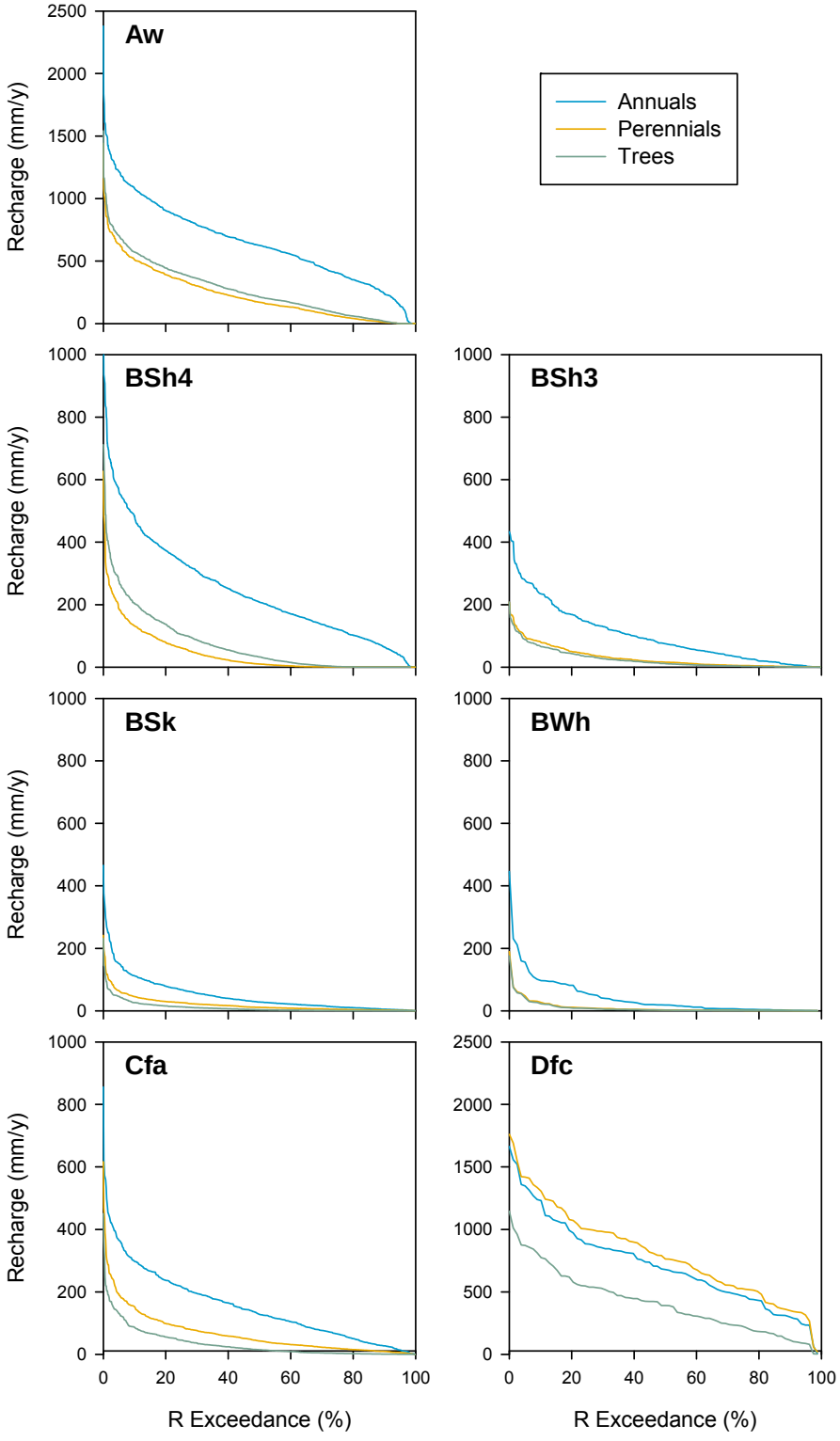

Figure A-10. Probability of exceedance of annual recharge for various vegetation, climate types and highly permeable soils (K=1m/d)

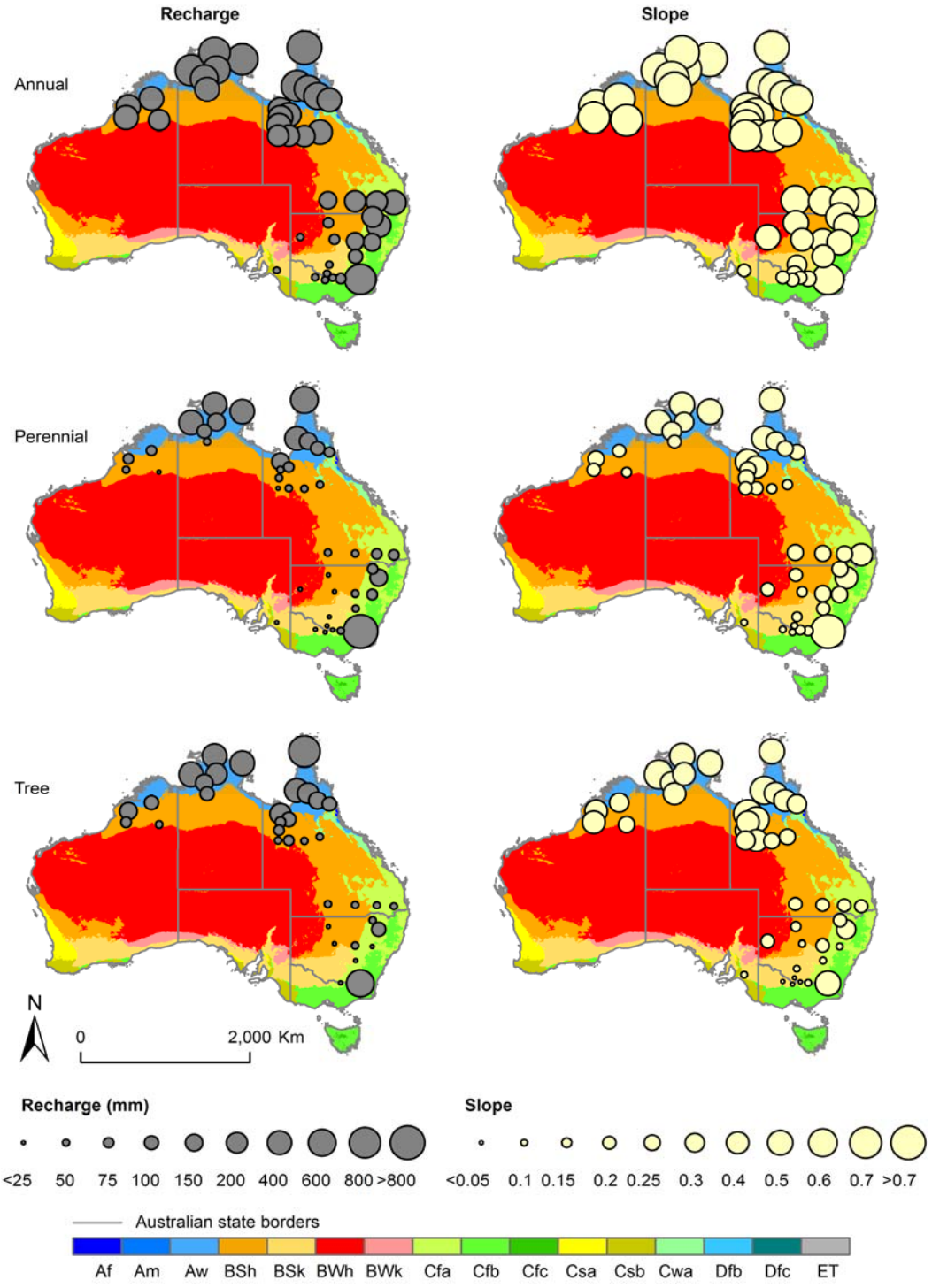

Figure A-11. Annual average recharge (a, c and e) and a (slope) of the relationship between recharge and annual average rainfall (b, d and f) for annual vegetation (a and b), perennial vegetation (c and d), trees (e and f) under soil with high hydraulic conductivity, plotted over the climate types

REFERENCES

Allen, D.M., Mackie, D.C. and Wei, M., 2004. Groundwater and climate change: a sensitivity analysis for the Grand Forks aquifer, southern British Columbia, Canada. Hydrogeology Journal, 12(3): 270–290.

Austin, J., Zhang, L., Jones, R., Durack, P., Dawes, W. and Hairsine, P., 2010. Climate change impact on water and salt balances: an assessment of the impact of climate change on catchment salt and water balances in the Murray-Darling Basin, Australia. Climatic Change, 100(3–4): 607–631.

Berti, M., Bari, M., Charles, S. and Hauck, E., 2004. Climate change, catchment runoff and risks to water supply in the south-west of Western Australia, Department on Environment, East Perth.

Bouraoui, F., Vachaud, G., Li, L.Z.X., Le Treut, H. and Chen, T., 1999. Evaluation of the impact of climate changes on water storage and groundwater recharge at the watershed scale. Climate Dynamics, 15(2): 153–161.

Brouyère, S., Carabin, G. and Dassargues, A., 2004. Climate change impacts on groundwater resources: modelled deficits in a chalky aquifer, Geer Basin, Belgium. Hydrogeology Journal, 12(2): 123–134.

BRS, 2008. Integrated vegetation cover 2008. Bureau of Rural Sciences, Canberra.

Candela, L., von Igel, W., Elorza, F.J. and Aronica, G., 2009. Impact assessment of combined climate and management scenarios on groundwater resources and associated wetland (Majorca, Spain). Journal of Hydrology, 376(3–4): 510–527.

Charles, S.P., Bari, M.A., Kitsios, A. and Bates, B.C., 2007. Effect of GCM bias on downscaled precipitation and runoff projections for the Serpentine catchment, Western Australia. International Journal of Climatology, 27(12): 1673–1690.

Charles, S.P., Bates, B.C. and Hughes, J.P., 1999. A spatio-temporal model for downscaling precipitation occurrence and amounts. Journal of Geophysical Research, 104(D24): 31657–31669.

Charles, S.P., Bates, B.C., Smith, I.N. and Hughes, J.P., 2004. Statistical downscaling of daily precipitation from observed and modelled atmospheric fields. Hydrological Processes, 18(8): 1373–1394.

Charles, S.P., Heneker, T.M. and Bates, B.C., 2008. Stochastically downscaled rainfall projections and modelled hydrological response for the Mount Lofty Ranges, South Australia, Water Down Under 2008. Engineers Australia, Adelaide, pp. 1144–1155.

Chiew, F.H.S., Kirono, D.G.C., Kent, D.M., Frost, A.J., Charles, S.P., Timbal, B., Nguyen, K.C. and Fu, G., 2010. Comparison of runoff modelled using rainfall from different downscaling methods for historical and future climates. Journal of Hydrology, 387(1–2): 10–23.

Chiew, F.H.S., Peel, M. and Western, A., 2002. Application and testing of the simple rainfall-runoff model SIMHYD. In: V.P. Singh and D.K. Frevert (Editors), Mathematical models of small watershed hydrology and applications. Water Resources Publication, Littleton, Colorado.

Chiew, F.H.S., Teng, J., Kirono, D., Frost, A.J., Bathols, J.M., Vaze, J., Viney, N.R., Young, W.J., Hennessy, K.J. and Cai, W.J., 2008. Climate data for hydrologic scenario modelling across the Murray-Darling Basin. A report to the Australian Government from the CSIRO Murray-Darling Basin Sustainable Yields Project. CSIRO, Canberra.

Cook, P.G., Leaney, F.W. and Miles, M., 2004. Groundwater recharge in the north-east Mallee Region, South Australia. CSIRO Land and Water, Technical Report 25/04, Adelaide.

Croley, T.E. and Luukkonen, C.L., 2003. Potential effects of climate change on ground water in Lansing, Michigan. Journal of the American Water Resources Association, 39(1): 149–163.

Crosbie, R.S., McCallum, J., Walker, G.R. and Chiew, F.H.S., 2008. Diffuse groundwater recharge modelling across the Murray-Darling Basin. A report to the Australian government from the CSIRO Murray-Darling Basin Sustainable Yields project. CSIRO Water for a Healthy Country Flagship, Canberra, http://www.csiro.au/files/files/pn7z.pdf.

Crosbie, R.S., McCallum, J.L. and Harrington, G.A., 2009. Diffuse groundwater recharge modelling across Northern Australia. A report to the Australian Government from the CSIRO Northern Australia Sustainable Yields Project. CSIRO Water for a Healthy Country Flagship, Canberra.

Crosbie, R.S., McCallum, J.L., Walker, G.R. and Chiew, F.H.S., 2010a. The impact of climate change on the episodicity of groundwater recharge. Submitted to Hydrogeology Journal.

Crosbie, R.S., McCallum, J.L., Walker, G.R. and Chiew, F.H.S., 2010b. Modelling the climate change impact on groundwater recharge in the Murray-Darling Basin. Hydrogeology Journal, DOI 10.1007/s10040-010-0625-x.

CSIRO, 2009. Water in northern Australia: summary of reports to the Australian Government from the CSIRO Northern Australia Sustainable Yields Project. CSIRO Water for a Healthy Country Flagship National Research Flagship, Canberra.

Dawes, W., Zhang, L. and Dyce, P., 1998. WAVES v3.5 user manual. CSIRO Land and Water, Canberra.

Dawes, W., Zhang, L. and Dyce, P., 2004. WAVES v3.5 user manual, CSIRO Land and Water, Canberra.

Dawes, W.R. and Short, D.L., 1993. The efficient numerical solution of differential equations for coupled water and solute dynamics: the WAVES model, CSIRO Division of Water Resources Technical Memorandum 93/18. CSIRO, Canberra.

Doll, P., 2009. Vulnerability to the impact of climate change on renewable groundwater resources: a global-scale assessment. Environmental Research Letters, 4(3): 35006.

Duan, Q.A., Sorooshian, S., and Gupta, V.K., 1994. Optimal use of the SCE-UA global optimisation method for calibrating watershed models, Journal of Hydrology, Vol. 158, pp. 265-284.

Eckhardt, K. and Ulbrich, U., 2003. Potential impacts of climate change on groundwater recharge and streamflow in a central European low mountain range. Journal of Hydrology, 236: 244–252.

Fowler, H.J., Blenkinsop, S. and Tebaldi, C., 2007. Linking climate change modelling to impacts studies: recent advances in downscaling techniques for hydrological modelling. International Journal of Climatology, 27(12): 1547–1578.

Fu G., Viney, N.R., Charles, S. P AND Liu, J 2010. Long-Term Temporal Variation of Extreme Rainfall Events in Australia: 1910–2006. Journal of Hydrometeorology 11, 950-965.

Goderniaux, P., Brouyere, S., Fowler, H.J., Blenkinsop, S., Therrien, R., Orban, P. and Dassargues, A., 2009. Large scale surface-subsurface hydrological model to assess climate change impacts on groundwater reserves. Journal of Hydrology, 373(1-2): 122–138.

Green, T.R., Bates, B.C., Charles, S.P. and Fleming, P.M., 2007. Physically based simulation of potential effects of carbon dioxide-altered climates on groundwater recharge. Vadose Zone Journal, 6(3): 597–609.

Gromping, U., 2006. Relative importance for linear regression in R: the package relaimpo. Journal of Statistical Software, 17(1).

Hanson, R.T. and Dettinger, M.D., 2005. Ground water/surface water responses to global climate simulations, Santa Clara-Calleguas Basin, Ventura, California. Journal of the American Water Resources Association, 41(3): 517–536.

Hatton, T.J., Walker, J., Dawes, W.R. and Dunin, F.X., 1992. Simulations of hydroecological responses to elevated CO_2 at the catchment scale. Australian Journal of Botany, 40(5): 679–696.

Herrera-Pantoja, M. and Hiscock, K.M., 2008. The effects of climate change on potential groundwater recharge in Great Britain. Hydrological Processes, 22(1): 73–86.

Holman, I.P., Tascone, D. and Hess, T.M., 2009. A comparison of stochastic and deterministic downscaling methods for modelling potential groundwater recharge under climate change in East Anglia, UK: implications for groundwater resource management. Hydrogeology Journal, 17(7): 1629–1641.

Hughes, J.P., Guttorp, P. and Charles, S.P., 1999. A non-homogeneous hidden Markov model for precipitation occurrence. Applied Statistics, 48(1): 15–30.

IPCC, 2007. Climate change 2007: the physical science basis. Contribution of Working Group I to the Fourth Assessment Report of the Intergovernmental Panel on Climate Change. Cambridge University Press, Cambridge UK, 996 pp.

Johnston, R.M., Barry, S.J., Bleys, E., Bui, E.N., Moran, C.J., Simon, D.A.P., Carlile, P., McKenzie, N.J., Henderson, B.L., Chapman, G., Imhoff, M., Maschmedt, D., Howe, D., Grose, C., Schoknecht, N., Powell, B. and Grundy, M., 2003. ASRIS: the database. Australian Journal of Soil Research, 41(6): 1021–1036.

Jones, D.A., Wang, W. and Fawcett, R., 2009. High-quality spatial climate data-sets for Australia. Australian Meteorological and Oceanographic Journal, 58(4): 233–248.

Jyrkama, M.I. and Sykes, J.F., 2007. The impact of climate change on spatially varying groundwater recharge in the grand river watershed (Ontario). Journal of Hydrology, 338(3-4): 237–250.

Kalnay, E., Kanamitsu, M., Kistler, R., Collins, W., Deaven, D., Gandin, L., Iredell, M., Saha, S., White, G., Woollen, J., Zhu, Y., Chelliah, M., Ebisuzaki, W., Higgins, W., Janowiak, J., Mo, K.C., Ropelewski, C., Wang, J., Leetmaa, A., Reynolds, R., Jenne, R. and Joseph, D., 1996. The NCEP/NCAR 40-year reanalysis project. Bulletin of the American Meteorological Society, 77: 437–471.

Kingston, D.G. and Taylor, R.G., 2010. Sources of uncertainty in climate change impacts on river discharge and groundwater in a headwater catchment of the Upper Nile Basin, Uganda. Hydrology and Earth System Sciences, 14(7): 1297–1308.

Kirshner, S., 2005. Modeling of multivariate time series using hidden Markov models. PhD Thesis, University of California, Irvine, 202 pp.

Kitsios, A., Bari, M.A., Charles, S.P. and Bates, B.C., 2006. Projected streamflow reduction in Serpentine catchment Western Australia: downscaling from multiple GCMs. Department of Water, Perth.

Lindeman, R.H., Merenda, P.F. and Gold, R.Z., 1980. Introduction to bivariate and multivariate analysis. Scott, Foresman, Glenview, IL.

Loáiciga, H.A., Maidment, D.R. and Valdes, J.B., 2000. Climate-change impacts in a regional karst aquifer, Texas, USA. Journal of Hydrology, 227(1–4): 173–194.

Maraun, D., Wetterhall, F., Ireson, A.M., Chandler, R.E., Kendon, E.J., Widmann, M., Brienen, S., Rust, H.W., Sauter, T., Themessl, M., Venema, V.K.C., Chun, K.P., Goodess, C.M., Jones, R.G., Onof, C.J., Vrac, M. and Thiele-Eich, I., 2010. Precipitation downscaling under climate change. Recent developments to bridge the gap between dynamical models and the end user. Rev. Geophys., in press.

McCallum, J.L., Crosbie, R.S., Walker, G.R. and Dawes, W.R., 2010. Impacts of climate change on groundwater in Australia: a sensitivity analysis of recharge. Hydrogeology Journal, 18(7): 1625–1638.

McCarthy, J.J., Canziani, O.F., Leary, N.A. and Dokken, D.J. (Editors), 2001. Climate change 2001, impacts, adaption, and vulnerability. Contribution of Working Group II to the Third Assessment Report of the Intergovernmental Panel on Climate Change. Cambridge University Press, Cambridge, UK.

McGregor, J.L., 2005. C-CAM: geometric aspects and dynamical formulation, CSIRO Atmospheric Research Technical Paper No. 70. CSIRO, Canberra.

Mileham, L., Taylor, R.G., Todd, M., Tindimugaya, C. and Thompson, J., 2009. The impact of climate change on groundwater recharge and runoff in a humid, equatorial catchment: sensitivity of projections to rainfall intensity. Hydrological Sciences Journal-Journal Des Sciences Hydrologiques, 54(4): 727–738.

Mpelasoka, F.S. and Chiew, F.H.S., 2009. Influence of rainfall scenario construction methods on runoff projections. Journal of Hydrometeorology, 10(5): 1168–1183.

Nash, J.E. and Sutcliffe, J.V., 1970. River flow forecasting through conceptual models part I -- a discussion of principles. Journal of Hydrology, 10(3): 282–290.

Ng, G.H.C., McLaughlin, D., Entekhabi, D. and Scanlon, B.R., 2010. Probabilistic analysis of the effects of climate change on groundwater recharge. Water Resources Research, 46: 7502–7502.

Okkonen, J., Jyrkama, M. and Klove, B., 2010. A conceptual approach for assessing the impact of climate change on groundwater and related surface waters in cold regions (Finland). Hydrogeology Journal, 18(2): 429–439.

Parry, M.L., Canziani, O.F., Palutikof, J.P., van der Linden, P.J. and Hanson, C.E. (Editors), 2007. Contribution of Working Group II to the Fourth Assessment Report of the Intergovernmental Panel on Climate Change. Cambridge University Press, Cambridge, UK.

Peel, M.C., Finlayson, B.L. and McMahon, T.A., 2007. Updated world map of the Köppen-Geiger climate classification. Hydrol. Earth Syst. Sci., 11(5): 1633–1644.

Raper, G.P. and Sharma, M.L., 1989. Prediction of groundwater recharge to a sandy aquifer using a simulation model. In: M.L. Sharma (Editor), Groundwater recharge. Balkema Publishing Co., Rotterdam/Boston, pp. 99–108.

Rosenberg, N.J., Epstein, D.J., Wang, D., Vail, L., Srinivasan, R. and Arnold, J.G., 1999. Possible impacts of global warming on the hydrology of the Ogallala Aquifer Region. Climatic Change, 42(4): 677–692.

Scanlon, B.R., Christman, M., Reedy, R.C., Porro, I., Simunek, J. and Flerchinger, G.N., 2002. Intercode comparisons for simulating water balance of surficial sediments in semiarid regions. Water Resources Research, 38(12): 1323–1323.

Schroeder, P.R., Dozier, T.S., Zappi, P.A., McEnroe, B.M., Sjostrom, J.W. and Peyton, R.L., 1994. The hydrologic evaluation of landfill performance (HELP) model: engineering documentation for version 3. EPA/600/R-94/168b, U.S. Environmental Protection Agency Office of Research and Development, Washington, DC.

Scibek, J. and Allen, D.M., 2006a. Comparing modelled responses of two high-permeability, unconfined aquifers to predicted climate change. Global and Planetary Change, 50(1-2): 50–62.

Scibek, J. and Allen, D.M., 2006b. Modeled impacts of predicted climate change on recharge and groundwater levels – art. no. W11405. Water Resources Research, 42(11): 11405–11405.

Scibek, J., Allen, D.M., Cannon, A.J. and Whitfield, P.H., 2007. Groundwater-surface water interaction under scenarios of climate change using a high-resolution transient groundwater model. Journal of Hydrology, 333(2–4): 165–181.

Serrat-Capdevila, A., Valdés, J.B., Pérez, J.G., Baird, K., Mata, L.J. and Maddock, T., 2007. Modeling climate change impacts – and uncertainty – on the hydrology of a riparian system: the San Pedro Basin (Arizona/Sonora). Journal of Hydrology, 347(1–2): 48–66.

Sharma, M.L., Barron, R.J.W. and Craig, A.B., 1991. Land use effects on groundwater recharge to an unconfined aquifer, CSIRO Division of Water Resources, Divisional Report 91/1, Perth.

Summerell, G.K., 2004. Understanding the processes of salt movement from the landscape to the stream in dryland catchments, PhD Thesis, The University of Melbourne.

Toews, M.W. and Allen, D.M., 2009. Simulated response of groundwater to predicted recharge in a semi-arid region using a scenario of modelled climate change. Environmental Research Letters, 4(3): 35003.

Vaccaro, J.J., 1992. Sensitivity of groundwater recharge estimates to climate variability and change, Columbia Plateau, Washington. Journal of Geophysical Research, 97(D3): 2821–2833.

van Roosmalen, L., Sonnenborg, T.O. and Jensen, K.H., 2009. Impact of climate and land use change on the hydrology of a large-scale agricultural catchment. Water Resources Research, 45: W00A15.

Vivoni, E.R., Aragon, C.A., Malczynski, L. and Tidwell, V.C., 2009. Semiarid watershed response in central New Mexico and its sensitivity to climate variability and change. Hydrology and Earth System Sciences, 13(6): 715–733.

Watson, R.T., Zinyowera, M.C. and Moss, R.H. (Editors), 1996. Climate change 1995, impacts, adaptions, and mitigation of climate change: scientific-technical analysis. Contribution of Working Group II to the Second Assessment of the Intergovernmental Panel on Climate Change. Cambridge University Press, Cambridge, UK.

Wilby, R.L., Charles, S.P., Zorita, E., Timbal, B., Whetton, P. and Mearns, L.O., 2004. Guidelines for the use of climate scenarios developed from statistical downscaling methods. Supporting material for the Intergovernmental Panel on Climate Change. Online at http://www.ipcc-data.org/guidelines/dgm_no2_v1_09_2004.pdf.

Woldeamlak, S.T., Batelaan, O. and De Smedt, F., 2007. Effects of climate change on the groundwater system in the Grote-Nete catchment, Belgium. Hydrogeology Journal, 15(5): 891–901.

Wood, A.W., Leung, L.R., Sridhar, V. and Lettenmaier, D.P., 2004. Hydrologic implications of dynamical and statistical approaches to downscaling climate model outputs. Climatic Change, 62(1/3): 189–216.

Zhang, L. and Dawes, W., 1998. WAVES – an integrated energy and water balance model. Technical Report No. 31/98, CSIRO Land and Water.

Zhang, L., Dawes, W.R. and Hatton, T.J., 1996. Modelling hydrologic processes using a biophysically based model – application of WAVES to FIFE and HAPEX-MOBILHY. Journal of Hydrology, 185(1–4): 147–169.

Zhang, L., Dawes, W.R., Hatton, T.J., Reece, P.H., Beale, G.T.H. and Packer, I., 1999. Estimation of soil moisture and groundwater recharge using the TOPOG_IRM model. Water Resources Research, 35(1): 149–161.

Contact Us
Phone: 1300 363 400
+61 3 9545 2176
Email: enquiries@csiro.au
Web: www.csiro.au

Your CSIRO

Australia is founding its future on science and innovation. Its national science agency, CSIRO, is a powerhouse of ideas, technologies and skills for building prosperity, growth, health and sustainability. It serves governments, industries, business and communities across the nation.